**MARMARA UNIVERSITY**
**INSTITUTE FOR GRADUATE STUDIES**
**IN PURE AND APPLIED SCIENCES**

# ELECTRODE MODIFICATION BASED ON METALLOPHTHALOCYANINES AND THEIR ELECTROCHEMICAL APPLICATIONS

MEHMET AYDEMİR

**MASTER THESIS**
Department of Chemical Engineering

**ADVISOR**
Prof. Dr. Atıf KOCA

ISTANBUL, 2014

**MARMARA UNIVERSITY**
**INSTITUTE FOR GRADUATE STUDIES**
**IN PURE AND APPLIED SCIENCES**

# ELECTRODE MODIFICATION BASED ON METALLOPHTHALOCYANINES AND THEIR ELECTROCHEMICAL APPLICATIONS

MEHMET AYDEMİR

(524511009)

**MASTER THESIS**
Department of Chemical Engineering

**ADVISOR**
Prof. Dr. Atıf KOCA

ISTANBUL, 2014

# ACKNOWLEDGEMENT

I owe thanks to several people during the research and conduction of this thesis for their precious contributions and I am truly grateful.

I would like to express my sincere gratitude to my thesis supervisor, Prof. Dr. Atıf KOCA, for his constant encouragement, guidance, valuable comments, suggestions, and helpful criticism throughout this research.

I would like to give my special thanks to Yeliz İPEK for her friendly support, contributions and never-ending help in the laboratory.

I am also thankful to Prof. Dr. Halit KANTEKİN for procurement of phthalocyanine analytes. Also many thanks to Prof. Dr. Zehra BAYIR and Prof. Dr. Makbule KOÇAK their remarkable contribution with newly synthesized phthalocyanines.

Finally, during all stages involved in the beginning of this thesis I want to thank to my spouse for her persistent support and encouragement.

**May, 2014** **Mehmet AYDEMİR**

# TABLE OF CONTENTS

# ABSTRACT


## ELECTRODE MODIFICATION BASED ON METALLOPHTHALOCYANINES AND THEIR ELECTROCHEMICAL APPLICATIONS

Metallophthalocyanine complexes (MPc) are colouring materials which present high thermal stability, light fastness, and inertness to acids and alkalis. In recent years there has been considerable interest in developing their use in electrochromic devices, organic catalysis, electrocatalysis, photocatalysis, photovoltaic devices, lithium batteries, fuel cells, pollution control (especially desulfurisation) etc.

This study represents the electrochemical and spectroelectrochemical characterizations of three sets of newly synthesized metallophthalocyanine (MPc) complexes and the results for their possible applications in technological fields. Voltammetric and in situ spectroelectrochemical characterization of the compounds bearing $In^{III}$, $Mn^{III}$, and $Ti^{IV}$ metal centers have shown that while $In^{III}$ClPc gives only Pc based, $Mn^{III}$ClPc and $Ti^{IV}$OPc undergo both Pc and metal based reduction reactions. During the electrochemical measurements, the interaction of the compounds with molecular oxygen both in solution and in solid states as Langmuir-Blodgett multilayer thin films was studied; $Mn^{III}$ClPc and $Ti^{IV}$OPc showed electrocatalytic activities for ORR which indicate possible usage of the complexes as molecular oxygen sensor.

In the second group, voltammetric and in situ spectroelectrochemical characterization of NiPc, ZnPc, CoPc and TiOPc complexes in solution were examined and the results were assessed. Electron transfer reactions of the CoPc and TiOPc compounds considerably altered the spectra of the complexes that are the most important expectations for the practical applications of the complexes especially in display technologies. The presence of molecular oxygen in the electrolyte affected the same complexes' electrocatalytic and electrosensing activity.

The last set of metallophthalocyanine (MPc) complexes; CuPc-odea, CoPc-odea and metal free $H_2$Pc-odea were analyzed and their electrochromic properties were studied oxidatively on ITO/MPc-odea electrodes constructed by electropolymerization. The affects of solvent, salt and the layer coated on ITO electrode were also investigated. In situ spectrochronocoulometric measurements indicate that ITO/CuPc-odea and ITO/CoPc-odea illustrate fast response time, high efficiency, high columbic and optic stability, and high optical contrast which make them use in display technology.


**May, 2014** **Mehmet AYDEMİR**

# ÖZET

## METAL FİTALOSİYANİN TEMELLİ ELEKTROT MODİFİKASYONLARI VE ELEKTROKİMYASAL UYGULAMALARI

Fitosiyanin kompleksleri yüksek sıcaklık dayanıklılığına, ışık hassaslığına sahip asit ve bazlarla reaksiyon vermeyen boyar maddelerdir. Son yıllarda ise elektrokromik cihazlarda, organikkataliz, elektro kataliz, fotokataliz, fotovoltaik cihazlarla, lityum ve yakıt pilleri ve kirlilik kontrolü alanlarında gelişen yaygın kullanımı büyük ilgi odağı olmuştur.

Bu çalışma, yeni sentezlenmiş üç grup metal fitalosiyanin komplekslerinin elektrokimyasal ve in-situ spektroelektrokimyasal özelliklerini ve sonuçlarıyla birlikte muhtemel teknolojik uygulama alanlarını içerir. $In^{III}$, $Mn^{III}$, and $Ti^{IV}$ metal merkezli komplekslerin voltametrik ve spektroelektrokimyasal analizleri, $In^{III}$ClPc kompleksinin sadece metal bazlı indirgenme reaksiyonu verirken $Mn^{III}$ClPc ve $Ti^{IV}$OPc komplekslerinin hem metal hem de fitalosiyanın bazlı indirgenme reaksiyonları verdiği gözlemlenmiştir. Elektrokimyasal ölçümler sırasında, maddelerin çözeltide ve Langmuir-Blodgett çok katmanlı ince filmlerinin moleküler oksijenle etkileşimleri çalışılmış, $Mn^{III}$ClPc ve $Ti^{IV}$OPc komplekslerinin oksijen sensörü olarak kullanılabileceğini gösteren ORR aktivitelerinde değişiklikler gözlemlenmiştir.

İkinci grupta, NiPc, ZnPc, CoPc ve TiOPc maddelerinin çözelti içinde voltametrik ve in-situ spektroelektrokimyasal özellikleri incelenmiş ve sonuçları değerlendirilmiştir.
CoPc ve TiOPc komplekslerinin elektron transferleri, bu maddelerinin spektrumlarını önemli ölçüde değiştirmiş, bu da maddelerin özellikle görüntüleme teknolojilerinde pratik uygulamaları için en önemli beklentilerinden biridir. Çözelti içerisinde moleküler oksijenin bulunması, aynı maddelerin elektrokatalitik ve elektrolitik algılama aktivitelerini etkilemiştir.

Son grupta, CuPc-odea, CoPc-odea ve metalsiz $H_2$Pc-odea kompleksleri analiz edildi ve bunların elektrokromik özellikleri, yükseltgenme reaksiyonları sırasında elektropolimerleştirilmiş ITO/MPc-odea elektrotlarında çalışıldı. Çözücü, elektrolit tuzu ve ITO üzerinde katma etkileri de ayrıca incelendi. İn situ elektrokronokolometrik ölçümler, ITO/CuPc-odea and ITO/CoPc-odea komplekslerinin hızlı değişim, yüksek verimlilik, kolombik verilerle birlikte, optik kararlılık ve kontrast gibi optimum elektrokromik özellikler göstermektedir ve bu özellikler display teknolojisinde kullanılmasını mümkün kılar.

**May, 2014** **Mehmet AYDEMİR**

# SYMBOLS

**A** : analyte

**A** : area of the electrode

**C** : electrocatalyst

**C** : analyte concentration ($mol/cm^3$)

$\mathbf{C_{ox}}$ : concentrations of oxidized form

$\mathbf{C_{red}}$ : concentrations of reduced form

**D** : diffusion coefficient ($cm^2/s$).

$\mathbf{E_0}$ : standard electrode potential for redox reaction

**F** : faraday constant

$\mathbf{i_d}$ : limiting current (μA)

$\mathbf{i_p}$ : the peak current

**m** : mass flow rate (mg/sec)

**n** : number of electrons involved in overall electrode reaction

**Ox** : oxidized form of redox couple

**Ox** : oxidized form of redox couple

$\mathbf{R_{ed}}$ : reduced form of redox couple

**Red** : reduced form of redox couple

**t** : drop lifetime in seconds(s)

**v** : scan rate of the applied potential

# ABBREVIATIONS

**AN** : acetonitrile

**CME** : chemically modified electrode

**CV** : cyclic voltammetry

**DCM** : dichloromethane

**DMF** : dimethylformamide

**DMSO** : dimethylsulfoxide

**DPV** : differential pulse voltammetry

**EDTA** : ethylenediaminetetraacetic acid

**HOMO** : highest occupied molecular orbital

**ITO** : indium tin oxide

**LB** : langmuir-blodgett

**LMCT** : ligand to metal charge transfer

**LUMO** : lowest unoccupied molecular orbital

**MLCT** : metal to ligand charge transfer

**MPc** : metallophthalocyanine

**NHE** : normal hydrogen electrode

**NPV** : normal pulse voltammetry

**OTE** : optically transparent electrode

**OTTLE** : optically transparent thin layer electrode

**Pc** : phthalocyanine

**PDT** : photodynamic therapy

**RE** : reference electrode

**SCE** : saturated calomel electrode

**SWV** : square wave voltammetry

**$TBABF_4$** : tetrabutylammonium tetrafluoroborate

**TBAP** : tetrabutylammonium perchlorate

**TEAP** : tetraethylammonium perchlorate

**WE** : working electrode

# LIST OF FIGURES

# LIST OF TABLES

# 1. INTRODUCTION

## 1.1. Discovery and Industrial Importance of Phthalocyanines

Since their accidental synthesis in Scotland, by Imperial Chemical Industries, in 1928, phthalocyanines (Pc) have drawn great attention for their industrial application in variety of fields such as, in dyestuffs, paints, colours for metal surfaces, fabrics and plastics. In recent years there has been considerable interest in developing their use in electrochromic devices, organic catalysis, electrocatalysis, photocatalysis, photovoltaic devices, lithium batteries, fuel cells, pollution control (especially desulfurisation) etc. [1].

Phthalocyanines (Pcs) are man's synthetic analogues of the porphyrins, such as chlorophyll, cyanocobalamine (vitamin B12) and hemoglobin [2]. The structure of phthalocyanines was elucidated and confirmed by X-ray diffraction (XRD) method.
Iron (II) phthalocyanine, a green/blue compound, was produced from phthalic anhydride and ammonia and granted being the first metal Pc [3].

Tinctorial properties in a region of the visible spectrum, moderate cost of manufacture, and good stability have led the Pcs to become a new class of coloring matter.

Copper (II) phthalocyanine as a pigment began to be traded under the name Monastral Blue in 1935 [4].

Water-soluble dyes based on sulfonated phthalocyanines and, subsequently, reactive dyes for permanent textile coloration were developed in the 1950s and 1960s.

## 1.2. General Features of Phthalocyanines

Phthalocyanines are conjugated two dimensional symmetrical molecules with a general formula of $C_{32}H_{18}N_8$ **(Fig. 1.1)**. The conjugated two dimensional 18 π-electron system enables phthalocyanines to be incorporated more than 70 metals and non-metals into their inner core [5].

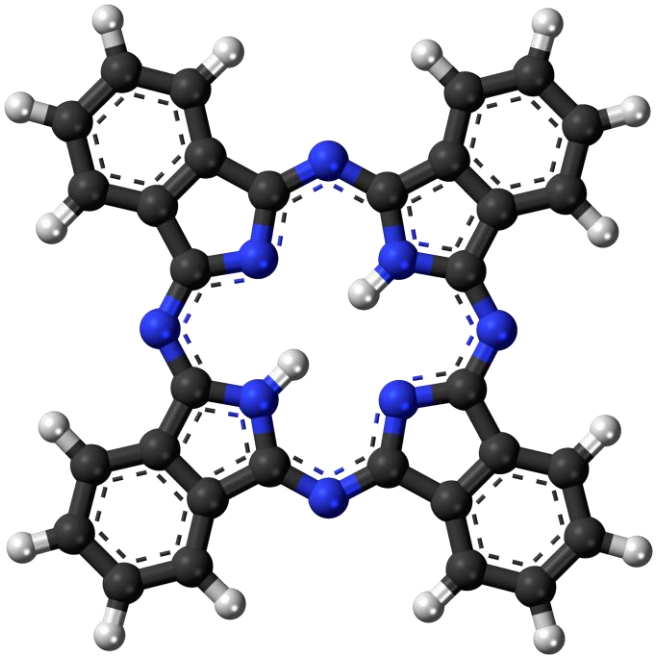

**Figure 1.1** The structure of phthalocyanine.

Metal phthalocyanines (MPcs) are of $D_4$h geometry, while metal free ($H_2$Pc) counterparts exhibit $D_2$h symmetry as a result of insertion of a metal ion to the cavity of the $H_2$Pc without disturbing the planarity. Replacing the two hydrogen atoms with a metal leads to an increase in symmetry from $D_2$h to $D_4$h **(Fig. 1.2)**.

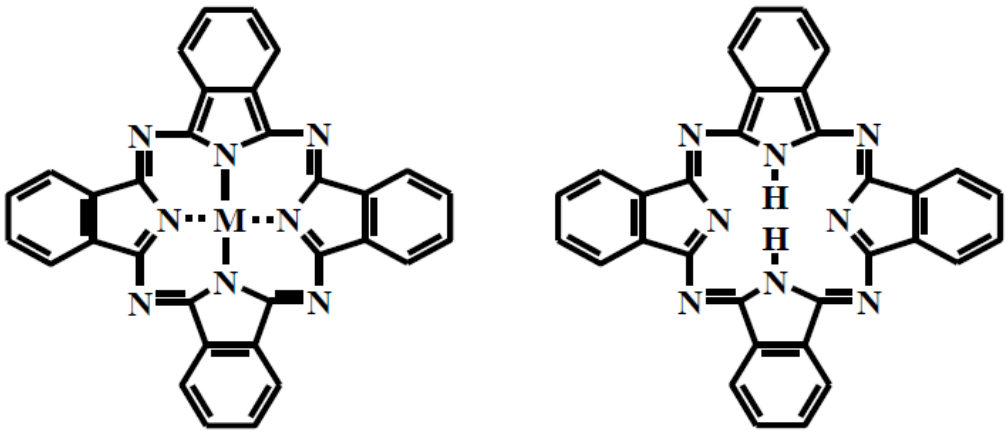


$D_4$h symmetry $D_2$h symmetry

**Figure 1.2** The molecular structures MPc and $H_2$Pc phthalocyanines.

However some larger metal ions (such as Pb, Sb and Ta) distort the geometry as they do not perfectly fit into the cavity of the ring, thus, leading to change in planarity to a square pyramidal and reduction of the symmetry from $D_2h$ to a $C_4v$ symmetry **(Fig. 1.3)** [6].

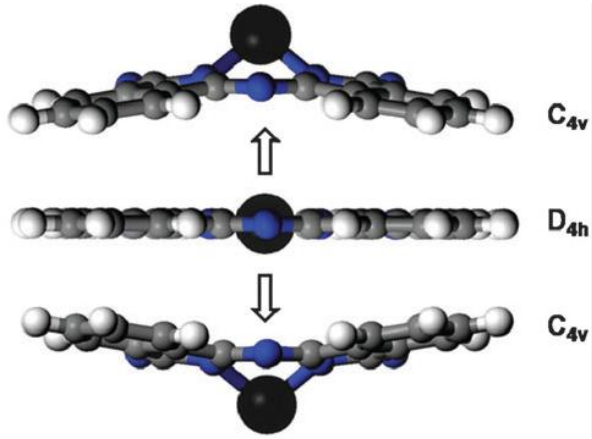


**Figure 1.3** The structure of MPc with $C_{4v}$ symmetry (shuttlecock-shaped).

Sometimes the metal center of a phthalocyanine bears ligands in axial position resulting different coordination geometry. In some cases sandwich complexes are formed when a large metal ion combines with two or more Pc units (**Fig. 1.4)**.

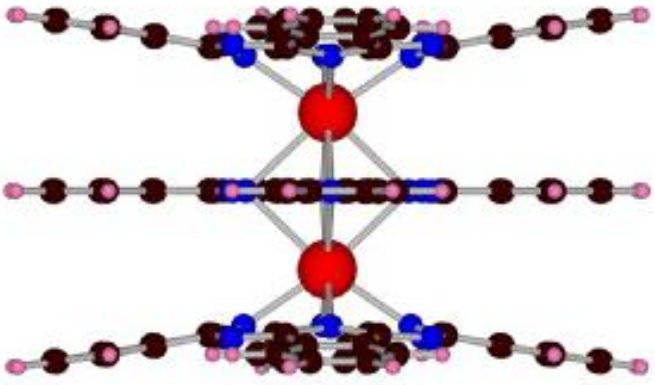

**Figure 1.4** A sandwich structure MPc with a large metal ion center.

The color of most phthalocyanines ranges from blue-black to a metallic bronze, depending on the manufacturing process and the chemical and crystalline form of the material. The colors of the newly divided pigment forms vary from dark blue to green, as

phthalocyanines absorb in the visible region at 600–700nm. Most compounds do not melt but sublime above 200°C. CuPc can be sublimed without decomposition at 500–580°C under an inert gas and normal pressure and at 900° C under vacuum. It decomposes vigorously, however, at 405–420°C in air and in nitrogen between 460–630° C.

### 1.3. Methods of Phthalocyanine Synthesis

Phthalocyanines contain four isoindoline molecules linked together over 1,3 positions by azo bridges, phthalocyanine synthesis is therefore a kind of cyclotetramerization process. Several routes can be employed depending on the desired product. In general ortho-disubstituted benzene derivatives serve as starting materials. Phathalic acid, phathalic anhydride, phthalonitrile, o-cyanobenzamide, o-dibromobenzene, diiminoisoindoline are among them **(Fig. 1.5)**.

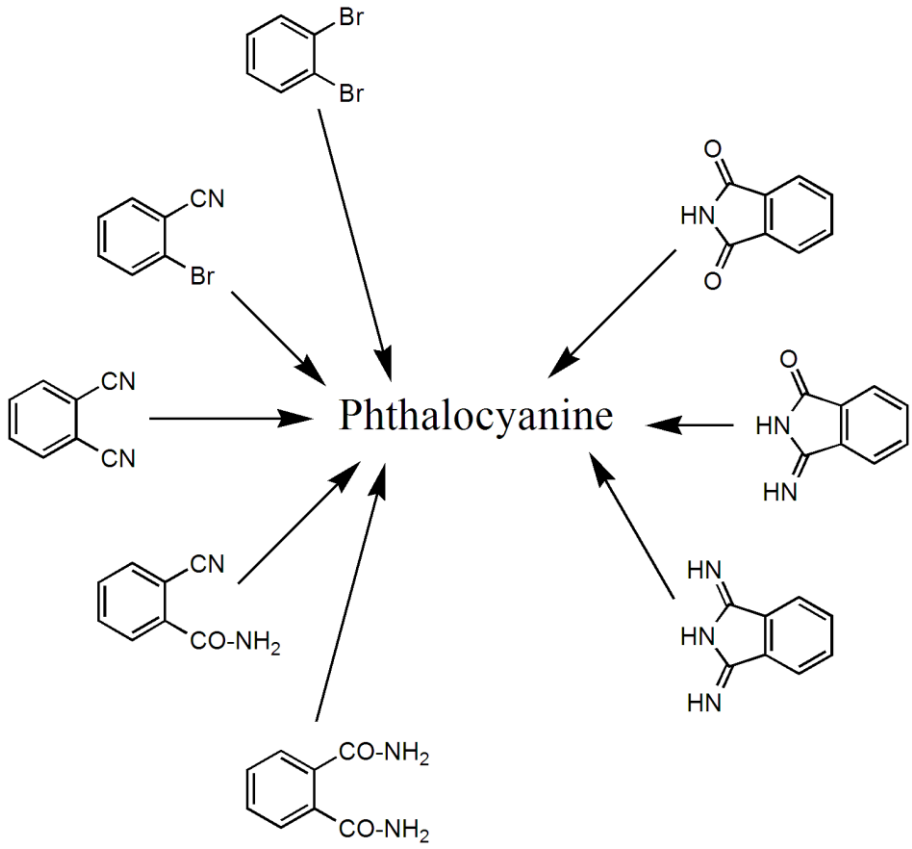


**Figure 1.5** Synthesis of metallophthalocyanines (MPcs) from typical starting materials.

First accidental phthalocyanine was synthesized by heating o-cyanobenzamide with ethanol **(Fig. 1.6)**.

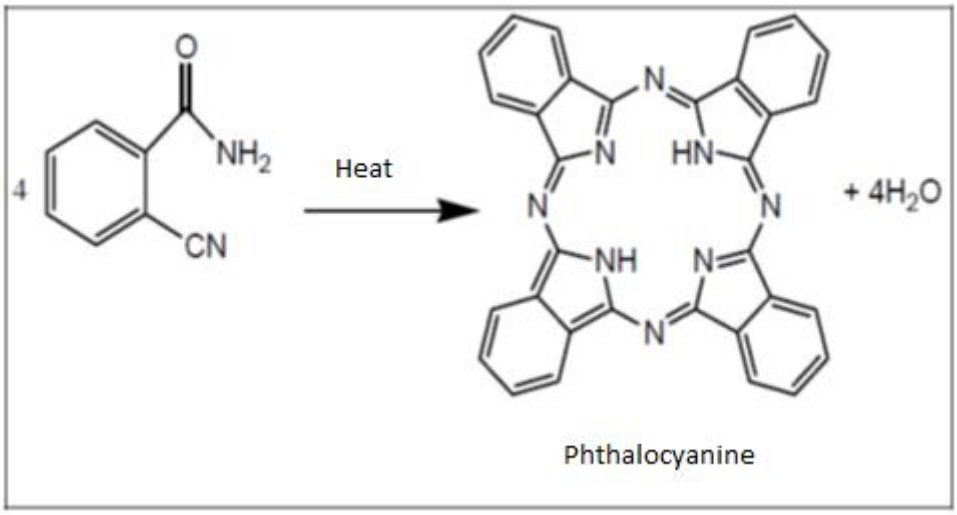


**Figure 1.6** The accidental discovery of phthalocyanine from o-cyanobenzamide.

Phthalonitrile is the most preferable precursor for laboratory scale phthalocyanine production, since it requires mild reaction process and readily gives good yield but costly of MPc. The reaction involves heating phthalonitrile in the presence of a base or high boiling point solvent with a metal ion source.

### 1.4. Application Fields of Phthalocyanines

Metallophthalocyanines (MPcs) have very wide range of application fields due to their unique electrochemical and spectroscopic characteristics. Over the years their increased coordination properties and feasible synthesis methods have made them valuable industrial subject.

Metallophthalocyanines (MPcs) have potential application usage as catalysis sensors and photodynamic therapy (PDT). New applications of MPcs are emerging, these include ink jet printing, electrophotography, photocopying and laser printing, electrochromic display devices, optical computer re-writable discs and information storage systems, liquid crystal display devices, photovoltaic cells, fuel cells, molecular electronics, semi-conductor devices and electrochemical sensors [7].

### 1.4.1. Dyes and Pigments

Phthalocyanines are highly delocalized 18 π-electron aromatic molecules showing strong absorption in the visible region, for this reason, they are extensively used as dyestuffs for textiles and printing inks [5,8].

Their characteristic blue-green color and robustness account for their traditional use as industrial dyes pigments [9,10]. Phthalocyanines are second only to the ubiquitous azo colorants in terms of commercial importance. The commercial importance of phthalocyanines mainly relies on three factors; the first is their beautiful bright blue to green colors and high tinting strength; the second is their remarkable thermal and chemical stability. The third factor is their excellent fastness to light. This combination of properties is extremely difficult, if not impossible, to achieve in other colorants. By comparison, the natural dyes such as chlorophyll and haemin are highly sensitive and easily destroyed by light and mild chemical reagents [11].

The insolubility of phthalocyanines necessitates preparation of soluble derivatives for application as dyes for textile fibres. Dispersed aqueous phthalocyanine pigments are used in pad-dyeing with resin emulsions. Because of their excellent stability to acids, alkalis and solvents phthalocyanines are particularly useful in spin dying. They have also been used in coloring synthetic fibres, such as viscose, cuprommonium cellulose, nylon, etc; Phthalocyanines are widely used as paint pigments. Metal surfaces can be coated by forming the metal phthalocyanine directly on them [12].

Copper phthalocyanine-sodium sulfonate has been used in photography. Copper phthalocyanine is also used as food coloring [13].

### 1.4.2. Catalyst

The first mention of phthalocyanines as catalyst is on the activation of molecular hydrogen [14] and found that crystals of phthalocyanine and copper phthalocyanine catalyze atomic interchange between molecular hydrogen and water vapor, and oxygen [15]. Phthalocyanines catalyze the oxidation of many organic compounds [16,17]. The aerobic

oxidation of unsaturated fatty acids catalyzed by phthalocyanines has been reported [18]. Cobalt and other phthalocyanines derivatives have been used as rubber emulsification catalysts.

When cobalt tetrasulphophthalocyanine is attached to poly (vinylamine) it can catalyses the autooxidation of thiols [19].

α-Keto acids, eg. pyruvic, phenylpyruvic, α-ketobutyric, α-ketoglutaric and α-keto isocaproic undergo electrocatalysed reduction at carbon past electrode modified with cobalt phthalocyanine [20]. CoPc modified electrodes can catalyse numerous electron transfer processes in addition to those of hydrazine and thiol compounds [21]. Metal phthalocyanines have received much attention in the electocatalytic reduction of dioxygen [22-24]. The phthalocyanines assume importance in electrocatalysis for two reasons;

Metal phthalocyanines are structural and electronic analogues of porphyrins whose electrochemistry is important in understanding electron transfer processes in biological systems.

Electrocatalytic reduction of dioxygen is important in fuel cells [25]. Because of the lower solubility of phthalocyanines, water soluble phthalocyanines such as tetrasulphophthalocyanine [26], and tetracarboxy phthalocyanine [27], have been used as facile catalysts in aqueous medium. The electrocatalytic activity of dioxygen reduction was improved at a glassy carbon electrode when modified with polypyrrole /tetrasulfonato-phthalocyaniato cobalt electrode [28]. The glassy carbon /polypyrrole/cobalt tetrasulfophthalocyanine (GC/PPY /CoTSP) electrode was formed by electropolymerization of pyrrole on a glassy carbon electrode in methanol solution containing CoTSP. Oxygen reduction reaction at the GC/PPY/CoTSP electrode in 0.5 M $H_2SO_4$ showed about 0.5 V more anodic onset potential than the value obtained with a GC electrode in the same medium.

The reduction of dioxygen at iron tetrasulfonatophthalocyanine (FeTSP) incorporated into polypyrrole was also studied [29]. It was found that thicker films are stable and mediate four-electron reduction of dioxygen. It was indicated that dimeric FeTSP species are responsible for the marked shift in the reduction onset potential.

Polymeric iron phthalocyanine precipitated on activated carbon, when heated to 200-500 $^0$C showed a higher rate of deactivation for the electrochemical reduction of dioxygen [30].

The iron phthalocyanine functions as a catalyst layer and oxygen sensor in fuel cells and air battery [31]. A porous electrocatalyst material was prepared by soaking activated carbon in iron phthalocyanine pyridine solution and in perfluorodecalin – $CCl_4$ solution and then mixing with PTFE. The material in the form of sheet was bonded on a nickel mesh. The electrode was used in a zinc-air battery having a discharge current density of 63 $MA/m^2$.

### 14.3. Electrochromism

Electrochromism is a reversible phenomenon in which so-called electrochromic substances undergo color change upon application of specific potential. Electrochromism occur due to electrochemical redox reaction taking place in the electrochromic substances. Color change is commonly observed between transparent (bleached) state and colored state or between two colored states. When more than two redox states are possible, the electrochromic material may reflect multi colors and such material is referred to as polyelectrochromic material.

Several application fields have been reported the electrochromic materials are in use; Electrochromic anti-glare car ear-view mirrors [32,33], electrochromic strips as battery state-of-charge indicators and electrochromic sunglasses. ‘smart windows’ for use in cars cars and in buildings [33], re-usable price labels, protective eyewear, controllable aircraft canopies, glare-reduction systems for offices, devices for frozen-food monitoring [34], camouflage materials, spacecraft thermal control for military purposes, and controllable light-reflective or light-transmissive display devices for optical information and storage.
Electrochromic materials must provide high response time and be reversible between the transition states over a well-defined potential region and life cycle as well.

Numerous organic and inorganic electrochromic materials have been mentioned in literature. Prussian blue, transition metal oxides (e.g. tungsten oxides), viologens, conducting polymers, metallopolymers and metallophthalocyanines are of common.

Prussian blue [iron(III) hexacyanoferrate(II)] is an important inorganic pigment being used as colorant in paints, lacquers, printing inks. Many transition metal oxides have electrochromic property. A typical and most widely known is tungsten trioxide ($WO_3$). Tungsten trioxide is a transparent with the oxidation state of tungsten $W^{6+}$. On electrochemical reduction, tungsten becomes $W^{5+}$ to give the electrochromic blue coloration.

As violegens form an insoluble radical cation, it is coated on ITO surface in electrochromic rear-view mirror [35,36].

Conducting poylmers (CPs) have gained a lot of attention for ECDs. This is due to the fact that all electroactive and CPs are potentially electrochromic materials, and are more processable than inorganic electrochromic materials and offer the advantage of a high degree of color tailorability. This tailorability has been achieved through the modification of various polymer systems via monomer functionalization and copolymerization as well as with the use of blends, laminates and composites. Complex colors are achieved by mixing two existing colors in a dual polymer device.

In CPs, electrochromic changes are induced by redox processes which are accompanied by ion insertion/expulsion and results in a modification of the polymer's electronic properties giving rise to changes in color of the material. The color exhibited by the polymer is closely related to the band gap and the dopant ions. A major focus in the study of electrochromic polymeric materials has been that of controlling their colors by main-chain and pendant group structural modification. Polyheterocycles have proven to be of special interest for this due to their environmental stability under ambient and in use conditions [37]. Since 1970 by the discovery of electrochromism of lutetium diphthalocyanine, intensive studies on the electrochemical properties of various MPcs have been devoted.
Although lutetium diphthalocyanine can exhibit five colors, only the blue–green transition is utilised in most prototype ECDs [38] due to some mechanical problems, such as film fracture , adhesion diffuculty on the electrode substrate which lead switching between two colors.

There are numerous red, blue, and green electrochromic materials in literature. However, such a single material, which has the ability to switch between three primary additive colors is scarce. Over years, efforts on discovery of new electrochromic materials supplying more than two color changes, especially color changes between transparent, red green and blue have condensed [39-42].

Modification of metal centers or substituents enable various color alternatives of MPcs complexes. Electropolymerization of thiophene substituted nickel phthalocyanine and the electrochromic features of the modified electrode have been reported [43]. Another paper has reported electrochromism of ethoxythiophene substituted monomeric CoPc-odea [44].

Electrochromism of the electropolymerization of MPc type complexes bearing amino groups as substituents was reported before. Electrode modification with electropolymerization is the one of the most preferred electrode modification techniques due to its simplicity, and controllability to obtain the desired future of the modified electrode [45].

### 1.4.4. Sensors

Devices based on metal phthalocyanine show useful response towards $NO_2$. A thin film MPc sensor has successfully been used to monitor $NO_x$ produced by short firing in coal mines [46]. Phthalocyanine based devices offer much promise as resistance modulating sensors for toxic gases, sensors against toxic gases can be developed using the conductivity changes of phthalocyanines [47,48]. They are thus complementary to metal oxide devices which are most useful in the detection of flammable gases [49].

Quartz crystal microbalance (QCM) sensors with phthalocyanines (Pcs) as sensitive materials as chemical sensors for the detection of low ppm levels of organic compounds in water. QCM sensors coated with different nickel phthalocyanines having polyoxy and alkyloxy substituents are characterized in their liquid sensing properties. Several Pcs have been found very sensitive to a variety of organic solvents, which are also potential pollutants of water, with detection limits in the lower ppm range [50]. QCM can also serve for the direct detection and classification of explosives such as 2,4,6-trinitrotoluene (TNT) and 1,3,5-trinitro-1,3,5-triazinane (RDX) contained in aqueous samples.

The sensors are found to be very sensitive especially to TNT having sensitivities as high as 100 Hz/ppm and detection limits in the low parts-per-billion range for this explosive [51]. Chemical sensor array technology based on phthalocyanine coated quartz crystal microbalance sensors is evaluated for direct pesticide analysis in aqueous samples. chemically modified phthalocyanine core structure increases sensor sensitivity and create sensors with widely diverging analyte responses. The obtained sensors show high sensitivities and pesticides detection limits down to 0.03 mg/L for common organophosphorus and organonitrogen pesticides such as fenthion and methiocarb [52]. An organic compound Nickel (II) phthalocyanine-tetrasulfonic acid tetrasodium salt (NiTSPc) has been studied as a potential material for a solution based temperature sensor. Using NiTSPc, an ITO/NiTSPc solution/ITO chemical cell has been made and characterized in the temperature range of 20–85 $^0$C. The sensor works on the principle of change in the resistance and capacitance of the chemical cell caused by the temperature variation. Good response/recovery and small hysteresis have been attained [53].

### 1.4.5. Active Layers on Chemically Modified Electrodes

Electrodes derived from different types of phthalocyanines have been fabricated [54,55, 56], powdered carbon or metal is coated with the phthalocyanines by chemical vapour deposition, solvent evaporation or electrophoretic deposition. The powder of the same material has also been pressed with crystalline phthalocyanines into composite pellets. Various metal and semiconductor substrates demonstrated greatly enhanced activity for the electrolysis of the benzoquinone/hydroquinone redox couple when coated with multimolecular layers of chlorogallium phthalocyanine [57]. Exchange current density on GaPc-Cl/Au electrode irradiated with about 100 mW/cm$^2$ polychromatic light were about 103 times greater than on plain gold electrode. The role of GaPc-Cl in activating the substrate surface is also reported. The use of chemically modified carbon paste electrodes, which are modified by the incorporation of cobalt phthalocyanine, is able to oxidize or reduce solute species which are themselves electrolysed only irreversibly at conventional electrode surfaces." These electrodes decrease the over potential for the oxidation of thiols [58], hydrazine [59], α-keto acids and oxalic acid. A glassy carbon electrode modified with CoPc can be efficiently used as a liquid chromatographic detector for the clinical

assay of oxalic acid and a-ketoacids in blood and urine. Faulkner et al [60,61], have studied in detail the faradaic processes taking place on Pc modified electrode surfaces. Nearly reversible kinetics and a high degree of selectivity for the electrode process are observed on these films. Preduction of dioxygen takes place on certain phthalocyanines, when they adhere vacuum deposited to a thickness of 100-1000 $A^0$ on polished graphite. Photooxidation of oxalate takes place on 1 mm thick films of CuPc deposited on Pt [55].

Furthermore, phthalocyanines are useful for anode buffer layers [62,63] and can be used for emitting layers [64].

### 1.4.6. Batteries

Phthalocyanines and phthalocyanine derivatives have been used as cathode materials in batteries especially in fuel cells and air cathode batteries. In batteries the porous electroconductive material is loaded with metal phthalocyanine and a perfluoro compound. This composite material is used as the catalyst layer [65,66].

## 1.5. Spectroelectrochemistry of Phthalocyanines

The ultraviolet visible (UV-visible) absorption spectra of MPc are illustrated by two discrete bands arising from the transition of delocolised phthalocyanine ring system.
**(Fig. 1.7)**.

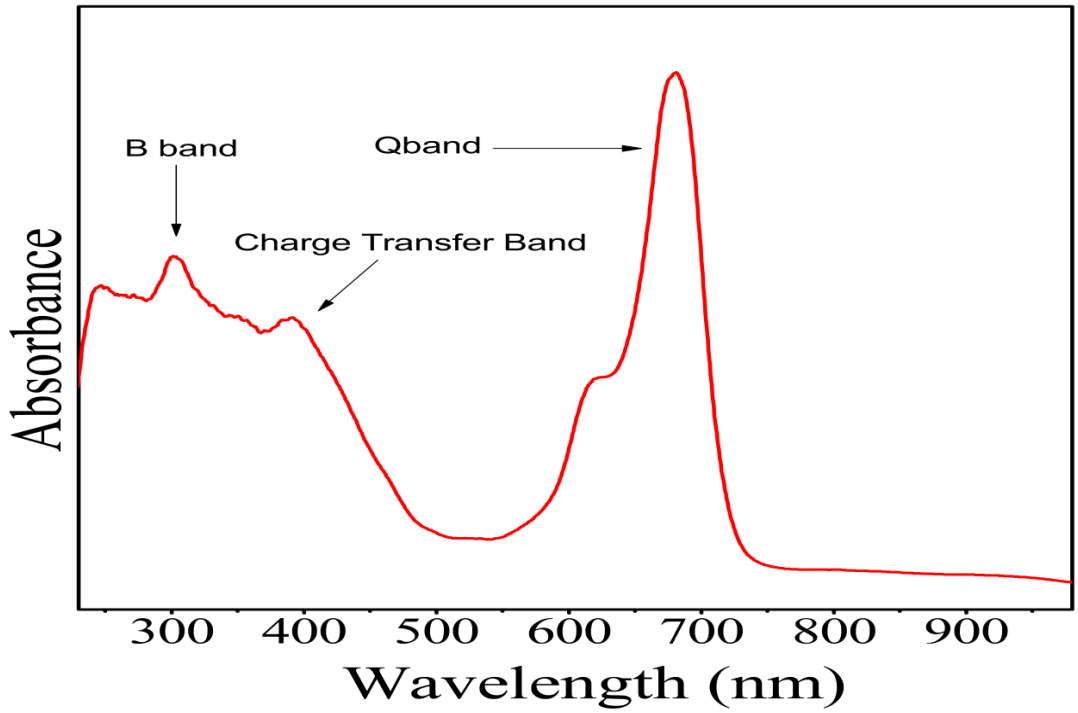


**Figure 1.7** Classic electronic absorption spectra MPc showing the common absorption bands.

The Q band originates from the π-π* electronic transitions from the highest occupied molecular orbital (HOMO) to the lowest unoccupied molecular orbital (LUMO) of the $Pc^{2-}$ ring while the B bands occur as a result of deeper π levels to LUMO transitions **(Fig. 1.8)**.

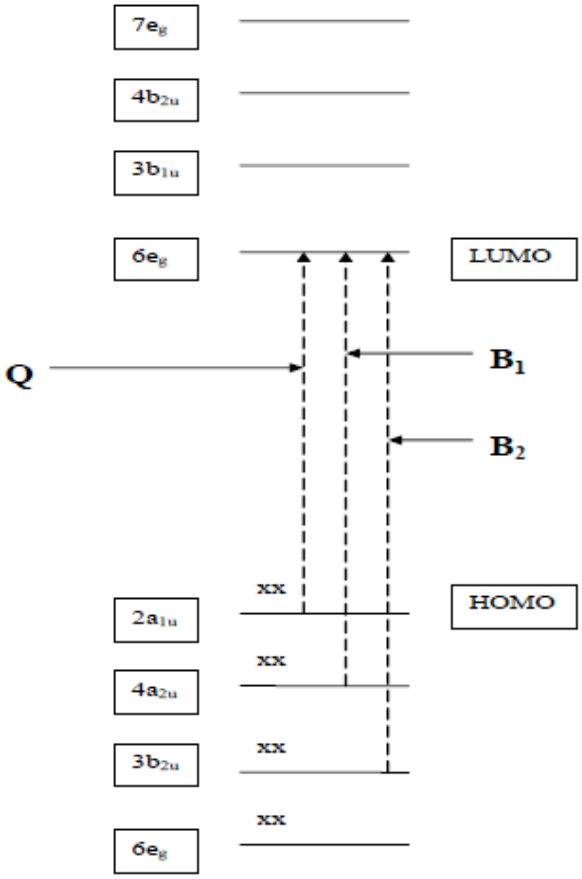


**Figure 1.8** Pc electronic transitions showing origin of the Q and B absorption bands.

The Q band is a transition from the highest occupied molecular orbital (HOMO), $a_{1}u$, to the lowest unoccupied molecular orbital, $e_g$, and appears in the far end of the visible region at around 650-750 nm. There is also the B band which is observed at the blue end of the spectrum, and consists of an overlap of $B_1$ and $B_2$ bands. $B_1$ is due to a transition from the $a_{2u}$ to the $e_g$ and $B_2$ is due to a transition from the lower lying $b_{2u}$ to the $e_g$ orbital. The $B_1$ and $B_2$ bands are usually observed as a single broad band around the 340 nm region [67]. The spectral position and intensity of the Q are affected by several factors such as central metal, symmetry, substituent, aggregation, and solvents [68,69].

The nature of the central metal has been observed to influence the position of the Q band, with a bath chromic shift being observed with an increase in the size of the central metal [68]. The oxidation state of the central metal also influences the Q band position, with a bath chromic shift being observed with increase in the oxidation state of the metal [69].

Normally an unmetallated MPc has a Q band that is split; this is due to the fact that the $e_g$ orbital of the LUMO is non-degenerate. It has been found that as the position of the Q band of the unmetallated Pc moves more to the infrared region; it becomes observed as single band. This is due to the fact that there is generation of degeneracy as the Q band shifts to the red region [70].

There can be metal to ligand charge transfer (MLCT) or a ligand to metal charge transfer (LMCT) bands [71], **(Fig. 1.9)**. These weak bands are normally observed in the visible region between the Q band and B band or after the Q band in the near infra red or infra red region. Charge transfer bands are observed for phthalocyanines with electro active metal centers.

This has been accounted by the fact that the d-orbitals of the electro active metal [72] are found within the HOMO and LUMO of the phthalocyanine. The observed CT bands are due to the movement of electrons between the d-orbitals of the metal centre and the HOMO/LUMO state of the phthalocyanine.

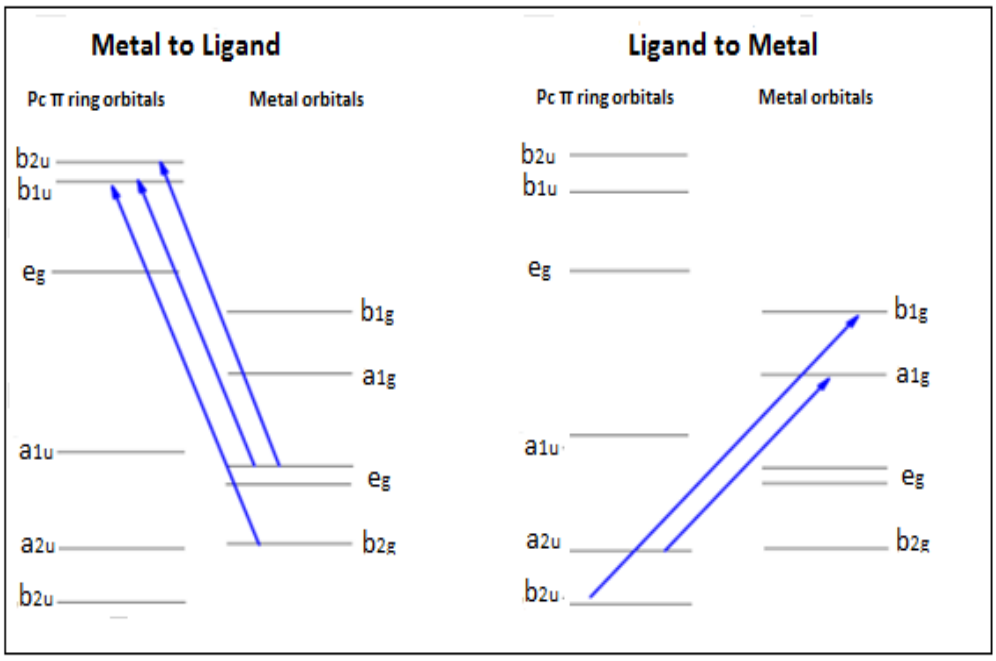


**Figure 1.9** Probable directions for charge transfer transitions between central metal and ligand.

### 1.6. Electrochemistry of Phthalocyanines

The electrochemistry of metallophthalocyanine species is vast with several redox processes involved [73,74]. Diverse electrochemical properties may be achieved by incorporating different metals into the core of the Pc ring and by varying the periphery substituents [73]. Redox processes occurring in MPc complexes may hence occur at the Pc ring or at the central metal and are influenced by: the nature of the substituents on the Pc ring; the nature and oxidation state of the central metal; the nature of any axial ligands and solvents [75].

The neutral form of Pc exists as a dianion, and may be represented as $Pc^{2-}$[76]. If metal orbitals lie at energies within the highest occupied molecular orbital-lowest unoccupied molecular orbital gap of the ring, oxidation or reduction, or both, may occur at the central metal [77,78]. Hence metals most commonly used in phthalocyanine electrochemistry are $Co^{II}$, $Fe^{II}$, and $Mn^{II}$. Typical oxidation and reduction processes of metal phthalocyanines may then be depicted as shown below where M represents the metal, Pc the phthalocyanine ring and $e^-$ an electron:

-Oxidation: $M^{2+}Pc^{2-} \rightarrow M^{3+}Pc^{2-} + e^-$

-Reduction: $M^{2+}Pc^{-2} + e^- \rightarrow M^{+2}Pc^{3-}$

Reduction of the Pc ring may occur by the successive gain of one to four electrons by the

LUMO of the MPc complex, resulting in the formation of $MPc^{3-}$, $MPc^{4-}$, $MPc^{5-}$ and $MPc^{6-}$ species **(Fig. 1.10)** [78].

Alterations in the oxidation state often result in reversible redox reactions and colour changes due to the ring based redox processes in MPc complexes [78]. A shift in the Q band wavelength is due to the oxidation or reduction of the central metal in MPcs [79]. The collapse of the Q band with the formation of new/weak bands pertains to a redox reaction on the Pc ring [80].

One may use cyclic voltammetric and spectroelectrochemical techniques in tandem to prove electron processes occurring during redox reactions. Other electrospectroscopic methods include electrochemically modulated infrared reflectance spectroscopy and

UV- vis electrochemically modulated reflectance spectroscopy.

The reactions of metal-free phthalocyanines and metal phthalocyaninates (peripherally octasusbstituted with various alkylthio-groups) with silver or palladium salts were investigated using spectroelechemistry in order to study their aggregation or disaggregation effects [81]. Peripherally substituted octabutylthiophthalocyanine complexes containing $Zn^{2+}$ and $Fe^{2+}$ have been synthesized and their electrochemical and spectral properties have been investigated [82]. There have been a small number of patents and publications describing the use of these compounds as IR absorbers, [83,84] mainly due to the shift of their high intensity Q bands to longer wavelengths. This work presents electrochemical and spectral attributes of novel thiol substituted phthalocyanines.

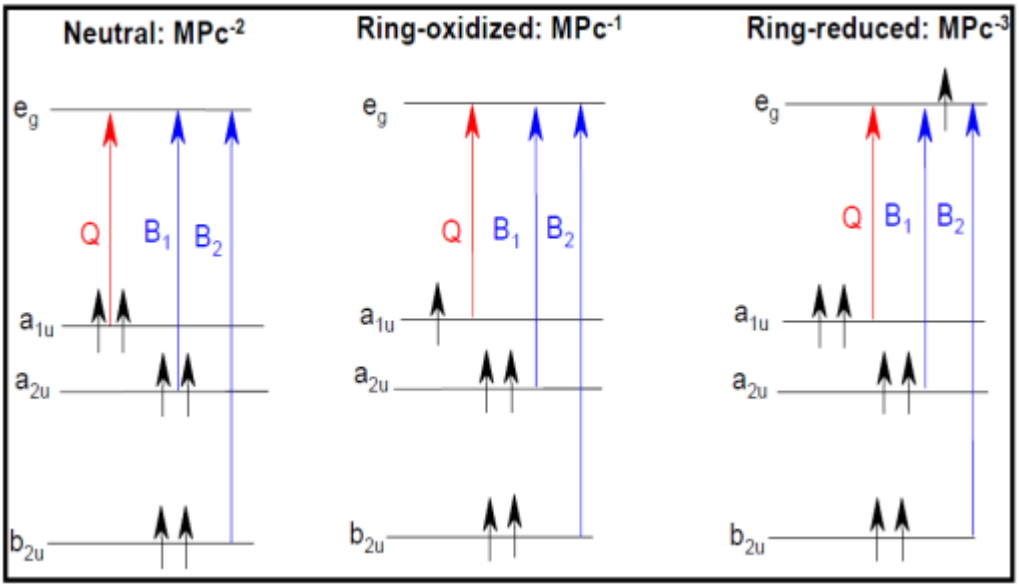


**Figure 1.10** Energy level diagrams of neutral, one-electron ring reduced, and one-electron ring oxidized MPc complexes.

### 1.7. Electroanalytical Techniques

The assessment of an analyte for possible technological applications, series of experiments are performed. Electrochemical and spectroelectrochemical characteristics of the material are measured and the data obtained is investigated. There are a wide variety of techniques employed for analysis, and within each major analytical technique there are many applications and variations.

### 1.7.1 Voltammetry

Voltammetry can be defined as an electrolysis process limited by the mass transport rate at which molecules move from the bulk of the solution to the electrode.

Voltammetry is a quick analytical tool, that is, simultaneous determination of several analytes by a single scan is often possible with a voltammetric procedure. The foremost advantage is sensitivity. Voltammetry ranks among the most sensitive analytical techniques available; it is routinely used for the determination of electro active substances in the sub-parts per million ranges. Of the other advantage is the capability to distinguish between oxidation states that may affect a substance's reactivity and toxicology.

The target of voltammetric studies is to provide a current response for analytes. In voltammetric technique, current is measured as an applied potential is changed over time. The current response of the analyte is measured as the electron transfer occurs throughout the redox process. For a general redox reaction;

$Ox + ne^- \rightarrow Red$

Cell potential equation known as Nernst equation can be written as

$$E = E^0 + \frac{0.059}{n} \log \left(\frac{C_{ox}}{C_{red}}\right)$$

where Here $C_{ox}$ and $C_{red}$ are the concentrations of oxidized and reduced form at the electrode surface and $E^0$ the standard electrode potential for redox reaction. The limiting current, using a dropping mercury electrode in voltammetry, can be quantified by Ilkovic equation;

$$i_d = 708.n.D^{1/2}.m^{2/3}t^{1/6}C$$

where $i_d$ is the limiting current (μA), $m$ is the mass flow rate of Hg through the capillary (mg/sec), t is the drop lifetime in seconds and $C$ is analyte concentration in mol/cm$^3$ , $n$ is number of electrons involved in overall electrode reaction and $D$ is diffusion coefficient (cm$^2$/s).

The voltammetric measurements are carried out in a three-electrode electrochemical cell **(Fig 1.11)**. Some electrochemical measurements are run in cells under an atmosphere of air. Oxygen however is electrochemically active and its solubility in water is sufficiently high that oxygen reduction interference can be a problem. As a consequence, most measurements are carried out under an inert atmosphere of either nitrogen or argon.

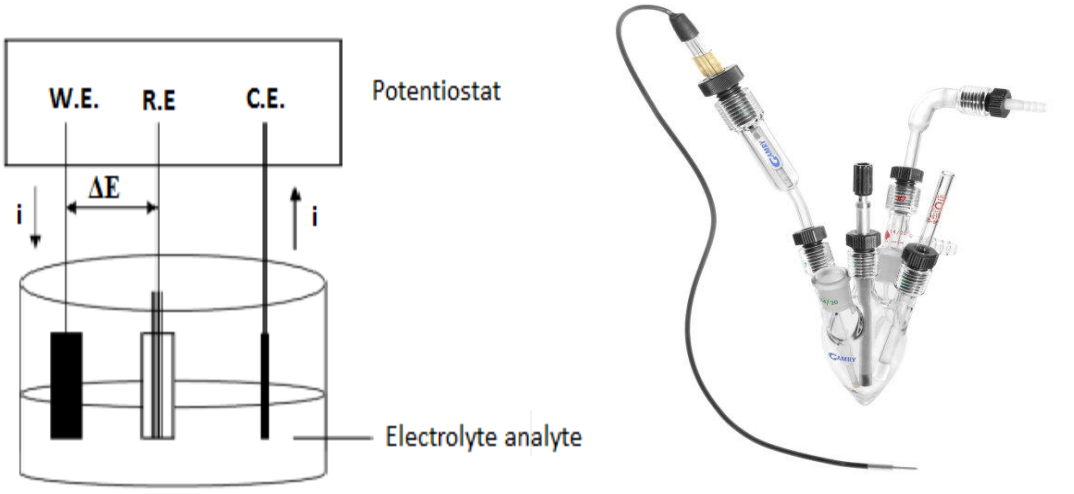


**Figure 1.11** A typical three-electrode electrochemical cell.

The electrochemical reaction takes place at the working W.E. This is the electrode at which the electrochemical phenomena being investigated takes place. The working electrode should provide high signal-to-noise characteristics, including a reproducible response [85]. Hence working electrode selection depends on essentially two factors: the redox behavior of the target analyte and the background current over the potential region required for the measurement. The reference electrode R.E. whose potential is constant enough that it can be taken as the reference standard against which the potentials of the other electrodes present in the cell can be measured [86]. Reference electrodes with large surface areas are often employed in order to maintain low current densities and hence minimize polarization. The complete elimination of reference electrode polarization is only possible with modern potentiostatic instrumentation based on operational amplifiers. The potentiostat maintains a potential difference, ΔE, between the R.E. and W.E., and supplies the current (i) needed for affecting the changes occurring at the W.E. [86,87]. An ideal R.E. is one whose potential does not shift from equilibrium (non-polarisable).

The counter (or auxiliary) electrode C.E. completes the electrochemical circuit. This is the electrode which serves as a source or sinks for electrons so that current can be passed from the external circuit through the cell. In general, neither its true potential nor current is ever measured or known [85].

The choice of an electrode material depends greatly on the useful potential range of the electrode in the particular solvent used and the qualities and purity of the material. One or more of the following limits the usable potential range [88].

- Solvent decomposition.
- Decomposition of the supporting electrolyte.
- Electrode dissolution or formation of a layer of an insulating/semiconducting substance on its surface.
- Poisoning through contact with solutions containing contaminants.

There are several reference electrodes used in electroanalytical experiments, (Ag | AgCl) being the most common. This consists of a piece of silver wire anodized with silver chloride in a glass tube. The wire is in contact with concentrated KCl or NaCl solution [89]. A semi-permeable salt bridge protects the electrode from the bulk solution. Many materials have been used as working electrodes. Mercury, carbon and "inert" (or noble) metals such as gold and platinum have been found to be essential working electrode materials. The geometry of these electrodes must also be considered. An inert conducting material, such as platinum wire or graphite rod, is usually used as the current carrying auxiliary electrode.

Supporting electrolytes are usually used in conjunction with solvents for electrochemical experiments. The choice of the solvent is based upon the solubility of the analyte including its redox activity and the solvent properties (e.g. electrical conductivity, electrochemical activity and chemical reactivity). The solvent should not react with the analyte (or

products) and should not undergo electrochemical reactions over a large potential range [86]. Solvent types include water, acetonitrile, dichloromethane, dimethylformamide (DMF), dimethylsulfoxide (DMSO) or methanol. Certain applications may require mixed solvents. Supporting electrolytes are necessary in order to decrease the resistance of the solution; eliminate electromigration effects; maintain constant ionic strength (by eliminating the effects of erratic amounts of naturally occurring electrolyte). The inert supporting electrolyte may be an inorganic salt, a mineral acid or a buffer. While potassium chloride or nitrate and sodium hydroxide are usually used when employing water as a solvent, tetraalkylammonium salts are often utilized in organic media.

#### 1.7.1.1. Cyclic voltammetry

Cyclic voltammetry in which the direction of the potential is reversed at the end of the first scan is a more commonly used technique **(Fig 1.12)**. This has the advantage that the product of the electron transfer reaction that occurred in the forward scan can be probed again in the reverse scan. In addition, it is a powerful tool for the determination formal redox potentials, detection of chemical reactions that precede or follow the electrochemical reaction and evaluation of electron transfer kinetics.

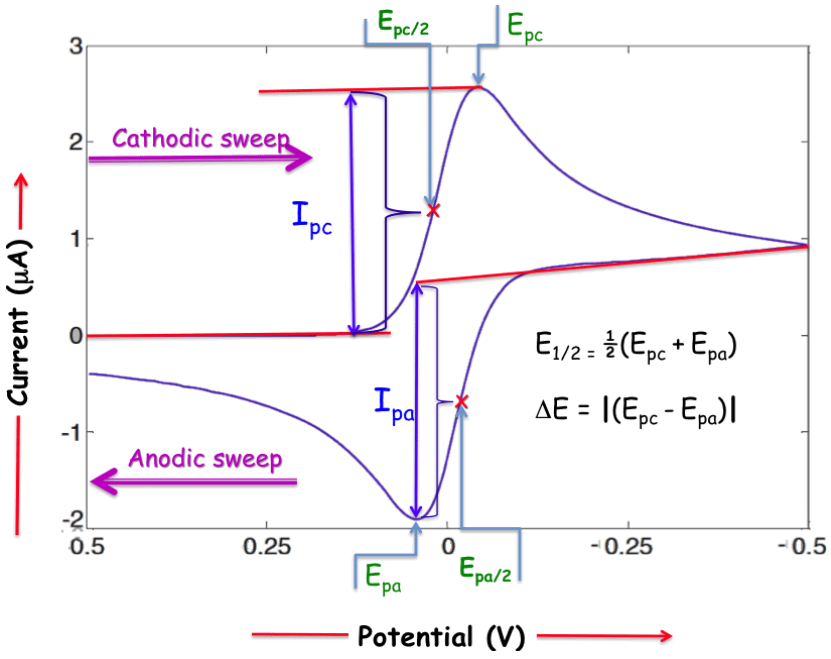


**Figure 1.12** A typical cyclic voltammogram for a reversible system.

CV is often the first experiment performed in an electro analytical study. In particular, it offers a rapid location of redox potentials of the electro active species, and convenient evaluation of the effect of media on the redox process.

Cyclic voltammetry involves the reduction and oxidation of the species. Oxidation occurs on application of a positive going potential, an increase in the peak current with an increase in the potential is observed until the potential where the analyte is oxidized is reached. Thereafter a decrease in current occurs. The reduction of the species occurs with application of a negative going potential. The movement of the species to the electrode can be facilitated by migration, convection and diffusion. Diffusion is the movement of analyte due to concentration gradient. The latter is the one that is of interest when dealing with electro analytical reactions. When working with voltammetry, specifically cyclic voltammetry, a system can be characterized as a reversible, quasi-reversible and irreversible. This is dependent on the ease of the redox reaction of the species and whether both the oxidized and reduced species are redox active. A reversible system shows the redox reaction of the species in the forward scan followed by the redox reaction upon application of a reverse scan. An irreversible system is observed by the occurrence of a forward peak with a peak in the reverse direction being very weak or not observed at all due to failure to regenerate the starting electro active species. A shift in the potential with change in scan rates is observed for an irreversible system because of the slow electron transfer.

The problem with cyclic voltammetry is that it has high background currents due to the charging current, this limits sensitivity. Hence another voltammetric method such as square wave voltammetry has to be used concurrently with cyclic voltammetry to increase the sensitivity.

Conclusions can also be drawn from the cyclic voltammograms regarding the rate of charge transfer, charge transport processes, and the interactions that occur within the polymer segments, at specific sites and between the polymer and the ions and solvent molecules. For very thin films and/or at low scan rates, when the charge transfer at the interfaces and charge transport processes within the film are fast, i.e., electrochemically reversible (equilibrium) behavior prevails, and if no specific interactions (attractive or

repulsive) occur between the redox species in the polymer film.

The electrochemical reaction is said to be reversible if a redox system remains in equilibrium throughout the potential scan that requires both the concentrations of oxidized and reduced forms to be at values supplied by Nernst equation.In an ideal cyclic voltammogram, the peak potential separation ($E_{pa}$ - $E_{pc}$) and the peak width are equal to 59/n mV and 28.5/n mV respectively for all scan rates, where n is the number of electron transferred in the process. The peak current ratio ($i_{pa}/i_{pc}$) is expected to be 1 as well.

In an irreversible reaction, the electrode reaction cannot be reversed. Slow electron exchange or chemical reactions at the electrode surface may result in irreversibility. A high kinetic barrier has to be overcome, achieved by the application of an extra potential (extra energy) called the overpotential (η). Cyclic voltammograms showing a single oxidation or reduction wave signify an irreversible system. A large peak current separation (> 200 mV) also indicates irreversibility.

Quasi-reversible reactions exhibit behaviors intermediate between reversible and irreversible reactions, the overpotential having a relatively small value, so that with this extra potential reactions can be reversed [88]. This phenomenon is observed when the return peak is smaller than its couple and/or a larger peak potential separation is observed in comparison to reversible systems. A peak separation of 80 to 200 mV is characteristic of a quasi-reversible system.

#### 1.7.1.2. Square Wave Voltammetry

It is a useful method for studying redox reactions with overlapping waves. In SWV a square wave potential superimposed to a staircase potential is applied to the working electrode **(Fig 1.13)**.

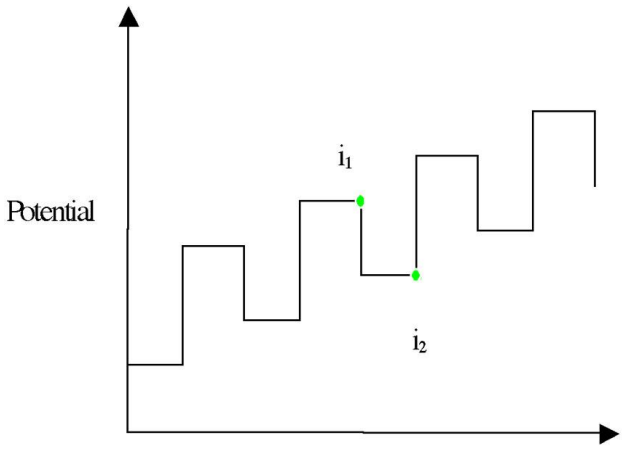


**Figure 1.13** Diagrammatic representation of a Square Wave curve.

For reversible processes the peaks are Gaussian shaped and the peak potentials ($E_p$) are equal to the half potentials ($E_{1/2}$) of the redox processes. An estimate of the number of electrons (n) involved in the redox process under each peak can be obtained from the peak height (i.e. the peak current), which is approximately proportional to n. A more exact evaluation of the number of electrons involved can be calculated from the half peak widths ($W_{1/2}$) which depend on factors such as temperature and the number of electrons involved. **(Fig 1.14)**. The ability to analyze both the forward and reverse currents as well as the net current in Square Wave Voltammetry proves useful as information about reaction reversibility can be obtained easily. Square wave voltammetry (SWV) is a sensitive electro analytical technique used to investigate redox reactions that may otherwise be impossible with CV [90].

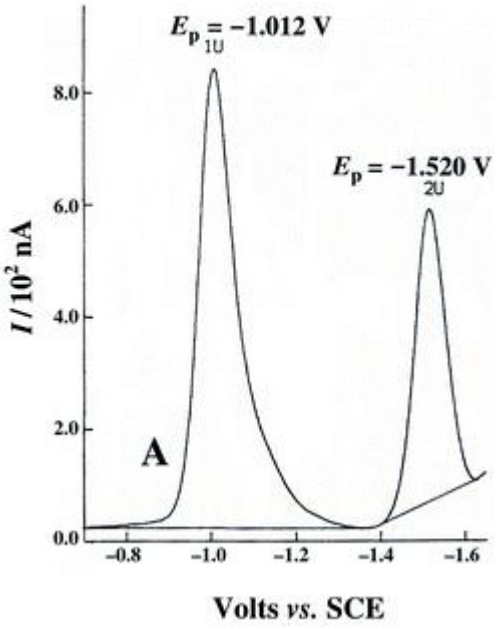


**Figure 1.14** Typical Square Wave voltammogram.

SWV eliminates the charging current caused by the electrode double layer, thus an increased signal-to-noise ratio results. Therefore shortcomings observed with CV, e.g. overlapping or closely spaced peaks with poor resolution are overcome by SWV. Optimal peak separation, greater analysis speed, lower electro active species consumption and lower detection limits of up to $10^{-8}$ M, are advantages obtained with this technique.

### 1.7.1.3. Pulse voltammetry

It was initially developed for the dropping mercury electrode, the objective being to synchronize the pulses with drop growth and reduce the capacitive current contribution by current sampling at the end of drop life. After applying a pulse of potential, the capacitive current dies away faster than the faradaic current; thus the current is measured at the end of the pulse [91].

**Normal Pulse Voltammetry (NPV)** uses a series of potential pulses of increasing amplitude. The current measurement is made near the end of each pulse, which allows time for the charging current to decay. It is usually car- ride out in an unstirred solution at

either DME (called normal pulse polarography) or solid electrodes. The potential is pulsed from an initial potential Ei. The duration of the pulse, t, is usually 1 to 100 msec and the interval between pulses typically 0.1 to 5 sec. The resulting voltammogram displays the sampled current on the vertical axis and the potential to which the pulse is stepped on the horizontal axis (**Fig 1.15)** [92].

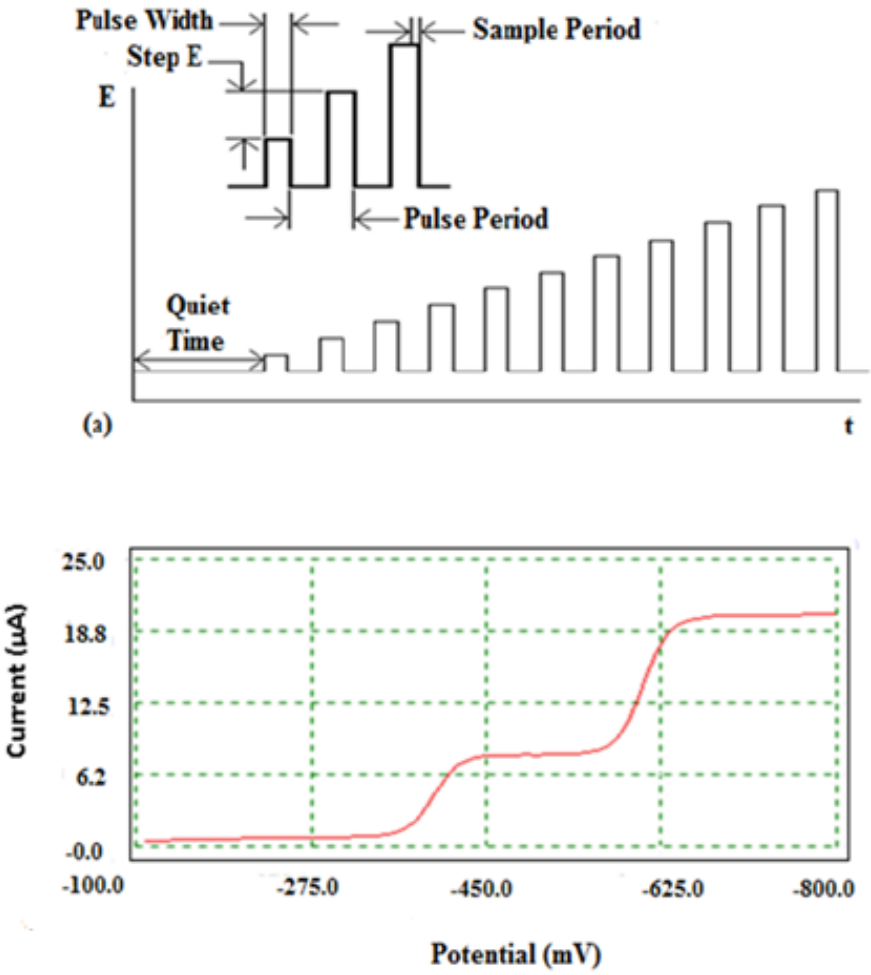


**Figure 1.15** Normal pulse voltammetry. (a) operation and (b) response.

### 1.7.2. Spectroelectrochemistry

Spectroelectrochemistry combine the use of electrochemistry and spectroscopy. The technique involves passing light beam through electrochemical cell, called an OTTLE (Optically Transparent Thin Layer Electrode) cell **(Fig. 1.16)**.

Spectroscopic measurements can be carried out concurrently with electrochemical control, by either transmission or reflection, and the measurements can be *in situ* or *ex situ*.

Spectroelectrochemistry allows the simultaneous acquisition of electrochemical and spectroscopic data, and the current and spectral absorbance bands are concurrently monitored.

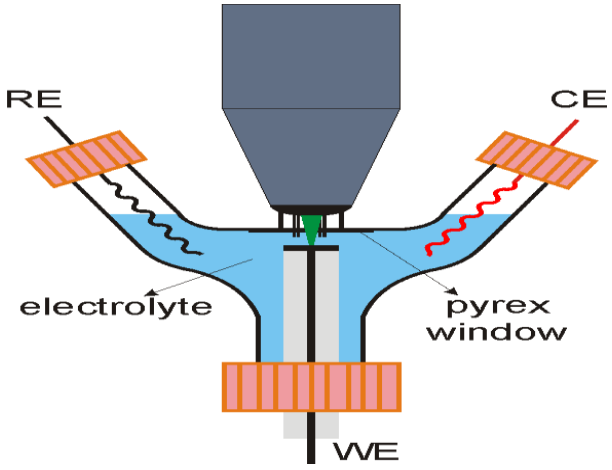


**Figure 1.16** Typical Spectroelectrochemical Cell.

The characterization of the products of oxidation or reduction of redox complexes can be made. The use of spectroelectrochemistry in MPc studies is based on the well known fact that the spectra of ring-based processes drastically affects the Q band while the metal-based redox processes result only in the shift in the Q band without much change in intensity.

Spectroelectrochemistry may consequently be used to: monitor electron transfer reactions; investigate the stability of the oxidation or reduction products; determine the reversibility of an electrochemical reaction. Information gathered from spectroelectrochemistry can be

applied to Faraday's Law

$Q = nFVC_o$

where Q is the charge read from the spectroelectrochemical instrument; F is Faraday's constant, V is the volume (usually 0.5 ml), and the initial concentration, $C_0$, is attained from Beer's Law ($A = \varepsilon col$). Hence one may find n, the number of electrons occurring in the electrochemical process.

The main problem encountered in *in situ* spectroelectrochemical experiments is that light must be able to pass through the electro analysis cell, so everything (cell walls, solution, and electrode) must be highly transparent.

To construct a cell from quartz or silica is simple, and to work with transparent solutions is generally problem-free, but transparent electrodes are a greater challenge. Nevertheless, the use of a wire mini-grid optically transparent electrode (OTE) overcomes this challenge. Modern methods commonly use a relatively cheap, thin (~0.3 μm) film of a semiconductor: either tin oxide doped with fluoride ($SnO_2$:F) or indium doped with tin oxide otherwise known as indium-tin oxide (ITO). This is a method that makes use of spectroscopy with electrochemistry. The simplest spectroelectrochemical method is the one that makes use of UV/Visible spectroscopy. There is passage of charge while a change in the species is monitored by the change in absorption. There are two modes that can be utilized when using UV/visible spectroscopy. There is use of optically transparent electrodes (OTEs); these can be made of thin film semiconductors such as tin oxide and indium oxide or a fine wire mesh that is made of metals such as platinum, gold. There is also the use of an optically transparent thin layer electrode (OTTLE), which is an enclosed chamber with the electrodes within the chamber together with the solution. Spectroscopic changes can be observed within a shorter time-frame, in seconds when making use of the OTTLE cell because of the low volumes used, 30-50 μl. Spectroelectrochemical experiments can be used to probe various adsorption-desorption processes. In particular, changes in the absorbance accrue from such processes can be probed utilizing the large ratio of surface area to solution volume of OTEs with long optical path length. In addition

to transmission experiments, it is possible to use more sensitive reflectance protocols. In particular, in internal reflectance, spectroscopy (IRS) the light beam is introduced to the electrode at an angle, and the spectrum is recorded from the reflected beam at the solid/solution interface. Prisms are used to allow the radiation enter and leave. In addition to its higher sensitivity, IRS is less prone to solution resistance effects.

### 1.8. Electrode Modification

Phthalocyanines are generally coated on as a quite thin film on electrode surfaces, in order to use the electrode with the chemical, electrochemical, optical, electrical, transport, and other desirable properties of the film in a rational, chemically designed manner and such process is referred to as electrode modification or chemically modified electrode (CME). For proper use selected methods are employed in coating electrodes with desired material.

#### 1.8.1. Dip-Coating

Dip-coating is an ideal method to prepare thin layers from chemical solutions since it is a low-cost and waste-free process that is easy to scale up and offers a good control on thickness.

This procedure involves immersing the electrode material in a solution of the polymer for a period sufficient for spontaneous film formation to occur by adsorption. The film quantity in this procedure may be augmented by withdrawing the electrode from the solution and allowing the film of polymer solution to dry on the electrode.

#### 1.8.2. Spin coating

In the spin coating process, solution is first deposited on the substrate, and the substrate is then accelerated rapidly to the desired rotation rate. Liquid flows radially, owing to the action of centrifugal force, and the excess is ejected off the edge of the substrate. The film continues to thin slowly until disjoining pressure effects cause the film to reach an equilibrium thickness or until it turns solid-like due to a dramatic rise in viscosity from solvent evaporation. The final thinning of the film is then due solely to solvent evaporation.

### 1.8.3. Langmuir-Bloddget Films

The Langmuir-Blodgett (LB) technique is one of the most promising methods for the preparation of thin films as it enables; precise control of the monolayer thickness, homogeneous deposition of the monolayer over large areas and the possibility to make multilayer structures with varying layer composition. An additional advantage of the LB technique is that monolayers can be deposited on almost any kind of solid substrate.

There exists a wide range of surfactants with an amphiphilic nature which drastically lower the surface tension of water. Many of these amphiphilic substances insoluble in water can, with the help of a volatile and water insoluble solvent, be easily spread on a water surface to form an insoluble monolayer at the air/water interface. These monolayers, also called Langmuir (L) films, represent the extreme case when considering adsorption to interfaces because all molecules are concentrated in a one molecule thick layer at the interface. The amphiphilic nature of the surfactants dictates the orientation of the molecules at the interface (air/water or oil/water) in such a way that the polar head group is immersed in the water and that the long hydrocarbon chain is pointing towards air, gas or oil.

The hydrocarbon chain of the substance used for monolayer studies has to be long enough in order to be able to form an insoluble monolayer. A rule of thumb is that there should be more than 12 hydrocarbons or groups in the chain ($(CH_2)n$, $n > 12$). If the chain is shorter, though still insoluble in water, the amphiphile on the water surface tend to form micelles.

These micelles are water soluble, which prevents the build-up of a monolayer at the interface. On the other hand if the length of the chain is too long the amphiphile tends to crystallize on the water surface and consequently does not form a monolayer. It is difficult to determine the optimal length for the hydrocarbon chain because its film forming ability also depends on the polar part of the amphiphile.

Furthermore, the amphiphile has to be soluble in some organic solvent which is highly volatile and water insoluble (to transport the surfactant to the surface, chloroform or hexane is commonly used). Langmuir-Blodgett films are built up by a process of successive deposition of individual Langmuir monolayers onto a solid substrate.

The monolayer is formed by spreading the organic molecules on the water subphase. The molecules usually have hydrophilic (head) and hydrophobic (tail) parts, so when the film is formed the molecules stand on their heads. When the molecules first are spread on the water they are very loosely packed and form a so called gas phase. This means that the area on the water available for each molecule is rather large and the surface pressure is low. The surface pressure is usually measured using a Wilhelmy plate and a precision scale. The surface pressure can be increased by means of one or two sliding barriers. At a certain point the surface pressure starts to rise more rapidly indicating a transition to the liquid phase. As the barrier is moved even further the onset of the solid phase can be noted by an even steeper rise in the surface pressure **(Fig. 1.17)**.

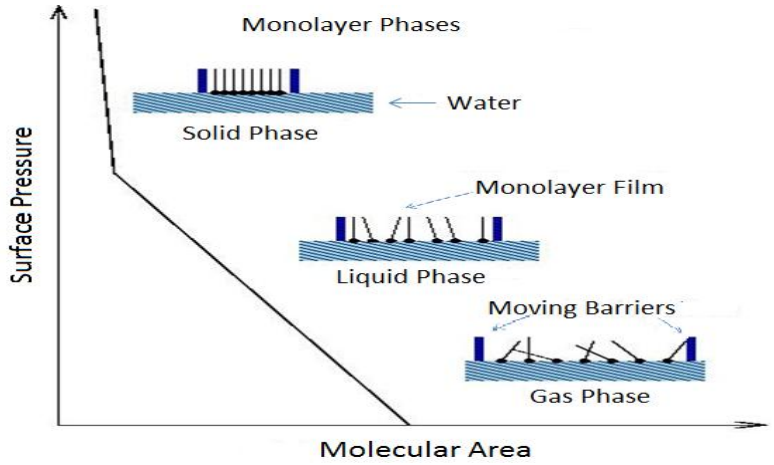


**Figure 1.17** Surface pressure - area isotherm.

One or more monolayers can be transfered to a substrate by dipping the substrate through the monolayer. The monolayer is kept uniform by controlling the surface pressure with the barriers throughout the process **(Fig. 1.18)**.

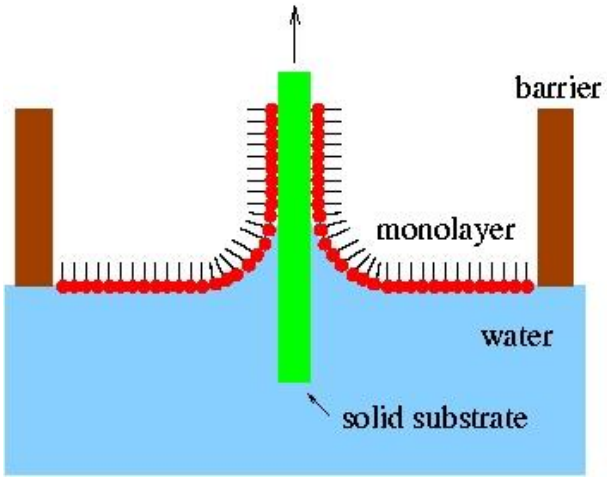


**Figure 1.18** Deposition of a monolayer on a solid substrate.

### 1.8.4. Electrochemical Polymerization

Electroactive multimolecular layer films of polymers are popular today because they are technically easier to apply to electrodes than are covalently bonded monolayers. They also contain multimolecular layers of electroactive sites, so that their electrochemistry can be more easily observed. Electroactive films can be used as electrocatlysts, as preconcentration media or as transport barrier, where the perfonnance of monolayer films are not reliable. A solution of monomer is oxidized or reduced to an activated form that polymerizes to form a polymer film directly on the electrode surface. This procedure results in few pinholes since polymerization would be accentuated at exposed (pinhole) sites at the electrode surface. Unless the polymer film itself is redox active, electrode passivation occurs and further film growth is prevented.

The electropolymerization of phthalocyanine complexes or ligands can be performed by continuously cycling the potential of a glassy carbon electrode between certain ranges or at constant rate.

The increase in polymerization current with the number of scan cycles indicates that the reaction of electrochemical polymerization an autocatalytic reaction. After certain point, the profile does not show signs of polymeric growth and the stability of the response indicate that the film obtained is conductive; otherwise, a diminution in the charge should be observed.

Sometimes voltammograms do not show growing signals electropolymerization changes the voltammetric profile of the modified electrode, but this change does not follow a common pattern. The different morphologies and chemical structures obtained when the complexes are electropolymerized are supported by the different voltammetric profiles of the monomer or polymer ligand.

On repeated potential cycling it is seen that the anodic peak current increases in magnitude. When the anodic peak does not exceed at a level, polymerization stops.

## 2. MATERIALS AND METHODS

This section explains the materials used and the procedure followed. Electrochemical and in situ spectroelectrochemical measurements of the complexes were investigated in solution and on modified electrodes to assess possible applications of the complexes in electrochemical technologies.

### 2.1. Materials

Ultra pure dimethylsulfoxides (DMSO), dichloromethane (DCM), Acetonitrile (AN) as solvent were consumed. Tetrabutylammonium perchlorate (TBAP), tetrabutylammonium borate (TBAB), tetrabutylammonium floride (TBAF), tetrabutylammonium chloride (TBAC), $LiClO_4$ and other reagents were purchased from Aldrich and used without further purification. A platinum disk electrode, glassy carbon electrode (GCE), and an indium tin oxide (ITO) electrode were employed as supporting electrolyte.Three sets of MPc complexes; bis(trifluoromethyl)phenylethynyl substituted complexes ($In^{III}ClPc$, $Mn^{III}ClPc$, and $Ti^{IV}OPc$), tetrakis 3-(4-methylphenyl)-5-phenyl-4H-1,2,4-triazol-4-yl]imino}methyl)phenoxy] substituted metal phthalocyanines **(**NiPc, ZnPc, CoPc, and TiOPc) and finally, octakis diethylamino-phenoxy substituted phthalocyanines ($H_2$Pc-odea, $Co^{2+}$ (CoPc-odea) and $Cu^{2+}$ (CuPc-odea) were the subjects of this study.

### 2.2. Electrochemical Measurements

The cyclic voltammetry (CV) and square wave voltammetry (SWV) measurements were carried out with Gamry Reference 600 potentiostat/galvanostat utilizing a three-electrode configuration at 25 ˚C. The working electrode was a Pt disc with a surface area of 0.071 $cm^2$. A Pt wire served as the counter electrode. Saturated calomel electrode (SCE) was employed as the reference electrode and separated from the bulk of the solution by a double bridge. Electrochemical grade TBAP in extra pure dichloromethane (DCM) and dimethylsulfoxide (DMSO), acetonitrile (AN) were employed as the supporting electrolyte at a concentration of 0.10 mol $dm^{-3}$. Ferrocene was used as universal indicator and $\Delta E_p$'s of ferrocene were changed from 60 to 110 mV with increasing scan rates from 0.010 to 1.00 $Vs^{-1}$ in our system.

High purity $N_2$ was bubled to remove dissolved $O_2$ at least 15 minute prior to each run and to maintain a nitrogen blanket during the measurements.

### 2.3. In-situ Spectroelectrochemical Measurements

UV-Vis absorption spectra and chromaticity diagrams were measured with OceanOptics QE65000 diode array spectrophotometer. In-situ spectroelectrochemical measurements were carried out by utilizing a three-electrode configuration of thin-layer quartz thin-layer spectroelectrochemical cell at 25˚C. The working electrode was a Pt tulle. A Pt wire counter electrode separated by a glass bridge and a SCE reference electrode separated from the bulk of the solution by a double bridge were used. In-situ electrocolorimetric measurements, under potentiostatic control, were obtained using Ocean Optics QE65000 diode array spectrophotometer at color measurement mode by utilizing a three-electrode configuration of thin-layer quartz spectroelectrochemical cell. The standard illuminant A with 2 degree observer at constant temperature in a light booth designed to exclude external light was used. Prior to each set of measurements, background color coordinates (x, y, and z values) were taken at open-circuit, using the electrolyte solution without the complexes under study. During the measurements, readings were taken as a function of time under kinetic control, however only the color coordinates at the beginning and final of each redox processes were reported.

Oxygen interaction experiments were followed in three cases;
*Case* 1: SWV responses of MPcs free electrolyte system bubbled gradually with molecular oxygen.
*Case* 2: SWV responses of MPcs in the electrolyte system purged with nitrogen.
*Case* 3: SWV responses of MPcs in the electrolyte system bubbled gradually with oxygen.

### 2.4 Langmuir-Blodgett Monolayer Coating

MPcs were coated on ITO electrode with Langmuir-Blodgett technique using KSV NIMA Langmuir-Blodgett monolayer coating device. $CdCl_2.H_2O$ solution was prepared with ultrapure water at a concentration of 1 mg/1ml that is used as a sub-phase in the trough of the device. In order to form well defined monolayer and controllable homogenous coating on ITO substrates, stearic acid (SA) solution was prepared (1mg/ml) with chloroform

solvent and mixed with MPCs solution (1:1 by volume). Then 1mg/1ml chloroform solutions of MPcs and SA mixtures were spread on the sub-phase solution drop by drop until the surface pressure rose up tob0.5 mN/m. Surface pressure ($\pi$)-area isotherm was recorded and the ideal surface pressure was detected as 35 mN/m for the formation of monolayers on the sub-phase. Finally MPc monolayers were transferred on the ITO substrates with 5 mm $s^{-1}$ "up stroke" and "down stroke" rate.

### 2.5. Electropolymerization

For the electropolymerization measurements, CV technique was employed with ITO working electrode. A Pt wire, and saturated calomel electrode (SCE) separated from the bulk of the solution by a double bridge were used as counter and reference electrodes respectively. Electrochemical TBAP in ultra-pure dichloromethane (DCM) was the supporting electrolyte at a concentration of 0.10 mol $dm^{-3}$. Repeating CV measurements between the potential windows of TBAP/DCM electrolyte system were employed to follow the formation of electropolymerized and/or electrodeposited film of MPcs on the working electrode. The ITO modified with the film was then removed from the electrolytic cell and rinsed with DCM and finally with water. The modified electrode is abbreviated as ITO/MPc. Similar CV parameters were used to prepare equivalent film thickness of the complexes.

# 3. RESULTS AND DISCUSSION

Electrochemical and in-situ spectroelectrochemical properties of three sets of MPcs with a total number of 10 complexes were investigated. Required meaurements of modified electrode were also performed to assess their possible technological usage.

It was noticed that the presence of molecular oxygen influenced the redox responses of some complexes which indicates possible usage of these substances as molecular oxygen sensor. Some others showed considerable spectal changes during electron tranfer, and by examining the response time and electrochromic properties, they were expected to be used in display technology. This part represents the investigation of the data obtained and the assesstment.

## 3.1. Tetrakis (3,5-bis(trifluoromethyl)phenylethynyl) Substituted Phthtalocyanines ($In^{III}ClPc$, $Mn^{III}ClPc$, and $Ti^{IV}OPc$)

The spectral, and electrochemical characterizations and the electrocatalytic and the electro sensing applications of $In^{III}ClPc$, $Mn^{III}ClPc$, and $Ti^{IV}OPc$ bearing (3,5-bis(trifluoromethyl)phenyl)ethynyl substituents were investigated here **(Fig. 3.1)**.

Since the metal centers of MPcs studied here have +3 and +4 oxidation states, each metal center has an axial ligand and forms $In^{III}Cl$, $Mn^{III}Cl$, and $Ti^{IV}O$. Binding ability of an axial ligand to the central metal ion of MPc donates it to behave as a possible functional material for the electrocatalytic reduction/oxidation and electrosensing applications. These type complexes bind the target species to the axial position of metal center and this interaction affects the electron transfer properties of MPcs and the target species. For this reason, $In^{III}ClPc$, $Mn^{III}ClPc$, and $Ti^{IV}OPc$ complexes were chosen for the usage as electrocatalyst and electrosensor for molecular oxygen. Indeed, the electrocatalytic reduction of $O_2$ is an important field of energy base researches as it is the main component in alternative fuel applications and lithium-ion cells. So the results of this study may open a way for the application of the complexes in these fields.

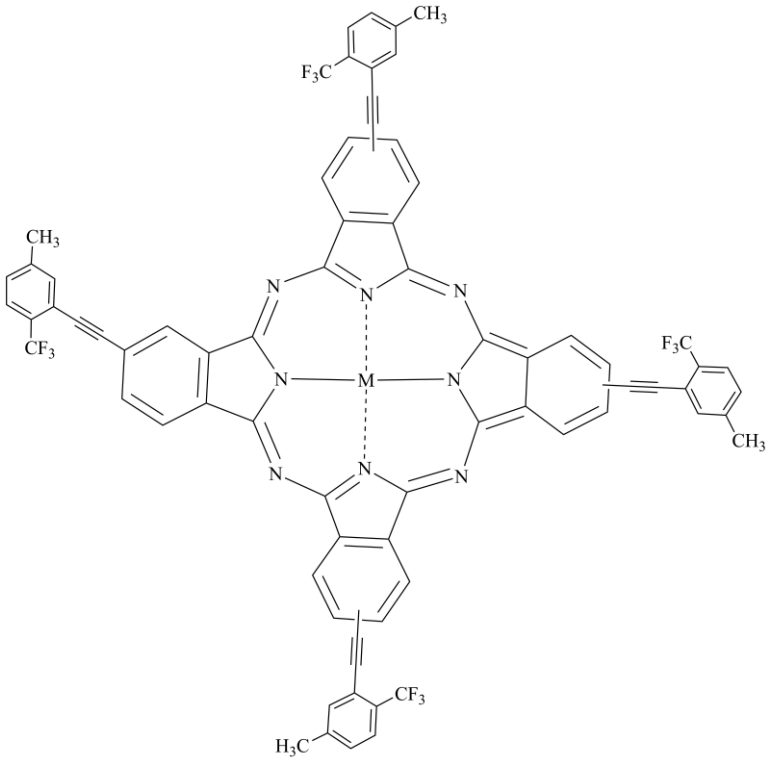


M: $TiO^{2+}$ (TiOPc), Cl-$Mn^{3+}$(MnClPc), Cl-$In^{3+}$(InClPc)

**Figure 3.1** The structure of 2,9,16,23-Tetrakis (3,5-bis(trifluoromethyl)phenyl)ethynyl phthalocyanines, $In^{III}$ClPc, $Mn^{III}$ClPc, and $Ti^{IV}$OPc.

### 3.1.1. Electrochemical Characterization of the Complexes in Solution

In order to understand the possible applications of a functional material in different electrochemical technologies, electrochemical behavior of this material must be determined in detail. For this purpose, voltammetric and in situ spectroelectrochemical analyses of $In^{III}$ClPc, $Mn^{III}$ClPc, and $Ti^{IV}$OPc were performed in different solutions and in solid states. Voltammetric analyses of the complexes were carried out in DCM/TBAP and DMSO/TBAP electrolyte systems on GCE working electrode with CV and SWV techniques. Voltammograms of the complexes were analyzed to derive fundamental electrochemical parameters including the half-wave peak potentials ($E_{1/2}$), ratio of anodic to cathodic peak currents ($I_{p,a}/I_{p,c}$), peak to peak potential separations ($\Delta E_p$), and the

difference between the first oxidation and reduction processes ($\Delta E_{1/2}$) **(Table 3.1)**. As shown in Table 1, only $In^{III}ClPc$ has a redox inactive metal center, thus, it gives only Pc based redox reactions as expected.

**Table 3.1** Voltammetric data of 2,9,16,23-Tetrakis (3,5- bis(trifluoromethyl)phenyl)ethynyl substituted MPc complexes vs. SCE.

| Complexes | Redox processes | [a] $E_{1/2}$ (V) | [b] $\Delta E_p$ (mV) | [c] $I_{p,a}/I_{p,c}$ | [d] $\Delta E_{1/2}$ |
|---|---|---|---|---|---|
| **$In^{III}ClPc$** (in DCM) | $[In^{III}ClPc^{2-}] / [In^{III}ClPc^{1-}]^{+1}$ | 1.00 | 95 | 0.93 | 1.58 |
| | $[In^{III}ClPc^{2-}] / [In^{III}ClPc^{3-}]^{-1}$ | -0.58 | 70 | 0.71 | |
| | $[In^{III}ClPc^{3-}]^{-1} / [In^{III}ClPc^{4-}]^{-2}$ | -0.87 | 95 | 0.75 | |
| | $[In^{III}ClPc^{4-}]^{-2} / [In^{III}ClPc^{5-}]^{-3}$ | -1.67 | - | - | |
| **$Ti^{IV}OPc$** (in DCM) | $[Ti^{IV}OPc^{1-}] / [Ti^{IV}OPc^{0}]^{+2}$ | 0.94 | 65 | 0.83 | 1.18 |
| | $[Ti^{IV}OPc^{2-}] / [Ti^{IV}OPc^{1-}]^{+1}$ | 0.60 | 61 | 0.94 | |
| | $[Ti^{IV}OPc^{2-}] / [Ti^{III}OPc^{2-}]^{-1}$ | -0.58 | 63 | 0.91 | |
| | $[Ti^{III}OPc^{2-}]^{-1} / [Ti^{III}OPc^{3-}]^{-2}$ | -0.98 | 75 | 0.85 | |
| | $[Ti^{III}OPc^{3-}]^{-2} / [Ti^{III}OPc^{4-}]^{-3}$ | -1.26 | - | - | |
| | $[Ti^{III}OPc^{4-}]^{-3} / [Ti^{II}OPc^{4-}]^{-4}$ | -1.53 | - | - | |
| **$Ti^{IV}OPc$** (in DMSO) | $[Ti^{IV}OPc^{1-}] / [Ti^{IV}OPc^{0}]^{+2}$ | 0.70 | 69 | 0.81 | 1.03 |
| | $[Ti^{IV}OPc^{2-}] / [Ti^{IV}OPc^{1-}]^{+1}$ | 0.43 | 64 | 0.96 | |
| | $[Ti^{IV}OPc^{2-}] / [Ti^{III}OPc^{2-}]^{-1}$ | -0.60 | 61 | 0.94 | |
| | $[Ti^{III}OPc^{2-}]^{-1} / [Ti^{III}OPc^{3-}]^{-2}$ | -1.00 | 70 | 0.95 | |
| | $[Ti^{III}OPc^{3-}]^{-2} / [Ti^{III}OPc^{4-}]^{-3}$ | -1.28 | 73 | 0.55 | |
| | $[Ti^{III}OPc^{4-}]^{-3} / [Ti^{II}OPc^{4-}]^{-4}$ | -1.55 | - | - | |
| **$Mn^{III}ClPc$** (in DCM) | $[Mn^{III}ClPc^{2-}] / [Mn^{III}ClPc^{1-}]^{+1}$ | 1.01 | 60 | 0.98 | 1.02 |
| | $[Mn^{III}ClPc^{2-}] / [Mn^{II}ClPc^{2-}]^{-1}$ | -0.010 | 80 | 0.96 | |
| | $[Mn^{II}ClPc^{2-}]^{-1} / [Mn^{I}ClPc^{2-}]^{-2}$ | -0.91 | 90 | 0.91 | |
| | $[Mn^{I}ClPc^{2-}]^{-2} / [Mn^{I}ClPc^{3-}]^{-3}$ | -1.49 | 190 | 0.74 | |
| **$Mn^{III}OClPc$** (in DMSO) | $[Mn^{III}ClPc^{2-}] / [Mn^{IV}ClPc^{1-}]^{+1}$ | 0.30 | 73 | 0.65 | 0.31 |
| | $[Mn^{III}ClPc^{2-}] / [Mn^{II}ClPc^{2-}]^{-1}$ | -0.012 | 65 | 0.96 | |
| | $[Mn^{II}ClPc^{2-}]^{-1} / [Mn^{I}ClPc^{2-}]^{-2}$ | -0.68 | 62 | 0.91 | |
| | $[Mn^{I}ClPc^{2-}]^{-2} / [Mn^{I}ClPc^{3-}]^{-3}$ | -1.28 | 66 | 0.92 | |

**[a]:** $E_{1/2}$ values (($E_{pa}$+$E_{pc}$)/2) were given versus SCE) at 0.100 $Vs^{-1}$ scan rate. **[b]:** $\Delta E_p = E_{pa}-E_{pc}$. **[c]**:$I_{p,a}/I_{p,c}$ for reduction ,$I_{p,c}/I_{p,a}$ for oxidation processes. **[d]**:$\Delta E_{1/2} = E_{1/2}$ (first oxidation)- $E_{1/2}$ (first reduction). **[e]**: $E_p$ value of aggregated species given in parentheses.

As shown in **Fig. 3.2**, $In^{III}ClPc$ gives three reductions, $R_1$ at -0.58 V ($\Delta E_p$ = 70 mV and $I_{p,a}/I_{p,c}$ = 0.71), $R_2$ at -0.87 V($\Delta E_p$ = 95 mV and $I_{p,a}/I_{p,c}$= 0.75), and $R_3$ at -1.67 V and an oxidation reaction $Oxd_1$ at 1.00 V($\Delta E_p$ = 95 mV and $I_{p,a}/I_{p,c}$= 0.93) within the potential window of DCM/TBAP electrolyte system.

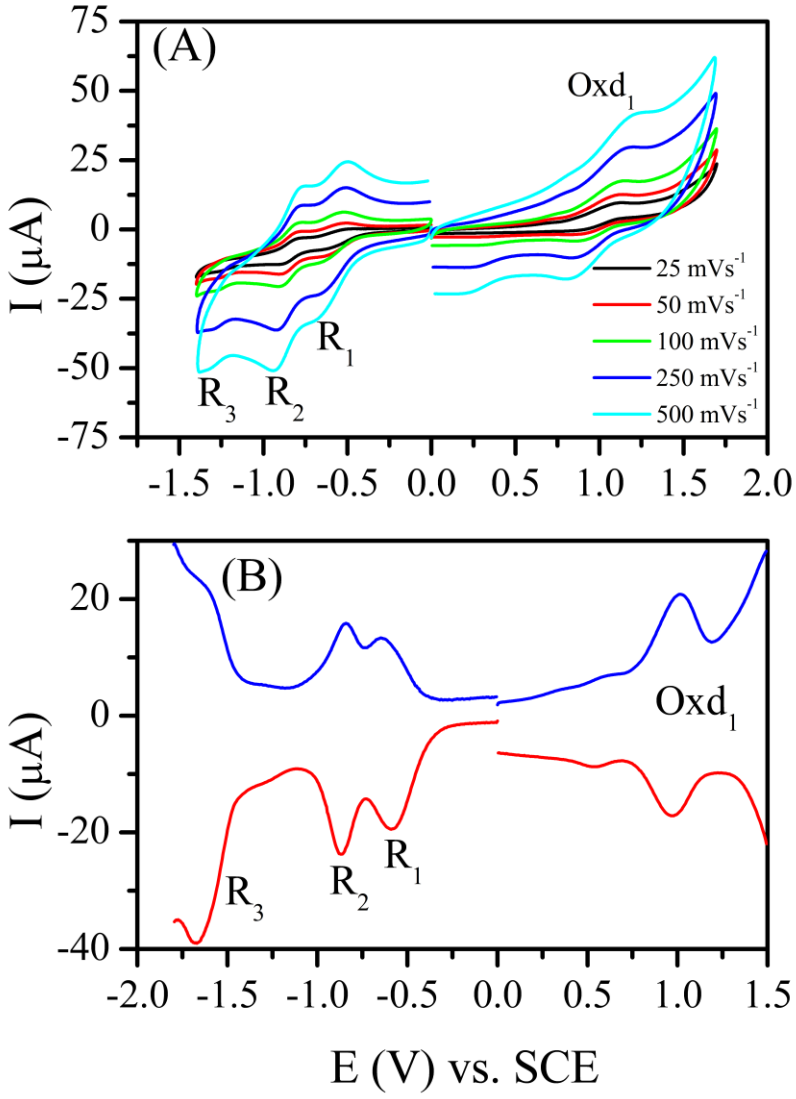


**Figure 3.2** (**a**) CVs of $In^{III}ClPc$ at various scan rates and (b) SWVs of $In^{III}ClPc$ recorded at 0.100 $Vs^{-1}$ scan rate on a GCE working electrode in DCM/TBAP.

While the electron transfer reactions of the complex are electrochemically quasi reversible with respect to $\Delta E_p$ values of the redox processes of $In^{III}ClPc$, the reduction reactions are complicated with a possible chemical reaction with respect to $I_{p,a}/I_{p,c}$, and $I_{p,c}$ vs. $\nu^{1/2}$ analyses [93]. $\Delta E_{1/2}$ value of the complex is in harmony with the MPcs having redox inactive metal centers. The only difference is the shifting of the redox processes toward the positive potentials with respect to similar complexes [94-97]. MPcs having redox inactive metal centers generally give the reduction reactions after ca. -0.80 V versus SCE with about ca. 0.30 V potential differences between first two reduction reactions ($\Delta E_{1/2(R1-R2)}$). $In^{III}ClPc$ studied here provides these basic electrochemical parameters reported in the literature and thus the redox properties of the complex support the proposed structure given on scheme 1.

$Mn^{III}ClPc$ and $Ti^{IV}OPc$ have redox active metal centers, thus they can generally give metal based redox based redox processes. Although, there is an inconsistency on the assignments of the redox couple of both of $Mn^{III}ClPc$ and $Ti^{IV}OPc$ in the literature, at least one metal based reduction reaction was reported for these type complexes. When a deep literature survey was carried out, it is easy to derive different reduction mechanisms for such complexes [95][98-103]. A controversy presents in the literature for the redox behaviors of TiPc type complexes. TiPc type complexes generally give four sequential reduction processes and while a metal-metal-ring-ring based reduction sequence was proposed in some papers, a metal-ring-metal-ring based reduction sequence was also commonly suggested. Differently, Nyokong et. al. also suggested an uncommon assignments in their study as a two electron reduction assigned to metal and ring reduction followed with a metal and then ring reduction sequence [104]. Nowadays, there have been intensive studies on TiPc type complexes for the clarification of this controversy and to understand the effects of substituents, axial ligands, and electrolyte systems to the redox assignment of the complexes [99,100,105]. For this purpose, the redox processes of $Ti^{IV}OPc$ with CW, SWV and in situ spectroelectrochemical analysis were studied. **Fig. 3.3** represents CV and SWV responses of $Ti^{IV}OPc$ in DCM/TBAP electrolyte on GCE working electrode. $Ti^{IV}OPc$ gives four reductions, $R_1$ at -0.58 V ($\Delta E_p$ = 63 mV and $I_{p,a}/I_{p,c}$ = 0.91), $R_2$ at -0.98

V($\Delta E_p$ = 75 mV and $I_{p,a}/I_{p,c}$= 0.85), $R_3$ at -1.26 V, and $R_4$ at -1.53 V and two oxidation reactions $Oxd_1$ at 0.60 V($\Delta E_p$ = 61 mV and $I_{p,a}/I_{p,c}$= 0.94) and $Oxd_2$ at 0.95 V($\Delta E_p$ = 65 mV and $I_{p,a}/I_{p,c}$= 0.83) within the potential window of DCM/TBAP electrolyte system.

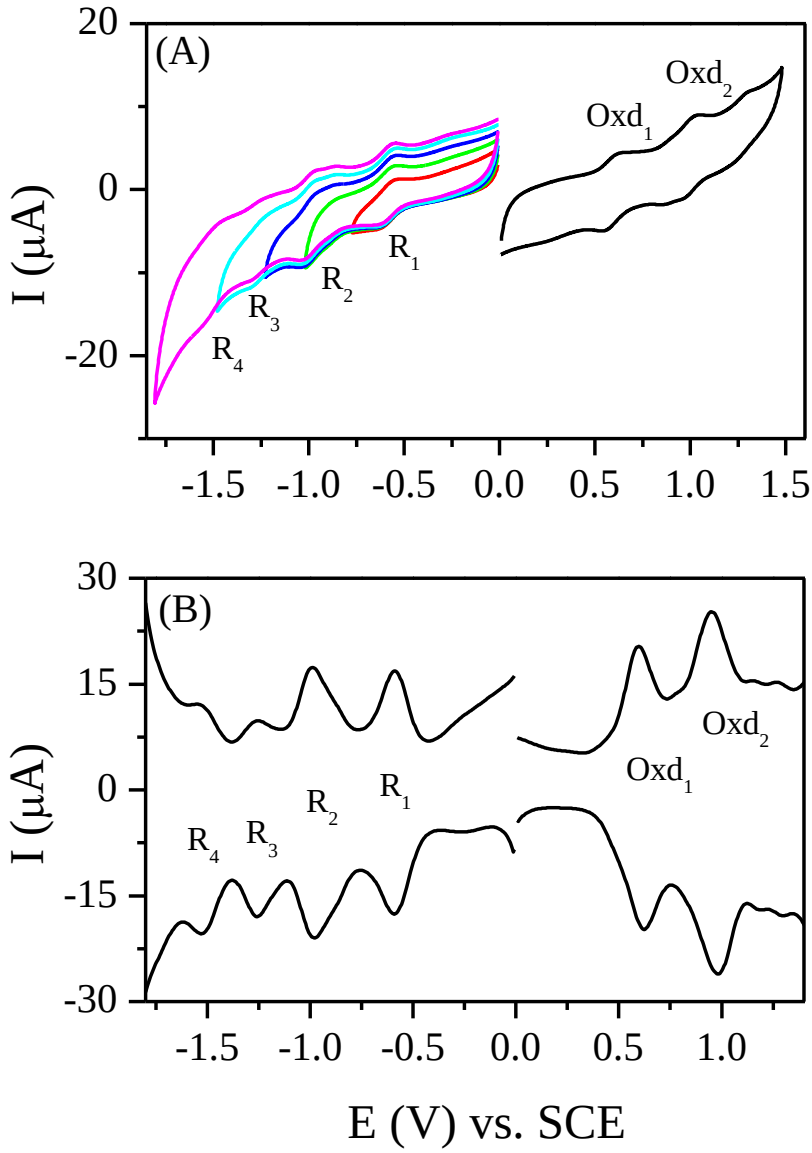


**Figure 3.3** (**a**) CVs of $Ti^{IV}OPc$ recorded with different vertex potentials at 0.100 $Vs^{-1}$ scan rate and (b) SWVs of $Ti^{IV}OPc$ recorded at 0.100 $Vs^{-1}$ scan rate on a GCE working electrode in DCM/TBAP.

While the first reduction ($R_1$) and first oxidation ($Oxd_1$) processes are chemically and electrochemically reversible with respect to $\Delta E_p$, $I_{p,a}/I_{p,c}$, and $I_{p,c}$ vs. $\nu^{1/2}$ analyses [94], the second reduction ($R_2$) and second oxidation ($Oxd_2$) processes are electrochemically quasi reversible, the third ($R_3$) and fourth ($R_4$) reduction processes have irreversible characters. The peak to peak separations between 0.30 and 0.40 V ($\Delta E_{1/2(R1\text{-}R2)}$, $\Delta E_{1/2(R2\text{-}R3)}$, and so on) are in harmony with those of the TiPc complexes. However, $\Delta E_{1/2(R1\text{-}Oxd1)}$ (1.18 V) is smaller than those of $In^{III}ClPc$ and MPcs bearing redox inactive metal centers. These differences indicate the location of the empty "d" orbitals of $Ti^{IV}O$ between the highest occupied molecular orbital (HOMO) and the lowest unoccupied molecular orbital (LUMO) of Pc ring. It is well known that when the empty "d" orbitals of the metal center of MPcs lie between HOMO and LUMO of Pc ring, metal center takes electrons before the Pc ring [106]. Thus, the first reduction process of $Ti^{IV}OPc$ must be a metal based reduction reaction. To support this phenomenon, the assignments of all redox reactions were also performed with in situ spectroelectrochemical measurements discussed below.

While a sequentially metal-ring-ring based reduction reactions were reported for various MnPc type complexes, there are many papers which reported a metal-metal-ring based reduction sequence [97][102][107-111]. Here, the redox behavior of $Mn^{III}ClPc$ was studied with CV, SWV, and in situ spectroelectrochemistry techniques and assignments of the electron transfer processes were performed and compared with similar complexes in the literature to clarify this inconsistency and/or to determine the substituent and solvent effects to this inconsistency. As shown in **Fig. 3.4**, CVs and SWVs of $Mn^{III}ClPc$ are completely different than those of $In^{III}ClPc$ and $Ti^{IV}OPc$ complexes. $Mn^{III}ClPc$ gives three reversible reduction and one reversible oxidation reactions. The first reduction reaction ($R_1$) of $Mn^{III}ClPc$ shifts up to -0.10 V due to the redox activity of the $Mn^{III}$ metal center. It is well known that $Mn^{III}$ metal center can be easily reduced to the more stable $Mn^{II}$ form at around 0.0 V.

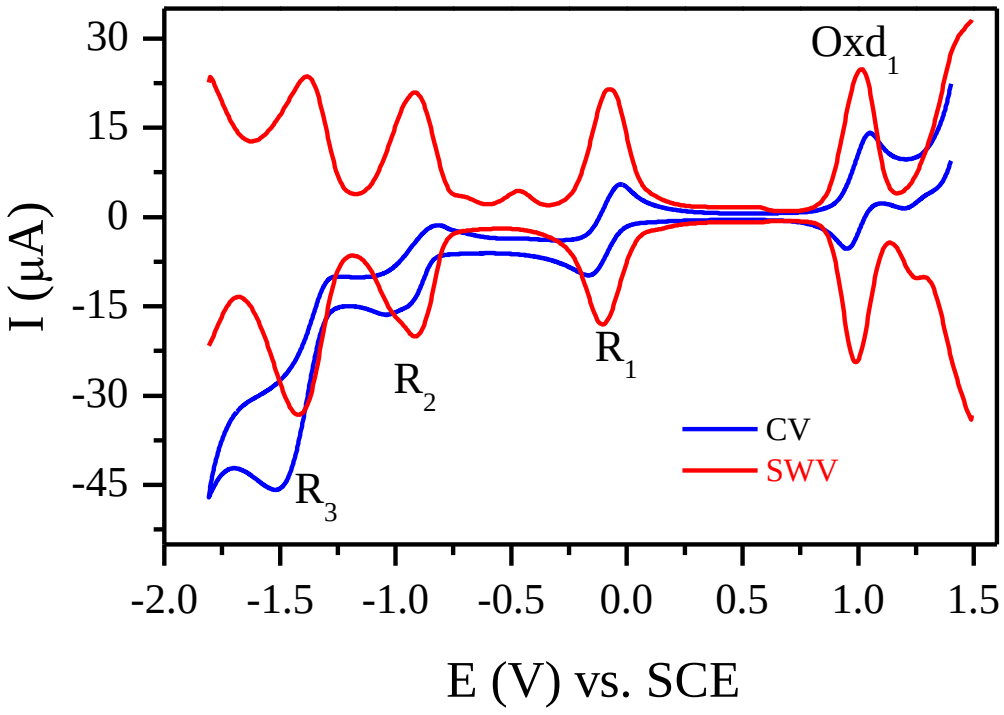


**Figure 3.4** CVs and SWVs of $Mn^{III}ClPc$ at 0.100 $Vs^{-1}$ scan rate on a GCE working electrode in DCM/TBAP.

In the literature, it is obviously presented that the second metal based reduction reaction ($[Mn^{II}CPc^{-2}]^{1-}$/ $[Mn^{I}ClPc^{-2}]^{2-}$) is observed after ca. 0.80 V than the first reduction reaction (($[Mn^{III}ClPc^{-2}]$/ $[Mn^{II}ClPc^{-2}]^{1-}$) [97,102][107-111]. Thus, the second reduction reaction ($R_2$) of $Mn^{III}ClPc$ recorded at -0.91 V can be easily assigned to $[Mn^{II}ClPc^{-2}]^{1-}$/ $[Mn^{I}ClPc^{-2}]^{2-}$ process. Assignments of all redox peaks were performed with in situ spectroelectrochemical measurements discussed below.

In order to analyze the effect of solvent to the electrochemistry of the complexes, voltammetric and in situ spectroelectrochemical measurements were also performed in a polar solvent DMSO instead of nonpolar DCM and the results are tabulated in Table 1. Redox reactions of the complexes were not significantly affected by the solvents. The redox reactions were generally shifted to the negative potentials due to the higher polarizing effect of DMSO. Moreover, the reversibility of the redox processes was also altered slightly by changing the solvent of the electrolyte. **Fig. 3.5** represents CV and

SWV responses of $Mn^{III}ClPc$ in DMSO/TBAP electrolyte on GCE working electrode as an example. The first reduction reaction ($R_1$) of $Mn^{III}ClPc$ is observed at -0.12 V and the first reduction reaction $Oxd_1$ at 0.30 V in DMSO. This large shift of $Oxd_1$ is most probably due to the metal based oxidation character of the complex in DMSO instead of the ring based oxidation in DCM. Moreover, $Oxd_1$ of $Mn^{III}ClPc$ has chemically irreversible character in DMSO and gives an extra peak at 0.10 V due to the chemical product formed after $Oxd_1$ process. Surprisingly, when $R_1$ of $Mn^{III}ClPc$ shifts to the positive potentials in DMSO with respect to those in DCM, the redox processes $R_2$ and $R_3$ shift to the positive potentials in DMSO. These uncommon shifts may be due to the coordination of DMSO to the $Mn^{III}$ center, which stabilizes $Mn^{I}Pc$.

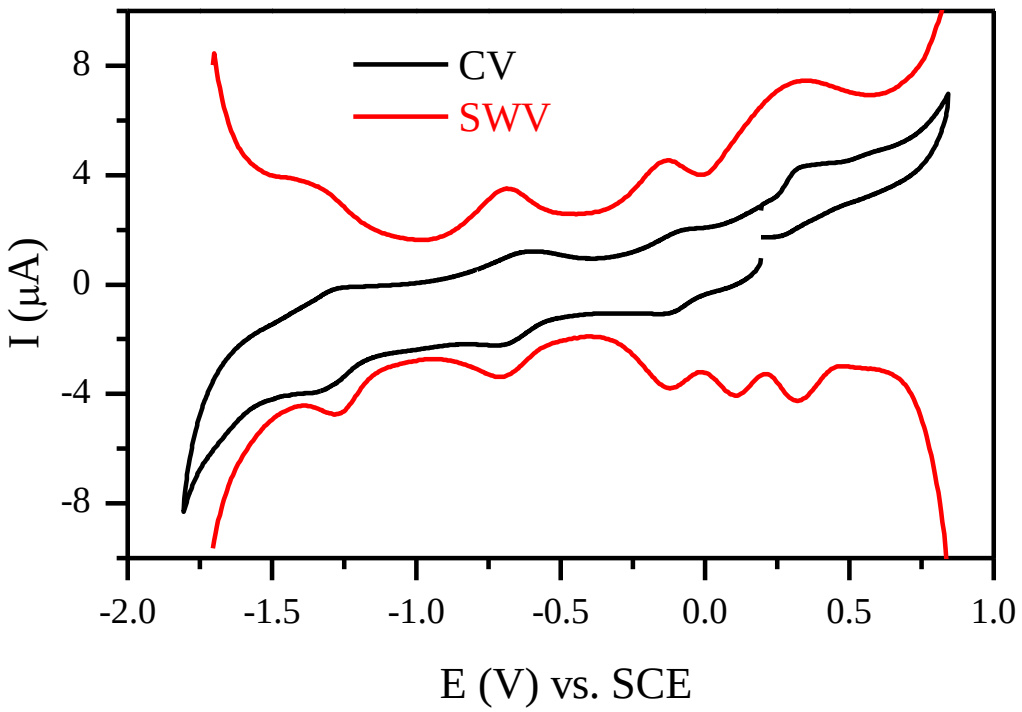


**Figure 3.5** CVs and SWVs of $Mn^{III}ClPc$ at 0.100 $Vs^{-1}$ scan rate on a GCE working electrode in DMSO/TBAP.

### 3.1.2. Spectroelectrochemical Measurements

In situ spectroelectrochemical measurements were performed to determine the assignments of the redox couples recorded with the CVs and SWVs of the complexes. $In^{III}ClPc$ complex has a redox inactive $In^{III}Cl$ center, thus the spectral changes recorded during the electron transfer processes of $In^{III}ClPc$ characterized the ring-based natures of the redox processes. **Fig. 3.6** shows in situ UV-Vis spectral changes and in situ recorded chromaticity diagram of $In^{III}ClPc$.

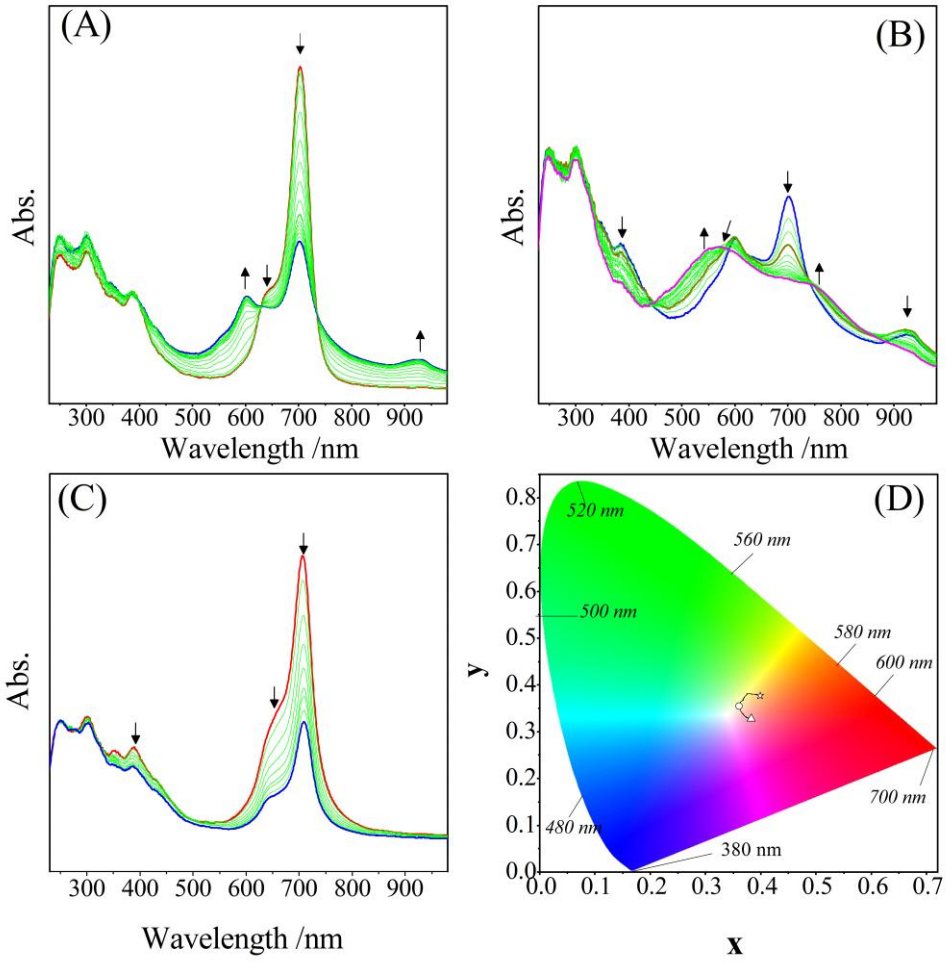


**Figure 3.6** In-situ UV-Vis spectral changes of $In^{III}ClPc$ in DCM/TBAP. **a**) $E_{app}$= -0.75 V. **b**) $E_{app}$= -1.10 V. **c**) $E_{app}$= = 1.30 V. **d**) Chromaticity diagram (each symbol represents the

color of electro-generated species; □: $[In^{III}ClPc^{-2}]$, ○:$[In^{III}ClPc^{-3}]^{-1}$; △: $[In^{III}ClPc^{-4}]^{-2}$; ☆: $[In^{III}ClPc^{-1}]^{+1}$.

During $R_1$ process at -0.75 V constant potential application, while the Q band at 702 nm decreases without a shift, new bands are observed at 601 and 624 nm **Fig. 3.6a**. Well-defined isosbestic points are observed at 388, 627, and 734 nm in the spectra which indicates the presence of one type of reduced species during the first reduction reaction. Decreasing of the Q band without shifting and observation of new bands at the ligand to metal charge transfer region (LMCT) characterize the Pc ring based electron transfer nature of the first reduction reaction. Thus, $R_1$ couple of $[In^{III}ClPc^{-2}]$ is assigned to $[In^{III}ClPc^{-2}]$ / $[In^{III}ClPc^{-3}]^{1-}$ [109-110]. The neutral form of $[In^{III}ClPc^{-2}]$ complex had a yellowish green color (x = 0.3769 and y = 0.3807) and this color changed into light yellow (x = 0.3605 and y = 0.3548) after the first reduction reaction **Fig. 3.6d**. The spectral changes given in **Fig. 3.6b** recorded under -1.10 V potential application are also characteristic spectral changes for a Pc based reduction reaction. Since, the Q band of the complex continues to decrease without a shift, when new bands are observed at 546 and 750 nm [109-110]. This process did not give well defined isosbestic points. The isosbestic points at around 585, 743, and 885 nm change continuously during the second reduction reaction. This behavior indicates the presence of a chemical reaction after $\mathbf{R_2}$ process and the formation of more than a single reduced type species during the second reduction reaction. Due to the chemical instability of the dianionic species formed after $\mathbf{R_2}$ process, the original spectrum was not obtained after applying 0.0 V to the working electrode. After the second reduction reaction, light yellow color of the monoaninic $[In^{III}ClPc^{-3}]^{1-}$ species turned into pink (x = 0.3833 and y = 0.3274) dianionic $[In^{III}ClPc^{-4}]^{2-}$ species **Fig. 3.6d**. During the oxidation of $[In^{III}ClPc^{-2}]$, all bands of the complex decrease in intensity due to the decomposition of the complex **Fig. 3.6c**.

**Fig. 3.7** illustrates in situ spectroelectrochemical and in situ electrocolorimetric results of $Ti^{IV}OPc$. $Ti^{IV}OPc$ gives spectral changes which are characteristic changes for metal-based redox reactions in addition to the ligand-based redox reactions, since the complex has a redox active $Ti^{IV}O$ center. In previous papers, the electrochemistry and in situ spectroelectrochemical behaviors of different TiPc type complexes were reported. Here it

was seen the substituent environment of the complexes alters both electrochemical and in situ spectroelectrochemical behaviors.

For example, while a metal-ring-metal-ring assignment was reported with TiOPc bearing octakis(2-dimethylaminoethylsulfanyl moieties [112], a metal-metal-ring-ring assignments was reported for TiOPc bearing tetra[4-(thiophen-3-yl)-phenoxy] moieties [97]. Nyokong et.al. also reported different assignments for different TiOPc complexes [91,93,97,100]. TiOPc studied here also has a metal- metal-ring-ring assignment with respect to in situ spectroelectrochemical and in situ electrocolorimetric results given below.

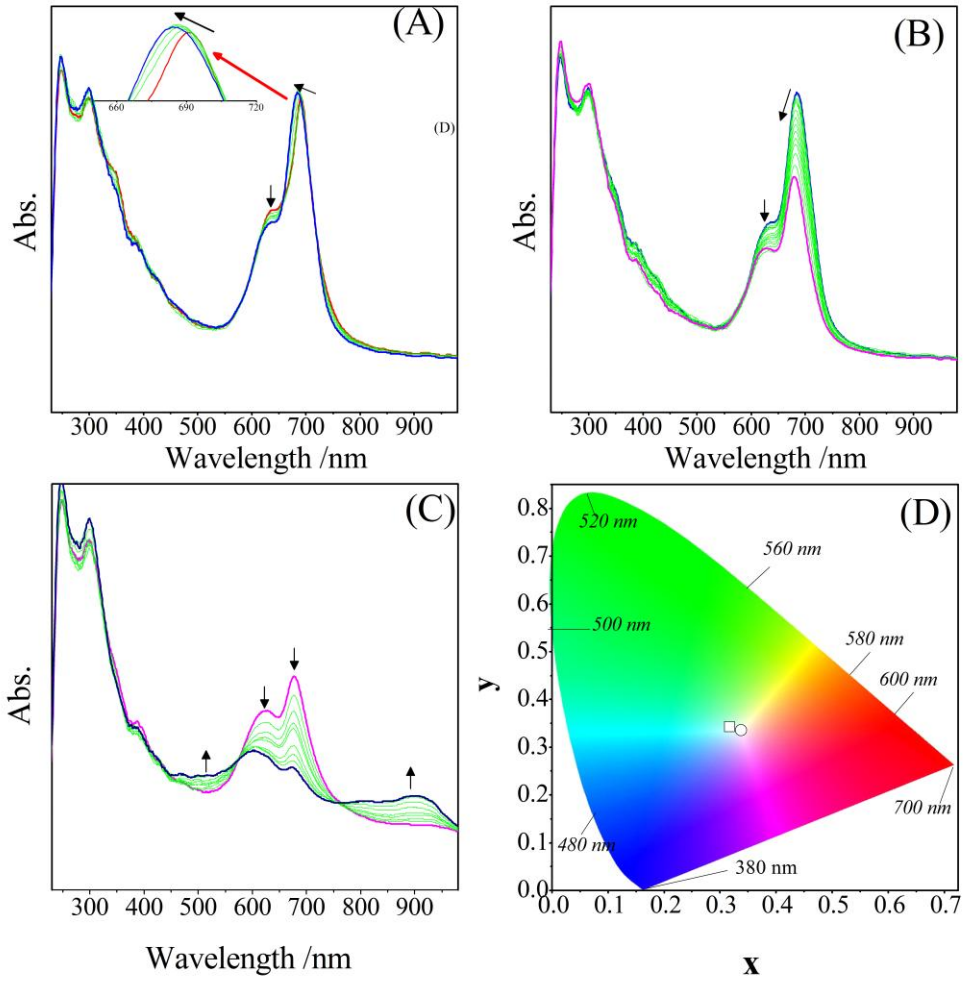


**Figure 3.7** In-situ UV-Vis spectral changes of $Ti^{IV}$OPc in DCM/TBAP. **a**) $E_{app}$= -0.75 V. **b**) $E_{app}$= -1.10 V. **c**) $E_{app}$= -1.35 V. **d**) Chromaticity diagram (each symbol represents the

color of electro-generated species; □: $[Ti^{IV}OPc^{-2}]$, ○: $[Ti^{II}OPc^{-3}]^{-3}$.

**Fig. 3.7a** shows the spectral changes recorded under -0. 75 V potential application. During this process, the Q band at 692 nm shifts to 684 nm, which can be easily assigned to $[TiO^{IV}Pc^{-2}]$/ $[TiO^{III}Pc^{-2}]^{1-}$ process [93][95][112,113] **Fig. 3.7a**. Clear isosbestic points were observed at 657 and 717 nm, which shows the formation of one type reduced species. During the second reduction reaction ($R_2$) of $Ti^{IV}OPc$, the Q band of the complex shifts from 684 to 678 nm with decreasing intensity **Fig. 3.7b**. The shift of the Q band indicates the metal-based character of $R_2$ process and assigned to $[TiO^{III}Pc^{-2}]^{1-}$/ $[TiO^{II}Pc^{-2}]^{2-}$ [91][95][112,113]. Further reduction reaction is a ring based process, since the Q band at 678 nm decreases in intensity without a shift, while new bands are observed at 517 and 905 nm **Fig. 3.7c**. Decreasing of the Q band without a shift and the observation of new bands at MLCT region are characteristic changes for a Pc ring based reduction reaction of MPc type complexes. During the oxidation of the complex, all bands decreased in intensity due to the decomposition of the complex. Color of the complex did not change significantly as shown in the chromaticity diagram given in **Fig. 3.7a**.

**Fig. 3.8** represents in situ spectroelectrochemical and in situ electrocolorimetric results of $Mn^{III}ClPc$. $Mn^{III}ClPc$ has redox active $Mn^{III}$ center, which can be easily reduced to $Mn^{II}$ and then to $Mn^{I}$ oxidation state depending on the substituents of Pc and ligand environment of the metal center. Metal reduction of MPcs generally shifts the Q band of the complexes and causes to the observation of new huge bands at the MLCT region. The spectral changes recorded here are in agreement with these characteristic spectral changes. **Fig. 3.8a** shows the spectral changes recorded under -0.30 V constant potential application. Neutral form of $Mn^{III}ClPc$ has a band at 515 nm and a red shifted Q band at 740 nm, which is a characteristic spectrum for the MnPcs having $Mn^{III}$ metal center [114-117]. During the reduction, while the Q band and the band at 515 nm decrease and finally disappear, a new Q band characterizing $Mn^{II}Pc$ is observed at 690 nm. The shift of the Q band from 740 nm to 690 nm and the disappearance of the band at 515 nm are characteristic changes for $[Mn^{III}ClPc^{-2}]$/ $[Mn^{II}ClPc^{-2}]^{1-}$ process [118-121]. This process gives clear isosbestic points at 536, 712, and 830 nm.

At the end of this reaction, reddish orange color (x = 0.3922 and y = 0.4065) of the complex turns into bluish green color (x = 0.2997 and y = 0.3544) as shown in the chromaticity diagram **Fig. 3.8d**.

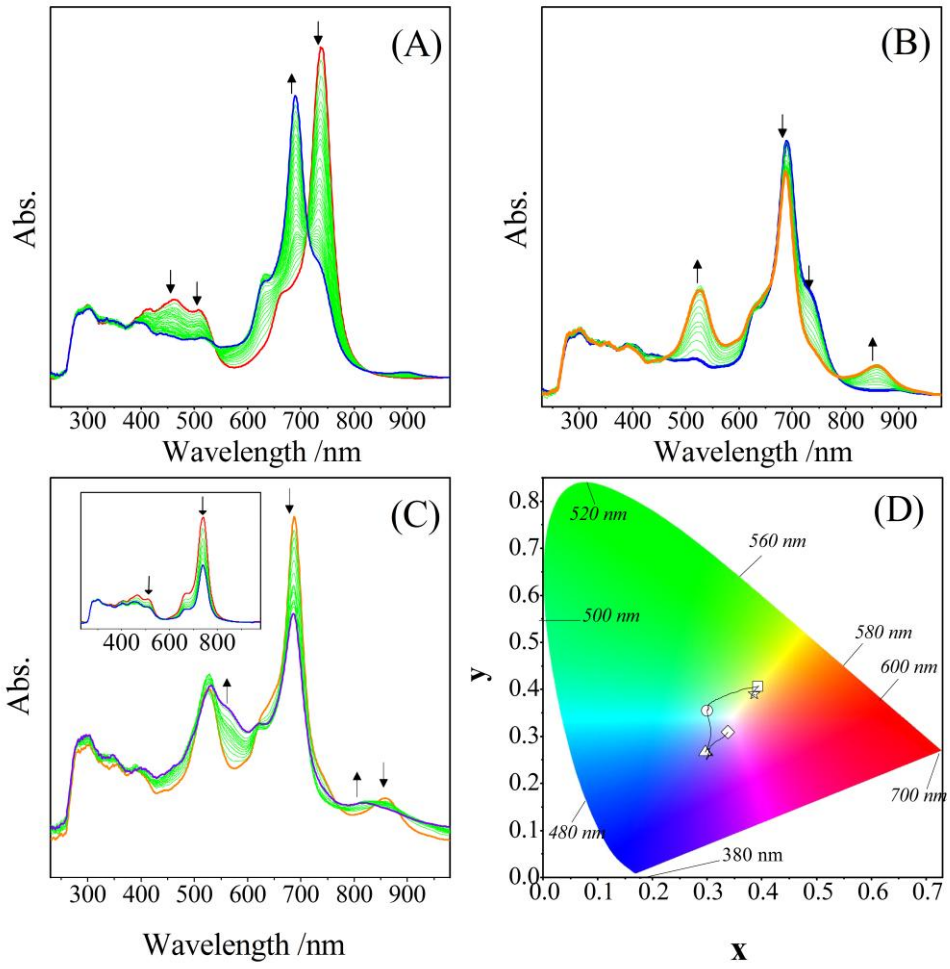


**Figure 3.8** In-situ UV-Vis spectral changes of $Mn^{III}ClPc$ in DCM/TBAP. a) $E_{app}$= -0.30 V. b) $E_{app}$= -1.20 V. c) $E_{app}$= = -1.60 V (inset: $E_{app}$ = 1.20 V). d) Chromaticity diagram (each symbol represents the color of electro-generated species; □: $[Mn^{III}ClPc^{-2}]$, ○:$[Mn^{II}ClPc^{-2}]^{-1}$; △: $[M^{I}ClPc^{-2}]^{-2}$; ◇: $[M^{I}ClPc^{-3}]^{-2}$; ☆: $[Mn^{III}ClPc^{-1}]^{+1}$.

Second reduction reaction of $Mn^{III}ClPc$ is also a metal based reduction reaction and it could be assigned to $[Mn^{II}ClPc^{-2}]^{1-}$ / $[Mn^{I}ClPc^{-2}]^{2-}$ process with respect to spectral changes under -1.20 V constant potential application **Fig. 3.8b**.

During this process, while the Q band decreases in intensity, a new band is observed at 527 nm. Moreover, another new band is also observed at 857 nm. The band at 527 nm especially characterizes $Mn^{I}$ form of the metal center of $Mn^{III}ClPc$ [118,119].

Clear isosbestic points at 461, 658, and 787 nm indicate chemical stability of the dianionic $[Mn^{I}ClPc^{-2}]^{2-}$ species. A deep blue color (x = 0.2964 and y = 0.2665) is observed for the dianionic $[Mn^{I}ClPc^{-2}]^{2-}$ species as shown in the chromaticity diagram Fig. 3.8d. Spectral changes given in **Fig. 3.8c** were recorded during the $R_3$ process of $Mn^{III}ClPc$. Observation of a new broad band (564 nm) at the higher wavelength side of the $Mn^{I}$ band is a characteristic change for a Pc-ring based reduction reaction [102][122-128]. This process gives clear isosbestic points at 502, 620,770, and 887 nm and a purple color (x = 0.3374 and y = 0.3093) at the end of the third reduction reaction. As shown in **Fig. 3.8c inset**, all bands of $Mn^{III}ClPc$ decrease in intensity due to the decomposition of the complex during the oxidation reaction.

### 3.1.3. Electrochemical Oxygen Reduction and Oxygen Sensing Measurements

It has been reported that presence of molecular oxygen in the electrolytes of voltammetry and spectroelectrochemical analysis systems alters the redox responses of MPcs and $O_2$ due to the interaction between $O_2$ and MPcs. The changes in the redox responses of MPcs and $O_2$ by virtue of this indicate electrocatalytic and/or electrosensing usability of MPcs. It was reported that MPcs having redox active metal centers, such as CoPc, MnPc and TiOPc, electrochemically catalyzes oxygen reduction reaction (ORR)[122,124,129-131]. Early studies indicated that substituents and metal center type of MPcs alter the electrocatalytic activity of the complexes. Now, the interaction of MPcs having (3,5-bis(trifluoromethyl)phenyl)ethynyl substituents was examined and compared the results with those of MPcs having different substituents and metal centers. To investigate the interaction between $O_2$ and MPcs, first of all, the voltammetric responses of MPcs in

solution with and without $O_2$ were reported.

The results of these measurements indicate that while $In^{III}ClPc$ did not interact with $O_2$ in solution, electrochemical responses of $Mn^{III}ClPc$ and $Ti^{IV}OPc$ changed considerably with the increasing $O_2$ concentration in solution. **Fig. 3.9** represents the SWV responses of $Ti^{IV}OPc$ recorded in DMSO/TBAP electrolyte bubbled with $O_2$ gradually (case 3).

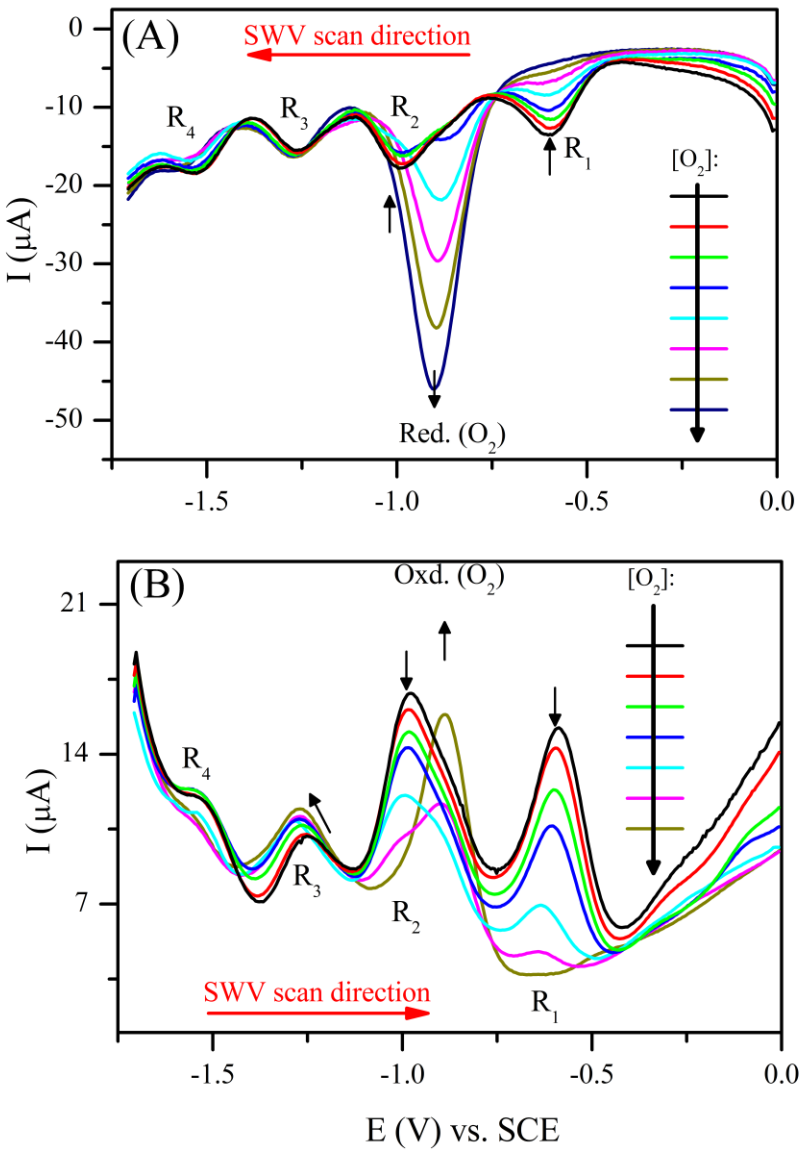


**Figure 3.9** SWV responses of $Ti^{IV}OPc$ recorded gas at 0.100 $Vs^{-1}$ scan rate on a GCE working electrode in DMSO/TBAP bubbled gradually with $O_2$.

Without $O_2$, $Ti^{IV}OPc$ gives four reduction peaks ($R_1$- $R_4$). During the gradual increasing of $O_2$ in DMSO/TBAP electrolyte, while both the cathodic and anodic peaks of $R_1$ and $R_2$ couples decrease in current intensity and disappear finally, a new couple (Red.($O_2$) /Oxd.($O_2$)) assigned to the ORR is observed at -0.91 V with increasing current intensity with respect to the increasing $O_2$ concentration. Moreover, $R_3$ and $R_4$ couples of the complex shift with slight current changes. These voltammetric data indicate that interaction of $O_2$ with $Ti^{IV}OPc$ especially alters the metal based reduction reactions ($R_1$ and $R_2$). The disappearances of $R_1$ and $R_2$ couples with respect to the increasing $O_2$ concentration show the coordination of $O_2$ to the $Ti^{IV}O$ center of $Ti^{IV}OPc$, and this coordination alters the $Ti^{IV}O$ based processes. The interaction of $O_2$ with $Ti^{IV}OPc$ also alters the SWV responses of $O_2$. While $O_2$ gives ORR at -1.25 V in $Ti^{IV}OPc$-free electrolyte, this reaction shifts to -0.91 V in $Ti^{IV}OPc$ dissolved in DMSO/TBAP electrolyte. These voltammetric differences between case 1 and case 2 indicate decreasing of the over potential of ORR as 0.34 V and thus attest the electrocatalytic activity of $Ti^{IV}OPc$ for the ORR.

**Fig. 3.10** shows the SWV responses of $Mn^{III}ClPc$ recorded in DMSO/TBAP electrolyte bubbled with $O_2$ gradually (case 3). $Mn^{III}OAcPc$ gives similar redox responses on the negative potential side of the SWV with those of the $Ti^{IV}OPc$. Without $O_2$, $Mn^{III}ClPc$ gives two metal based reduction couples ($R_1$ and $R_2$) and these redox processes were affected considerably from increasing $O_2$ concentration. As shown in Fig. 3.10 while the peaks $R_1$ and $R_2$ couples gradually decrease and disappear finally, the peaks of $R_3$ gradually shift as a result of increasing $O_2$ concentration. Moreover, the ORR couple (Red.($O_2$) /Oxd.($O_2$)) is observed at -0.79 V in $Mn^{III}ClPc$ dissolved in DMSO/TBAP electrolyte. These voltammetric data show that $O_2$ interacts with the $Mn^{III}Cl$ metal center of $Mn^{III}ClPc$ and this interaction causes the disappearance of $Mn^{III}Cl$ based redox processes. With respect to these voltammetric responses, it is easy to conclude that $Mn^{III}ClPc$ electrochemically catalyzes ORR reaction and the electrocatalytic activity of $Mn^{III}ClPc$ decreases the over potential of ORR as -0.46 V. In addition to the electrocatalytic activity, different SWV responses were recorded at the positive potential

side of the SWV of $Mn^{III}ClPc$.

Without $O_2$, $Mn^{III}ClPc$ gives an oxidation couples $Oxd_1$ at 0.35 V assigned to $[Mn^{III}ClPc^{-2}]$ /$[Mn^{IV}ClPc^{-2}]^{1+}$ process. When the solution is gradually bubbled with $O_2$, $Oxd_1$ couple of $Mn^{III}ClPc$ decreases in current intensity and a new couple ($ES_1$) increases to at 0.63 V. Continuous increase of the peaks of $ES_1$ couple with the increasing concentration indicates possible usage of $Mn^{III}ClPc$ as an electrochemical oxygen sensor.

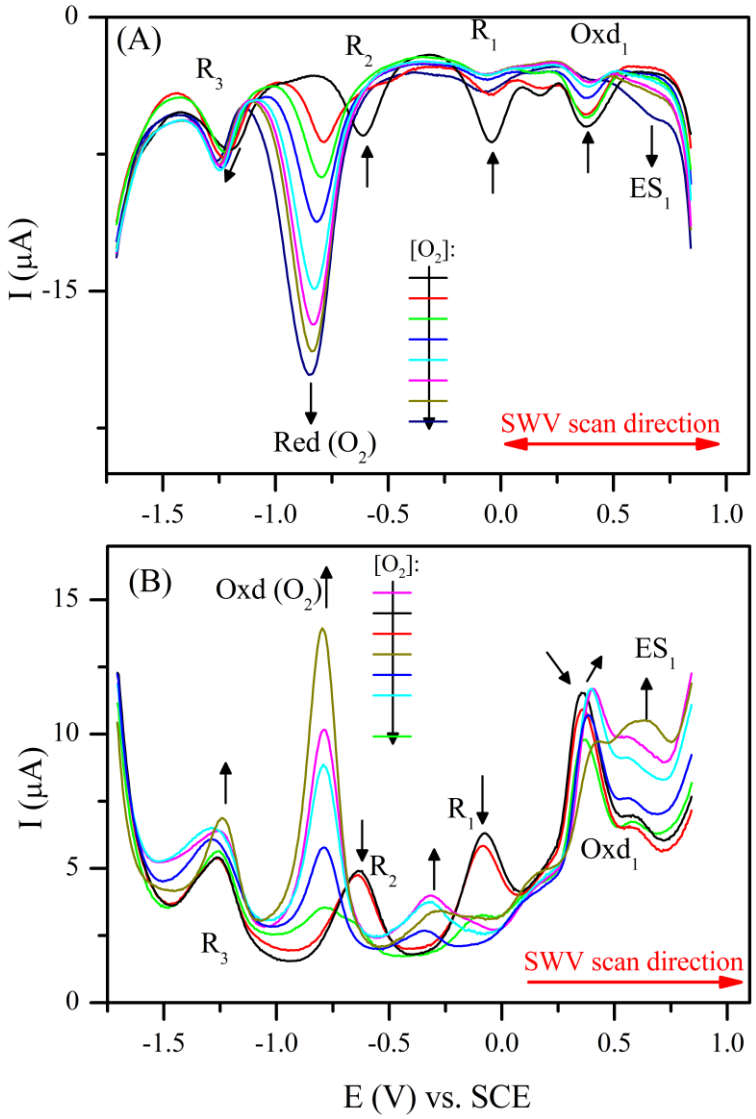


**Figure 3.10** SWV responses of $Mn^{III}ClPc$ recorded gas at 0.100 $Vs^{-1}$ scan rate on a GCE

working electrode in DMSO/TBAP bubbled gradually with $O_2$.

In-situ spectroelectrochemical studies were employed to support the interaction between MPcs and $O_2$. **Fig. 3.11** shows in-situ UV-vis spectral changes of $Ti^{IV}OPc$ in $O_2$ saturated DMSO/TBAP electrolyte system. Under open circuit potential, spectra of $Ti^{IV}OPc$ did not change in $O_2$ bubbled electrolyte, which shows that neutral form of $Ti^{IV}OPc$ did not interact with $O_2$ in *case 3*. While $Ti^{IV}OPc$ gives spectral changes assigned to metal based reduction reaction during the first ($R_1$) and second ($R_2$) reduction reactions in oxygen removed DMSO/TBAP electrolyte system (*case 2*), spectral changes assigned to the Pc based reduction reactions are observed in *$O_2$* saturated DMSO/TBAP electrolyte system as shown in **Fig. 3.11**. These in situ spectroelectrochemical results support SWV responses of $Ti^{IV}OPc$ (the disappearance of metal based peaks due to the interaction with $O_2$) and interaction of $O_2$ with reduced $Ti^{IV}OPc$ species.

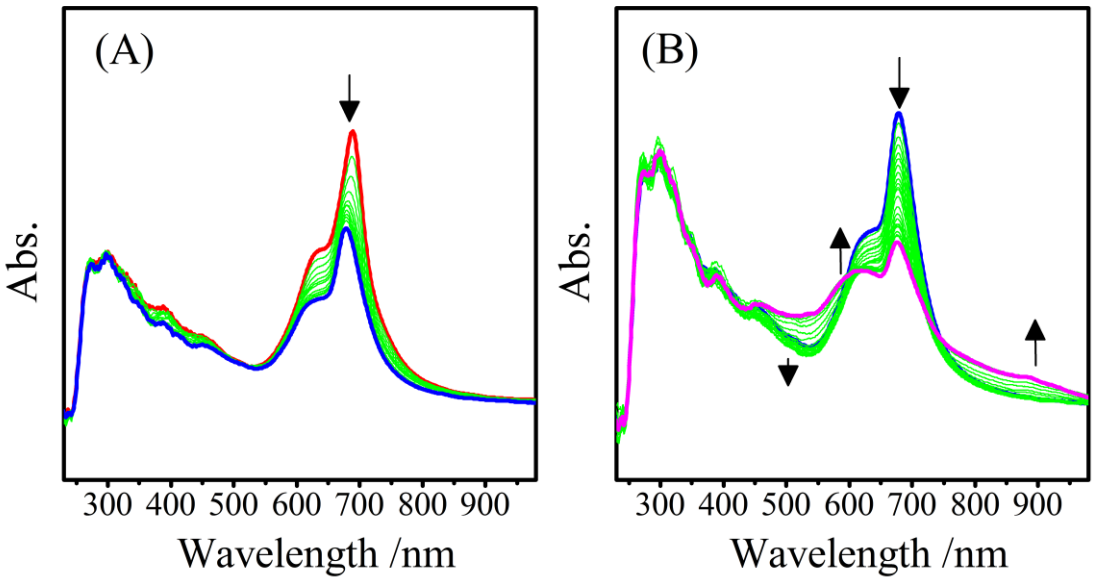


**Figure 3.11** In-situ UV-Vis spectral changes of **$Ti^{IV}OPc$** in DMSO/TBAP electrolyte saturated with $O_2$. **a**) $E_{app}$= -0.75 V. **b**) $E_{app}$ = -1.70 V.

In-situ UV-vis spectral changes of $Mn^{III}ClPc$ in $O_2$ saturated DMSO/TBAP electrolyte system also supports the interaction between $O_2$ and $Mn^{III}ClPc$. While spectral changes assigned to $[Mn^{III}ClPc^{-2}]$/ $[Mn^{II}ClPc^{-2}]^{1-}$ and $[Mn^{II}ClPc^{-2}]^{1-}$ / $[Mn^{I}ClPc^{-2}]^{2-}$ processes were observed in $O_2$ removed DMSO/TBAP electrolyte (*case 2*) during $R_1$ and $R_2$

reduction reactions, spectral changes recorded during $R_1$ and $R_2$ processes were completely different in $O_2$ bubbled electrolyte (*case 3*). Under -0.50 V potential application, while the Q band at 735 nm characterizing [$Mn^{III}ClPc^{-2}$] species decreases in absorbance intensity, a new band is observed at 645 nm **Fig. 3.12a**. This new band characterizes μ-oxo species. It is known that μ-oxo species, $PcMn^{III}$-Cl-$Mn^{III}Pc$, give a band at between 600-650 nm [118-121]. These spectral changes indicate that [$Mn^{III}ClPc^{-2}$] reduces to [$Mn^{III}ClPc^{-2}$]$^{1-}$ which immediately interacts with $O_2$ and forms $PcMn^{III}$-Cl-$Mn^{III}Pc$. When -1.30 V was applied to the working electrode, the spectral changes assigned to the [$Mn^{II}ClPc^{-2}$]$^{1-}$ / [$Mn^{I}ClPc^{-2}$]$^{2-}$ process could not be observed in $O_2$ saturated DMSO/TBAP electrolyte. Instead, the band of the μ-oxo species increases and the band assigned to the [$Mn^{III}ClPc^{-2}$] species disappears completely **Fig. 12a**. These spectral changes support the SWV responses of the complex and the interaction between $O_2$ and $Mn^{III}ClPc$.

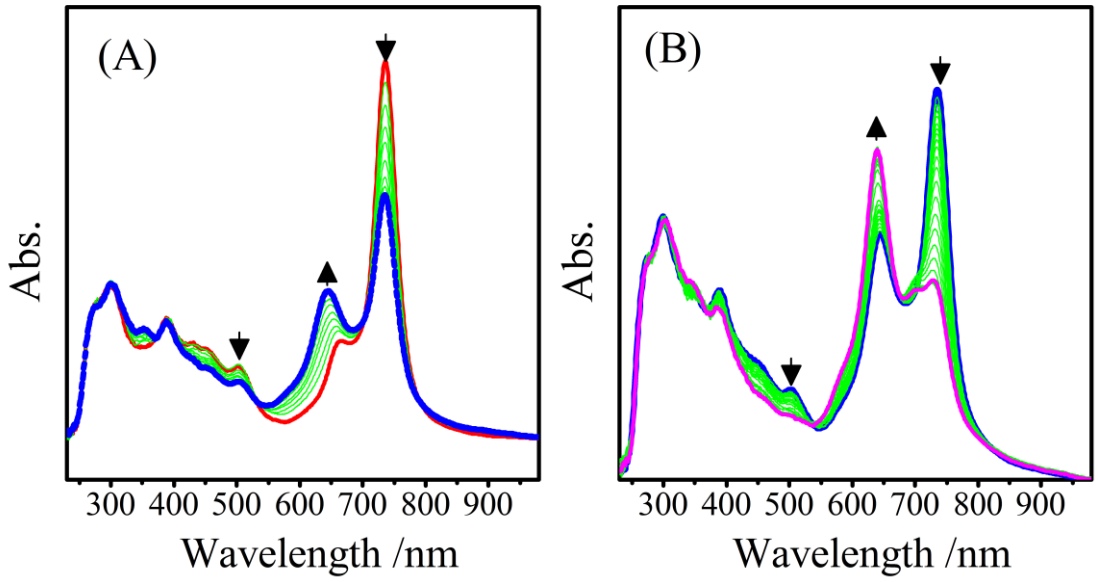


**Figure 3.12** In-situ UV-Vis spectral changes of $Mn^{III}ClPc$ in DMSO/TBAP electrolyte saturated with $O_2$. **a**) $E_{app}$= -0.30 V. **b**) $E_{app}$ = -1.30 V.

For the practical application of a functional material as ORR electrocatalyst and/or electrosensor, these materials should be coated on a substrate and tested for the desired applications. For this purpose, $Mn^{III}$ClPc and $Ti^{IV}$OPc were coated on ITO electrodes with Langmuir Blodgett (LB) technique (ITO/$Mn^{III}$ClPc and ITO/$Ti^{IV}$OPc), and these modified electrodes were used as electrocatalyst and sensors. **Fig. 3.13** represents the surface pressure ($\pi$)-area isotherm of $Mn^{III}$ClPc and $Ti^{IV}$OPc. Although the complexes formed well defined monolayer on the water sub-phase of the LB trough, it could not be transferred on ITO electrodes properly. Therefore, SA solution was added to the solution of $Mn^{III}$ClPc and $Ti^{IV}$OPc to supply formation of monolayers on ITO substrates. When 1:1 mixtures of SA:$Mn^{III}$ClPc and SA:$Ti^{IV}$OPc are used, all transfer ratios during both "up stroke" and "down stroke" are recorded as 1.0±0.1, which indicate coating of monolayer films with a Y type transfer. 20 LB monolayers were coated on ITO surface with all of the solution sprayed on the tray of the LB instrument in one trial.

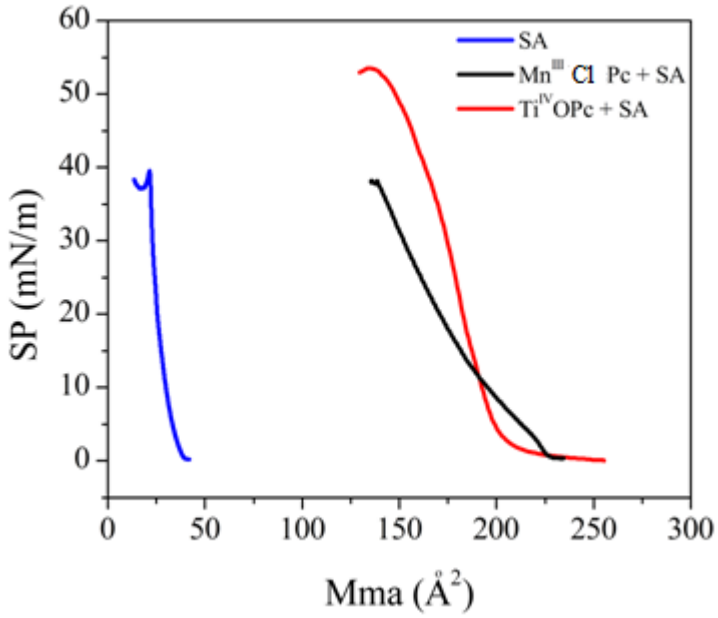


**Figure 3.13** Surface pressure ($\pi$)-area isotherm of $Mn^{III}$ClPc and $Ti^{IV}$OPc.

ITO/$Mn^{III}$ClPc and ITO/$Ti^{IV}$OPc were tested as ORR electrocatalyst and/or electrosensor in aqueous solution. **Fig. 3.14** shows the SWV responses of ITO/$Mn^{III}$ClPc electrode recorded in $H_2O/LiClO_4$ electrolyte bubbled with $O_2$ gradually.

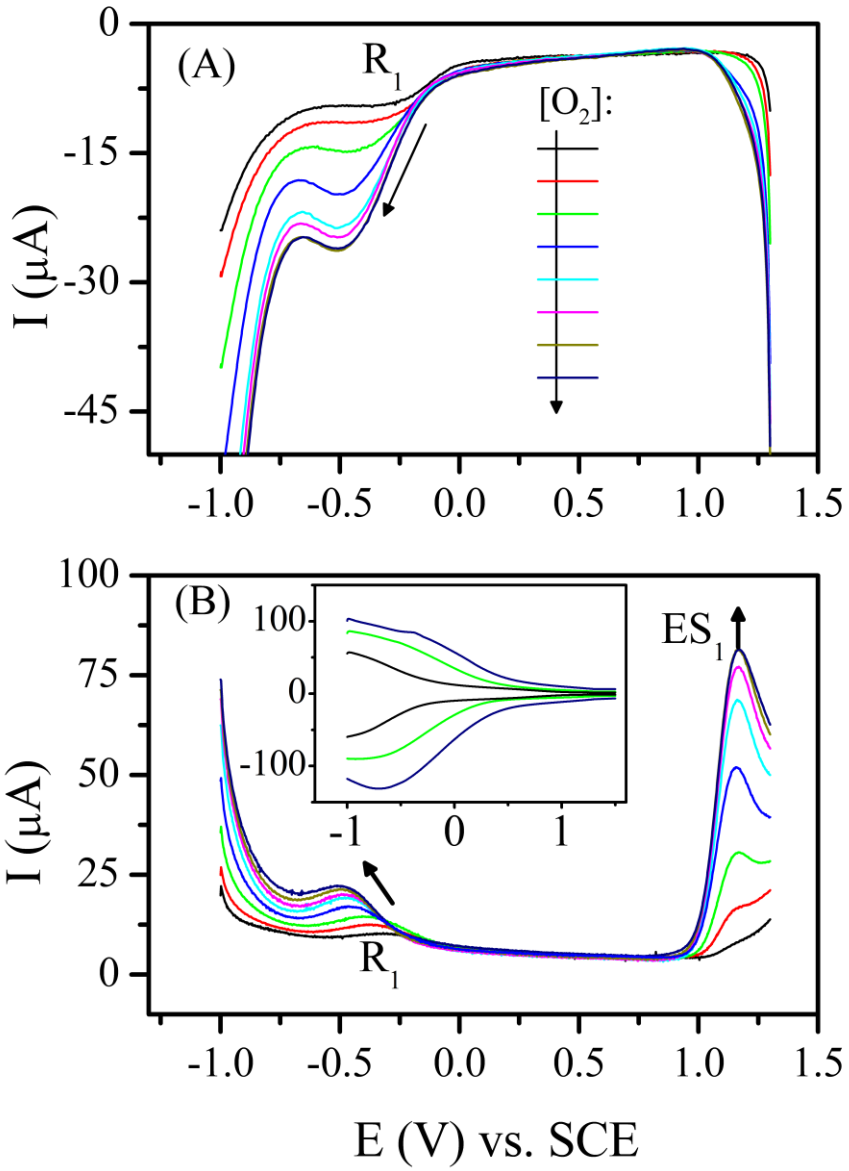


**Figure 3.14** SWV responses of ITO/$Mn^{III}$ClPc electrode recorded in $H_2O/LiClO_4$ bubbled gradually with $O_2$.

As shown in this figure, $Mn^{III}ClPc$ behaves as an ORR electocatalyst in the aqueous solution as a solid film. Since over potential of ORR decreases about 0.20 V with respect to the bare ITO electrode **Fig. 3.14b inset**. Recording of an anodic peak ($ES_1$) at 1.16 V with increasing current intensity with respect to the increasing $O_2$ concentration illustrates the sensor activity of the complex in aqueous solution. Similar SWV responses are also observed with ITO/$Ti^{IV}$OPc electrode **(Fig. 3.15)**.

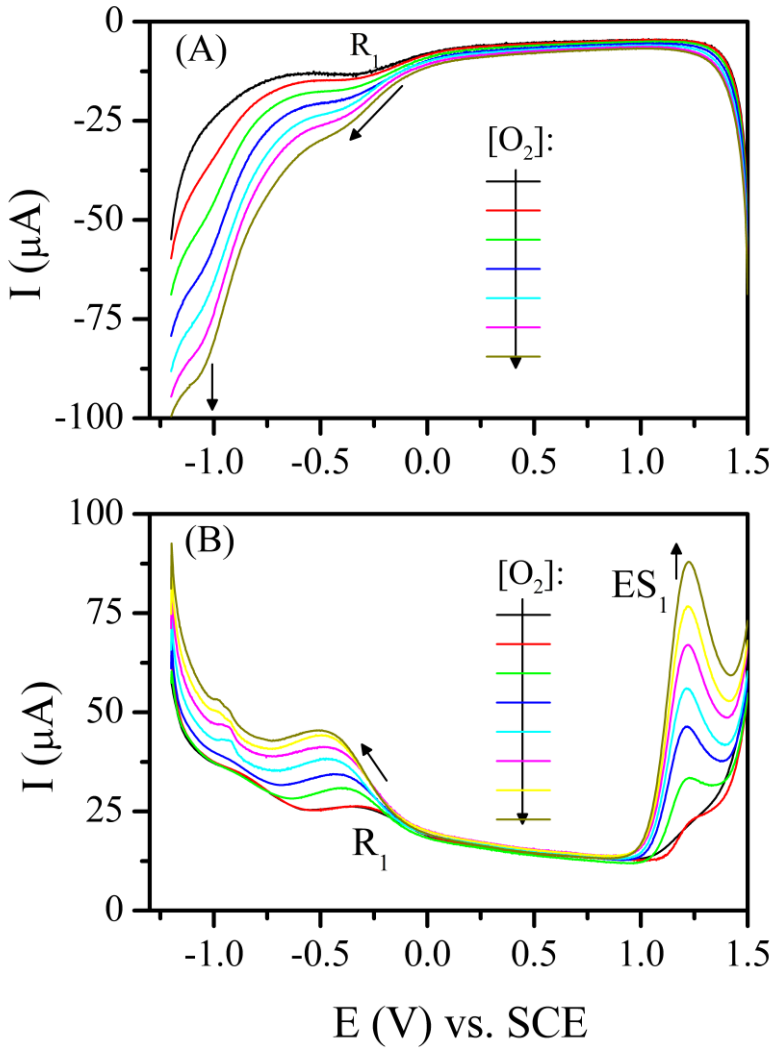


**Figure 3.15** SWV responses of ITO/$Ti^{IV}$OPc electrode recorded in $H_2O/LiClO_4$ bubbled gradually with $O_2$.

ORR reaction on ITO/$Ti^{IV}$OPc electrode gives a couple at around -0.30 V with a negative potential shift during increasing $O_2$ concentration. At the same time, $ES_1$ peak representing the sensing activity of the complex is observed at 1.23 V with increasing current intensity with respect to increasing $O_2$ concentration. The differences between ITO/$Mn^{III}$ClPc and ITO/$Ti^{IV}$OPc are the magnitude of the over potential decreases and the peak potentials of $ES_1$ peaks.

### 3.2. 3-(4-methylphenyl)-5-phenyl-4H-1,2,4-triazol-4-yl]imino}methyl)phenoxy] Substituted Phthalocyanines (NiPc, ZnPc, CoPc, and TiOPc)

Tailoring various substituents to the periphery and/or nonperiphery of phthalocyanines and different metal centers in the core of the Pc ring alter the redox activity of the complexes [102]. Each new complex may have extraordinary redox behaviors due to the effect of new substituents and metal centers. For this reason, electrochemical behavior of a newly synthesized complex should be determined to decide their possible application fields with respect to the electrochemical responses. Thus, the electrochemical and spectroelectrochemical features of NiPc, ZnPc, CoPc and TiOPc complexes bearing tetrakis3-(4-methylphenyl)-5-phenyl-4H-1,2,4-triazol-4-yl]imino}methyl)phenoxy] substituent were investigated in this section **(Fig. 3.16)**.

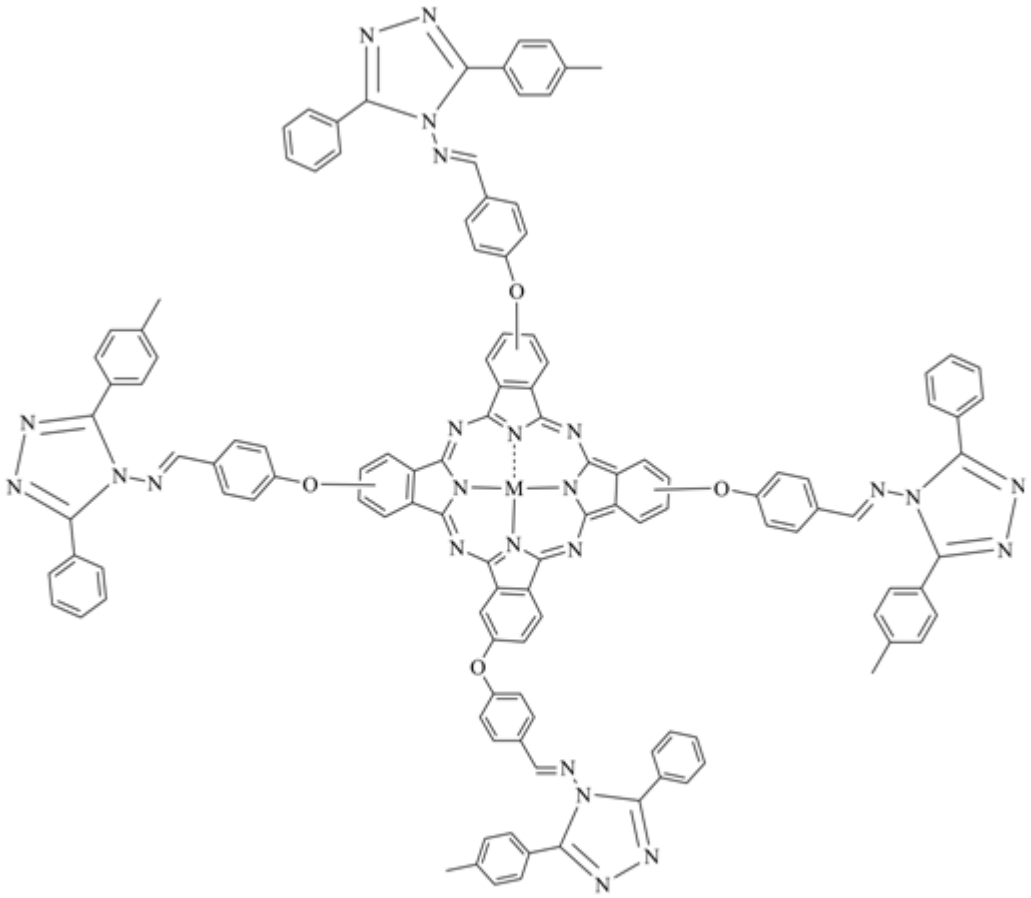


**Figure 3. 16** The structure of tetrakis 3-(4-methylphenyl)-5-phenyl-4H-1,2,4-triazol-4-yl]imino}methyl)phenoxy]phthalocyanines NiPc, ZnPc, CoPc and TiOPc.

### 3.2.1. Voltammetric Measurements

CV and SWV responses of the MnPc complexes were carried out in DCM/TBAP electrolyte system on a Pt working electrode to determine their electrochemical properties. CV and SWVs were analyzed and the results, the assignments of the redox couples and estimated electrochemical parameters including the half-wave peak potentials ($E_{1/2}$), ratio of anodic to cathodic peak currents ($I_{p,a}/I_{p,c}$), peak to peak potential separations ($\Delta E_p$), peak with ($\Delta E_p$), d$E_p$/dν values, and difference between the first oxidation and reduction processes ($\Delta E_{1/2}$) are tabulated in **Table 3.2**.

Among the complexes, NiPc and ZnPc have redox inactive metal centers, thus redox behaviors of these complexes are different than those of the CoPc and TiOPc, since CoPc and TiOPc give metal based reduction reactions due to the redox activity of the metal centers of these complexes. The general similarity of the complexes is aggregation behaviors of the complexes, which is reflected with the splitting of the redox processes due to the existence of equilibrium between aggregated and disaggregated species.

**Table 3.2** Voltammetric data of tetrakis 3-(4-methylphenyl)-5-phenyl-4H-1,2,4-triazol-4-yl]imino}methyl)phenoxy] substituted the complexes. vs. SCE.

| Complexes | Redox processes | [a] $E_{1/2}$ (V) | [b] $\Delta E_p$ (mV) | [c] $I_{p,a}/I_{p,c}$ | [d] $\Delta E_{1/2}$ |
|---|---|---|---|---|---|
| **NiPc** | $[Ni^{II}Pc^{2-}] / [Ni^{II}Pc^{1-}]^{+1}$ | 0.87 | 90 | 1.23 | 1.46 |
| | $[Ni^{II}Pc^{2-}] / [Ni^{II}Pc^{3-}]^{-1}$ | -0.74 (-0.59)[e] | 80 | 1.26 | |
| | $[Ni^{II}Pc^{3-}]^{-1} / [Ni^{II}Pc^{4-}]^{-2}$ | -1.07 | 62 | 0.95 | |
| **ZnPc** | $[Zn^{II}Pc^{2}] / [Zn^{II}Pc^{1-}]^{+1}$ | 0.79 (0.62)[e] | … | 0.94 | 1.49 |
| | $[Zn^{II}Pc^{2}] / [Zn^{II}Pc^{3-}]^{-1}$ | -0.87 | 61 | 0.94 | |
| | $[Zn^{II}Pc^{3-}]^{-1} / [Zn^{II}Pc^{4-}]^{-2}$ | -1.18 | 120 | 0.79 | |
| **CoPc** | $[Co^{II}Pc^{1-}]^{+1} / [Co^{III}Pc^{1-}]^{+2}$ | 0.98 (1.13) [e] | 65 | 0.83 | 1.16 |
| | $[Co^{II}Pc^{2-}] / [Co^{II}Pc^{1-}]^{+1}$ | 0.69 (0.83) | 62 | 0.90 | |
| | $[Co^{II}Pc^{2-}] / [Co^{I}Pc^{2-}]^{-1}$ | -0.47 (-0.91)[e] | 200 | 0.85 | |
| | $[Co^{I}Pc^{2-}]^{-1} / [Co^{I}Pc^{4-}]^{-2}$ | -1.28 | 90 | 0.72 | |
| **TiOPc** | $[Ti^{IV}OPc^{2-}] / [Ti^{IV}OPc^{1-}]^{+1}$ | 0.90 | 120 | 0.86 | 1.45 |
| | $[Ti^{IV}OPc^{2-}] / [Ti^{IV}OPc^{3-}]^{-1}$ | -0.55 | 61 | 0.96 | |
| | $[Ti^{IV}OPc^{3-}]^{-1} / [Ti^{III}OPc^{3-}]^{-2}$ | -0.74 | - | - | |
| | $[Ti^{III}OPc^{3-}]^{-2} / [Ti^{III}OPc^{4-}]^{-3}$ | -0.92 | 63 | 0.87 | |
| | $[Ti^{III}OPc^{4-}]^{-3} / [Ti^{II}OPc^{4-}]^{-4}$ | -1.08 | - | - | |

**[a]:** $E_{1/2}$ values (($E_{pa}$+$E_{pc}$)/2) were given versus SCE) at 0.100 $Vs^{-1}$ scan rate. **[b]:** $\Delta E_p = E_{pa}-E_{pc}$. **[c]**:$I_{p,a}/I_{p,c}$ for reduction ,$I_{p,c}/I_{p,a}$ for oxidation processes. **[d]**:$\Delta E_{1/2}$ = $E_{1/2}$ (first oxidation)- $E_{1/2}$ (first reduction). **[e]**: $E_p$ value of aggregated species given in parentheses.

**Fig. 3.17** shows the CV and SWV responses of NiPc recorded in DCM/TBAP electrolyte system on a Pt working electrode. NiPc gives two reductions processes, $R_1$ at -0.74 V ($\Delta E_p$ = 80 mV and $I_{p,a}/I_{p,c}$ = 1.26) and $R_2$ at -1.07 V($\Delta E_p$ = 62 mV and $I_{p,a}/I_{p,c}$= 0.95). First reduction reaction $R_1$ is complicated with a shoulder wave $R'_1$ (at -0.59 V), which is assigned to the reduction of the aggregated species. Splitting of the first reduction reaction decreases the chemical and electrochemical reversibility's of the process. The first reduction reaction peaks are broader and have smaller peak currents than those of the second ones. These behaviors are resulted from the aggregation of the complex. After the $R_1$ couple aggregated species turn into monomeric ones, which give higher peak currents due to the increase in the concentration of the monomeric ones. The second reduction couple of NiPc is electrochemically reversible at all scan rates with respect to $\Delta E_p$, $E_{p/2}$, $dE_p/d\nu$ and $I_{p,a}/I_{p,c}$ values. The process is also chemically reversible and diffusion controlled with respect to [$I_p \alpha \nu^{1/2}$] and $I_{p,a}/I_{p,c}$ values [65]. NiPc gives an oxidation reaction, $O_1$ at 0.87 V ($\Delta E_p$ = 90 mV and $I_{p,a}/I_{p,c}$ = 1.23) in addition to the reduction reactions. However the $O_1$ process gives broad waves with small peak currents. This different behavior may be due to the aggregation of the complex. $\Delta E_{1/2}$ value (1.46 V) and $\Delta E_{1/2(R1-R2)}$ (0.33 V) values of NiPc are in agreement with the similar complexes in the literature. It is well known that MPcs having redox inactive metal center generally gives a HOMO-LUMO gap ($\Delta E_{1/2}$) between 1.40 and 1.70 V. These type complexes give first two reduction reactions after ca. -0.60 V versus SCE with about 0.30 V potential differences between these two processes ($\Delta E_{1/2(R1-R2)}$).

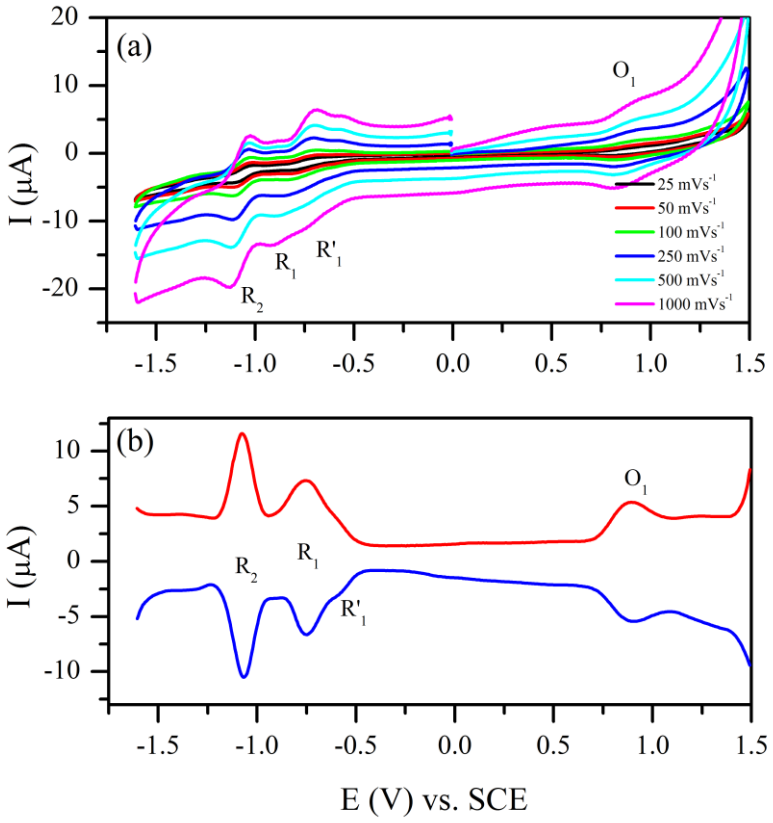


**Figure 3.17** (**a**) CVs of NiPc at various scan rates and (b) SWVs of NiPc recorded at 0.100 $Vs^{-1}$ scan rate on a Pt working electrode in DCM/TBAP.

**Fig. 3.18** represents the CV and SWV responses of ZnPc, which illustrates similar voltammetric responses with those of NiPc. Two reductions processes, $R_1$ at -0.87 V ($\Delta E_p$ = 61 mV and $I_{p,a}/I_{p,c}$ = 0.94) and $R_2$ at -1.18 V($\Delta E_p$ = 120 mV and $I_{p,a}/I_{p,c}$= 0.79) and one split oxidation process ($O'_1$ at 0.62 V and $O_1$ at 0.79 V) are observed with ZnPc. Main difference between these two complexes is the aggregation tendencies of them. While aggregation effect is clearly pronounced on the first reduction reaction of NiPc, the aggregation wave $R'_1$ recorded before $R_1$ is almost invisible for ZnPc. Thus, the $R_1$ of ZnPc is almost chemically and electrochemically reversible at all scan rates. Differently, effect of aggregation is more distinctive on the oxidation reaction of ZnPc. The oxidation reaction of ZnPc splits into two waves $O'_1$ assigned to the aggregated species and $O_1$ assigned to the monomeric species. Concentration effect on the SWVs of ZnPc illustrates the aggregation reaction of the complex more clearly as shown in **Fig. 3.19b**. $\Delta E_{1/2}$ value

(1.49 V) and $\Delta E_{1/2(R1-R2)}$ (0.31 V) values of ZnPc are in agreement with those of NiPc and the similar complexes in the literature [126-133]. When we compared $\Delta E_{1/2}$ values, it is clear that redox reaction of ZnPc shift about 0.130 V towards the negative potentials with respect to NiPc, due to the effective nuclear charge differences between $Zn^{II}$ and $Ni^{II}$ metal centers.

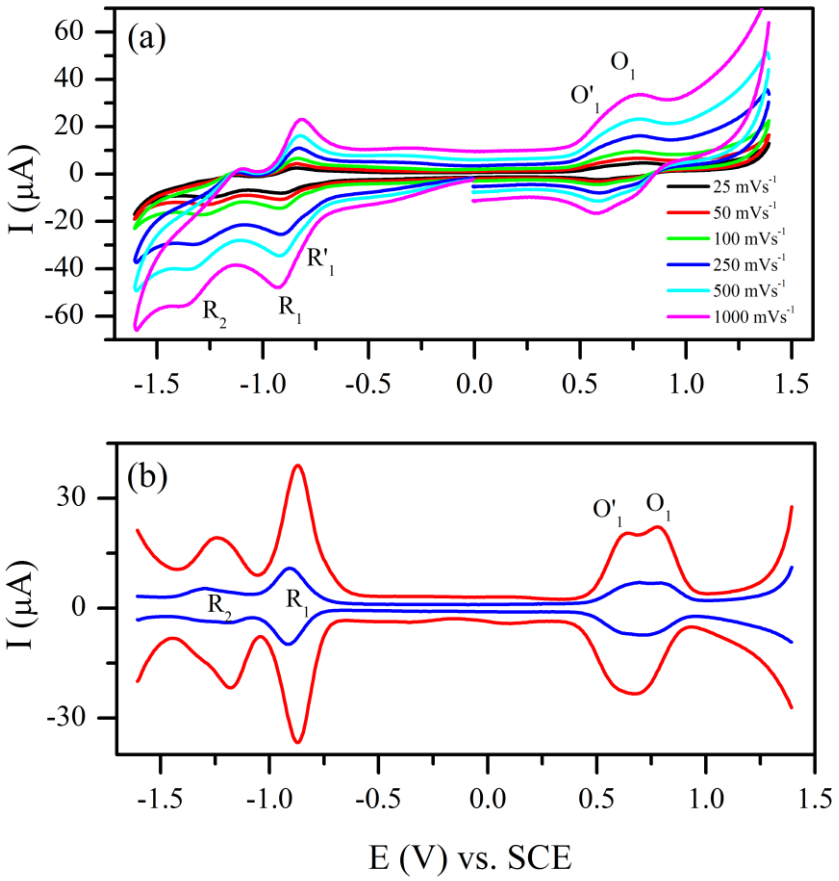


**Figure 3.18** (**a**) CVs of ZnPc at various scan rates and **(b)** SWVs of ZnPc recorded with two different concentrations at 0.100 $Vs^{-1}$ scan rate on a Pt working electrode in DCM/TBAP.

Electroactive nature of the $Co^{II}$ center of CoPc differentiates the redox responses of the complex from those of NiPc and ZnPc. Since CoPc gives a metal based reduction reaction $R_1$ at almost -0.47 V in addition to the Pc ring based reduction reaction at -1.28 V ($R_2$) (**Fig. 3.19)**. During the anodic potential scans CoPc illustrates two oxidation processes, $O_1$

at 0.69 V and $O_2$ at 1.13 V. Due to the aggregation of the complex, a reduction wave $R'_1$ at -0.92 V and oxidation waves $O'_1$ and $O'_2$ are also recorded. The first reduction reaction $R_1$ of CoPc deviates from reversibility at even slow scan rates with respect to $\Delta E_p$ and $I_{p,a}/I_{p,c}$ values ($\Delta E_p$ = 200 mV and $I_{p,a}/I_{p,c}$= 0.85 at 0.025 $Vs^{-1}$ scan rate). Moreover, $R_2$ of CoPc has electrochemically irreversible character and the oxidation processes have electrochemically reversible but chemically irreversible characters. SWVs of the complex illustrate these analyses results more clearly as shown in **Fig. 3.19b**. For instance, different peak current values of $R_1$ couple illustrate the chemical irreversibility of the process and presence of aggregation-disaggregation equilibrium coupled with this process. However, $R_2$ process seems as a chemically reversible process with respect to peak current ratio of the waves recorded with SWV.

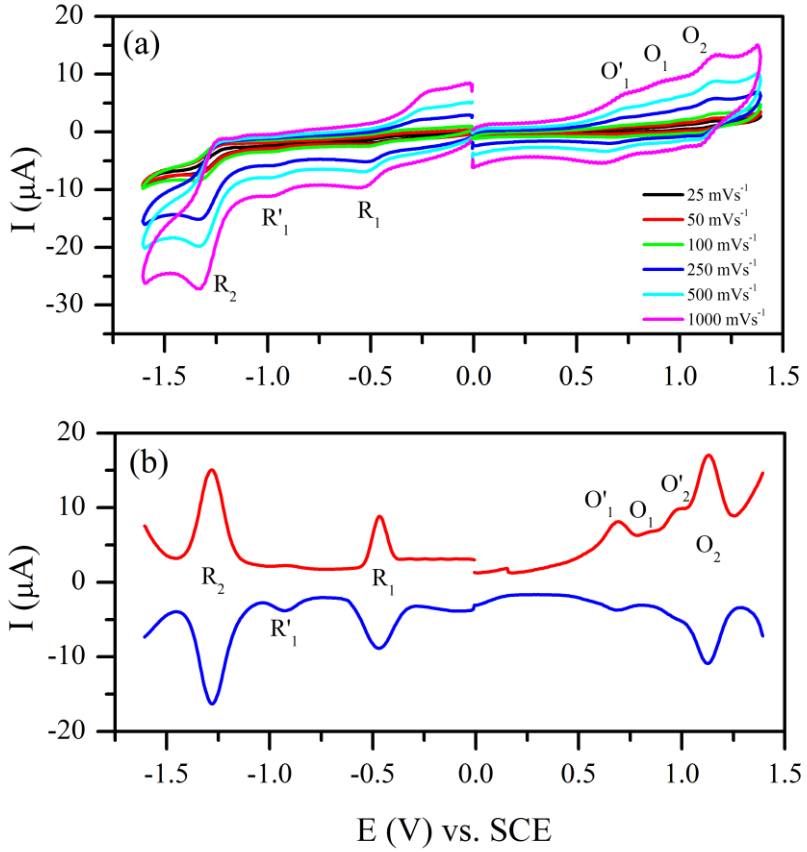


**Figure 3.19** (**a**) CVs of CoPc at various scan rates and **(b)** SWVs of CoPc recorded at 0.100 $Vs^{-1}$ scan rate on a Pt working electrode in DCM/TBAP.

TiOPc shows completely different electrochemical responses from all of the other complexes. Since two reduction reactions were observed with NiPc, ZnPc, and CoPc, TiOPc presents four reduction and one oxidation reactions (**Fig. 3.20)**.

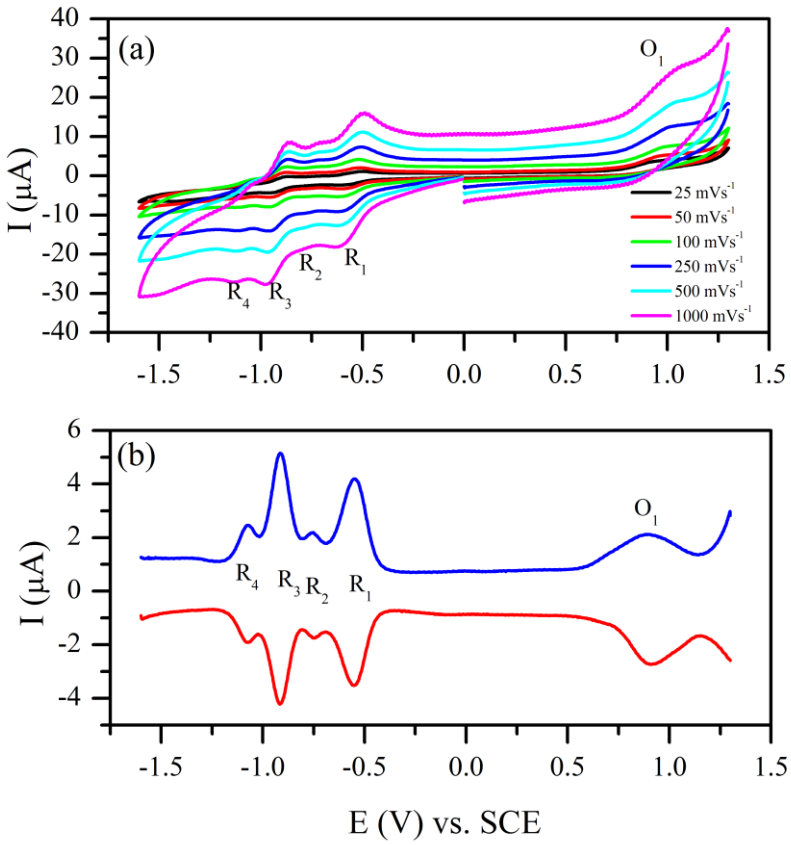


**Figure 3.20** (**a**) CVs of TiOPc at various scan rates and (b) SWVs of TiOPc recorded at 0.100 $Vs^{-1}$ scan rate on a Pt working electrode in DCM/TBAP.

While two reduction reactions ($R_1$ and $R_2$) have expected peak currents, other reduction couples ($R_3$ and $R_4$) have fivefold small peak currents than $R_1$ and $R_2$. These different peak currents may arise due to the different number of transferred electrons and/or different rates of the electron transfer reactions. It is well documented that electron transferring more than one is uncommon for MPc complexes [121,132]. Thus, all of these redox processes should be one-electron processes. However, peak current differences causes serious doubt about the electron transfer numbers. To clarify the number of electron transfers, CPC analyses of these peaks were performed. When the TiOPc solution was

electrolyzed at -0.60 V, the number of electron was found to be one for the first reduction peak. Electrolysis of a fresh TiOPc solution at -1.50 V gives the total number of electron transferred during reduction reactions as four. These CPC measurements indicate one electron character of each reduction reaction, even though they have different peak currents. These uncommon peak currents may be due to the different electron transfer rates of these processes. It is known that $Ti^{IV}O$ center of the TiOPc type complexes give metal based reduction reactions in addition to the Pc based processes [95-107,135,136]. These differently assigned processes may have different electron transfer rates. In situ spectroelectrochemical measurements (given below) were carried out to determine assignments of the redox reactions of TiOPc.

### 3.2.2. Spectroelectrochemical Measurements

In situ spectroelectrochemical measurements were carried out to execute assignments of the redox couples recorded in the CVs and SWVs of the complexes. NiPc and ZnPc complexes have redox inactive metal center, therefore spectral changes characterizing ring-based reduction reactions were only observed with these complexes. As a representative of these types complexes, in situ spectroelectrochemical and in situ electrocolorimetric analyses results were given in **(Fig. 3.21)**. **Fig. 3.21a** shows the in situ UV-Vis spectral changes and in situ recorded chromaticity diagram of ZnPc recorded during the first reduction process at -1.00 V constant potential. During this process, while the Q band at 675 nm decreases without shift, new bands are observed at ligand to metal charge transfer region (LMCT) (568, 865, and 956 nm). Well-defined isosbestic points are observed at 370, 600, and 700 nm in the spectra which indicates presence of one reduced species during the first reduction reaction. These spectral changes characterize the formation of monoanionic $[Zn^{II}Pc^{-3}]^{1-}$ species from the neutral $[Zn^{II}Pc^{-2}]$ [108-111]. While the neutral $[Zn^{II}Pc^{-2}]$ has cyan color (x = 0.2608 and y = 0.3349), its color changes to blue (x = 0.261 and y = 0.2898) after the first reduction process **(Fig. 3.21d)**. Under -1.40 V potential, the Q band continues to decrease and the band at 570 nm shifts to 552 nm with an increase. At the same time, while the band at 956 nm decreases, a new band enhances at 718 nm. These spectral changes are in consistent with the second reduction reaction of MPc type complexes and are easily assigned to $Zn^{II}Pc^{-3}]^{1-}$/ $Zn^{II}Pc^{-4}]^{2-}$ [108-

111]. These spectral changes cause to the color changes from blue to purple (x = 0.307 and y = 0.267) as shown in the chromaticity diagram **(Fig. 3.21b)**. During the oxidation of ZnPc, any significant spectral changes could not be observed. As the Q bands decrease slightly, a new band starts to enhance at 505 nm **(Fig. 3.21c)**.

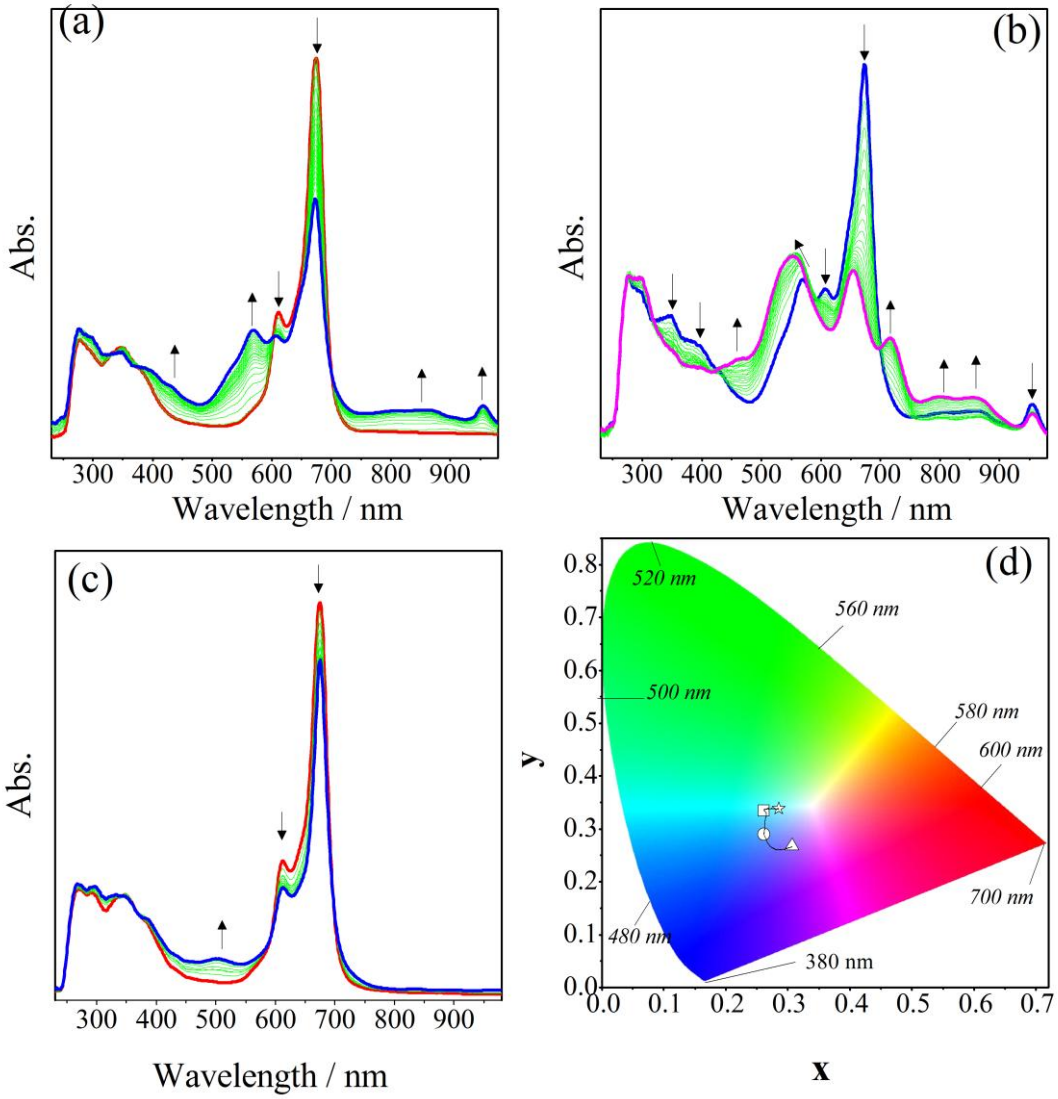


**Figure 3.21** In-situ UV-Vis spectral changes of ZnPc in DCM/TBAP. **a**) $E_{app}$= -1.00 V. **b**) $E_{app}$= -1.40 V. **b**) $E_{app}$= = 1.20 V. **d**) Chromaticity diagram (each symbol represents the color of electro-generated species; □: $[Zn^{II}Pc^{-2}]$, ○:$[ Zn^{II}Pc^{-3}]^{-1}$; △: $[Zn^{II}Pc^{-4}]^{-2}$; ☆: $[Zn^{II}Pc^{-1}]^{+1}$.

**Fig. 3.22** represents in situ spectroelectrochemical and in situ electrocolorimetric analysis results of CoPc. CoPc has redox active $Co^{II}$ center, therefore it gives different spectral changes than those of ZnPc and NiPc. In literature, spectroelectrochemical behaviors of various CoPc complexes were reported [102,122-124]. It was also represented in some studies that CoPc complexes illustrate characteristic spectral changes for the metal based and ring based electron transfer reactions [102,122-128]. The characteristic spectral changes recorded during the metal-based reduction reaction were shifting of the Q band to the longer wavelengths and observation of a new intense band between 400 and 550 nm. Surprisingly, CoPc, studied here shows different spectral changes than those of the similar CoPc complexes in the literature during the first reduction reaction as shown in **Fig. 3.22a**. Prior to potential application, the Q band at 665 nm has a shoulder at 612 nm due to the aggregation of the complex. Under -0.70 V potential, two distinct spectral changes were observed. First of all, common spectral changes assigned to $[Co^{II}Pc^{-2}]$/ $[Co^{I}Pc^{-2}]^{1-}$ process start to occur as shown in **Fig. 3.22a inset**. During this process, the Q band at 665 nm decreases and a new band at 702 nm starts to increase, a new band is observed at 465 nm. These spectral changes illustrate reduction of the monomeric CoPc species. Since, the band at 612 nm, which is assigned to the aggregated species, stays stable without any significant changes. Then the trend of the previous spectral behaviors starts to change. As the band at 465 nm continues to increase, the Q band at 665 nm increases in absorption intensity **(Fig. 322a)**. These spectral changes indicate the presence of aggregation-disaggregation equilibrium and turning the aggregated species into monomeric one due to the reduction reaction. At the end of the first reduction reaction, both the aggregated and monomeric species reduce to $[Co^{I}Pc^{-2}]^{1-}$ species. At the end of this reaction, greenish blue color (x = 0.2388 and y = 0.3137) of the complex turns into green color (x = 0.3012 and y = 0.3755) as shown in the chromaticity diagram. During the second reduction reaction, the Q band decreases in intensity, while the intensity of the region at around 540 nm increases. A light yellow color (x = 0.3676 and y = 0.3424) is observed at the end of the second reduction reaction. These spectral changes are characteristic changes for a Pc-ring based reduction reaction **(Fig. 3.22b)** [102,122-128]. **Fig. 3.22c** represents the Pc ring based oxidation of CoPc under the application of constant 0.80 V potential. During this process,

the Q band decreases without a shift, while new bands are observed at 530 and 740 nm. This process gives clear isosbestic points at 485 and 704 nm and a color changes from greenish blue to purple (x = 0.317 and y = 0.300).

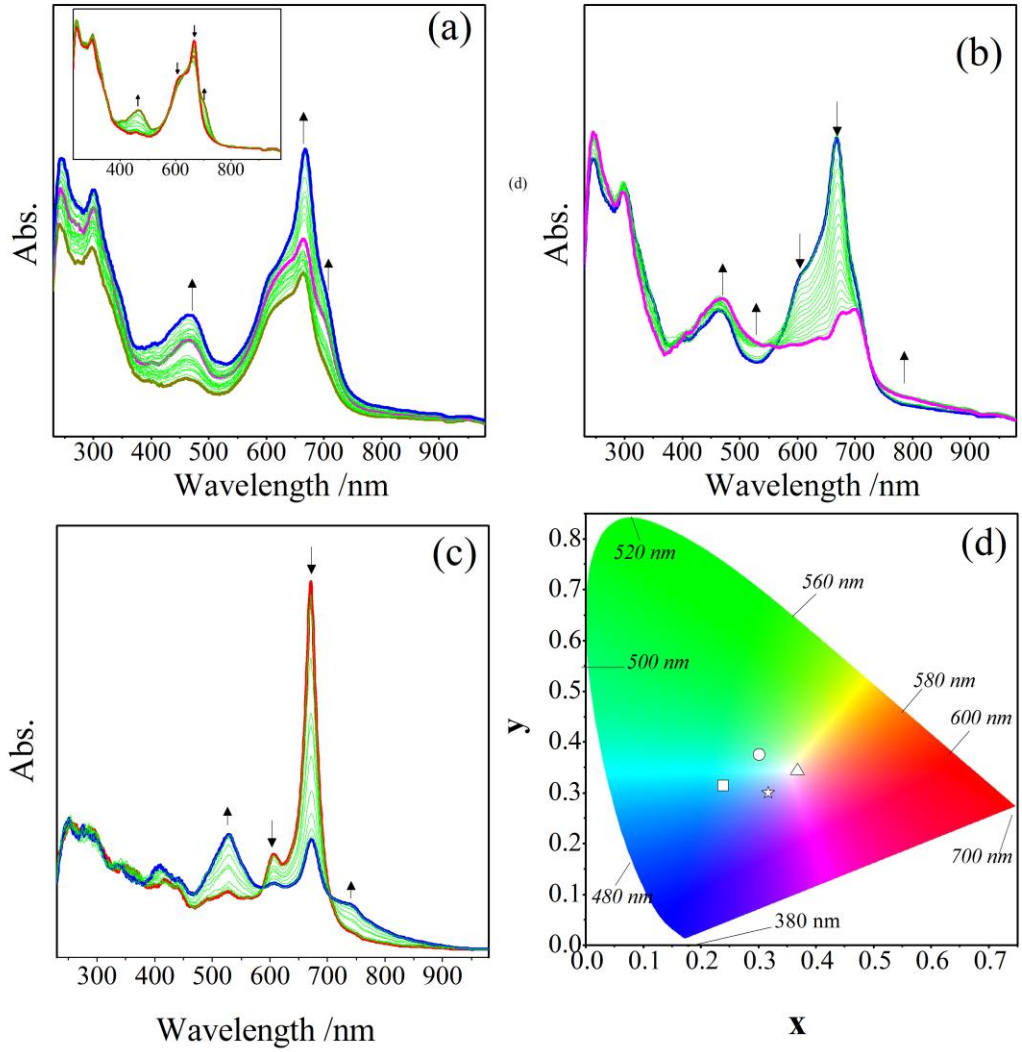


**Figure 3.22** In-situ UV-Vis spectral changes of CoPc in DCM/TBAP. **a**) $E_{app}$= -0.70 V. **b**) $E_{app}$= = -1.40 V. **c**) $E_{app}$= = 0.80 V. **d**) Chromaticity diagram (each symbol represents the color of electro-generated species; □: $[Co^{II}Pc^{-2}]$, ○:$[Co^{I}Pc^{-2}]^{-1}$; △: $[Co^{I}Pc^{-3}]^{-2}$; ☆: $[Co^{II}Pc^{-1}]^{+1}$.

**Fig. 3.23** represents in situ spectroelectrochemical and in situ electrocolorimetric analysis results of TiOPc. TiOPc has redox active $Ti^{IV}O$ center, thus it gives characteristics spectral changes for metal-based electron transfer reactions in addition to the ligand-based redox reactions. While peak assignments of CoPc, ZnPc, and NiPc do not change with redox inactive substituents, peak assignments of TiOPc type complexes alter with the substituents environment. For instance, while TiOPc bearing octakis(2-dimethylaminoethylsulfanyl moieties [116] has a metal-ring-metal-ring assignment, TiOPc bearing tetra[4-(thiophen-3-yl)-phenoxy] moieties [100] has a metal- metal-ring-ring assignments. Differently, TiOPc studied here shows a ring-metal-ring–metal assignment. Under -0. 60 V potential application, decreasing the Q band at 696 nm without shifting and observation of a new band at 712 nm are characteristic changes for a ring based redox reaction and assigned to $[TiO^{IV}Pc^{-2}]$ / $[TiO^{IV}Pc^{-3}]^{1-}$ process [134-136] **(Fig. 3.23)**. Clear isosbestic points at 408, 578, and 740 nm and a color change from bluish green (x= 0.2863 and y= 0.3551) to light green (x= 0.334 and y= 0.341) are observed during this process. Second reduction reaction of TiOPc ($R_2$) is a metal-based process ($[TiO^{IV}Pc^{-3}]^{1-}$/ $[TiO^{III}Pc^{-3}]^{2-}$) [95,99,100,116,117]. Since, the Q band of the complex shift from 696 to 674 nm while a new band is observed at 920 nm **(Fig. 3.23b)**. Simultaneously, the band at 712 nm disappears at the end of the second reduction reaction. Shifting of the Q band and observation of a new band at the metal to charge transfer (MLCT) region are characteristic changes for a metal based reduction reaction of MPc type complexes. Light green of the $[TiO^{IV}Pc^{-3}]^{1-}$ species turns into light yellow color (x= 0.341 and y= 0.344) after the second reduction reaction as shown in the chromaticity diagram given in **Fig. 3.23d**. Similarly third reduction reaction $R_3$ is a Pc ring-based reduction reaction ($[TiO^{III}Pc^{-3}]^{2-}$/ $[TiO^{III}Pc^{-4}]^{3-}$) [95,99,100,116,117]. During this reaction, the Q band decreases in intensity, while two new bands are observed at 600 and 752 nm **(Fig. 3.23b inset)**. Light yellow color of the $[TiO^{III}Pc^{-3}]^{2-}$ species turns into red color (x= 0.4078 and y= 0.3374) after the third reduction. Under -1.20 V potential application ($R_4$), the Q band at 674 nm shift to 634 nm and a new band is observed at 538 nm **(Fig. 3.23c)**. These changes are easily assigned to $[TiO^{III}Pc^{-4}]^{3-}$/ $[TiO^{II}Pc^{-4}]^{4-}$. At the end of the reduction reactions of TiOPc, a pink color (x= 0.3904 and y= 0.302) was observed as shown in the chromaticity diagram.

TiOPc decomposes during the oxidation reaction under constant potential application, since all bands decrease in absorption intensity without giving isosbestic points as shown in **Fig. 3.23a inset**.

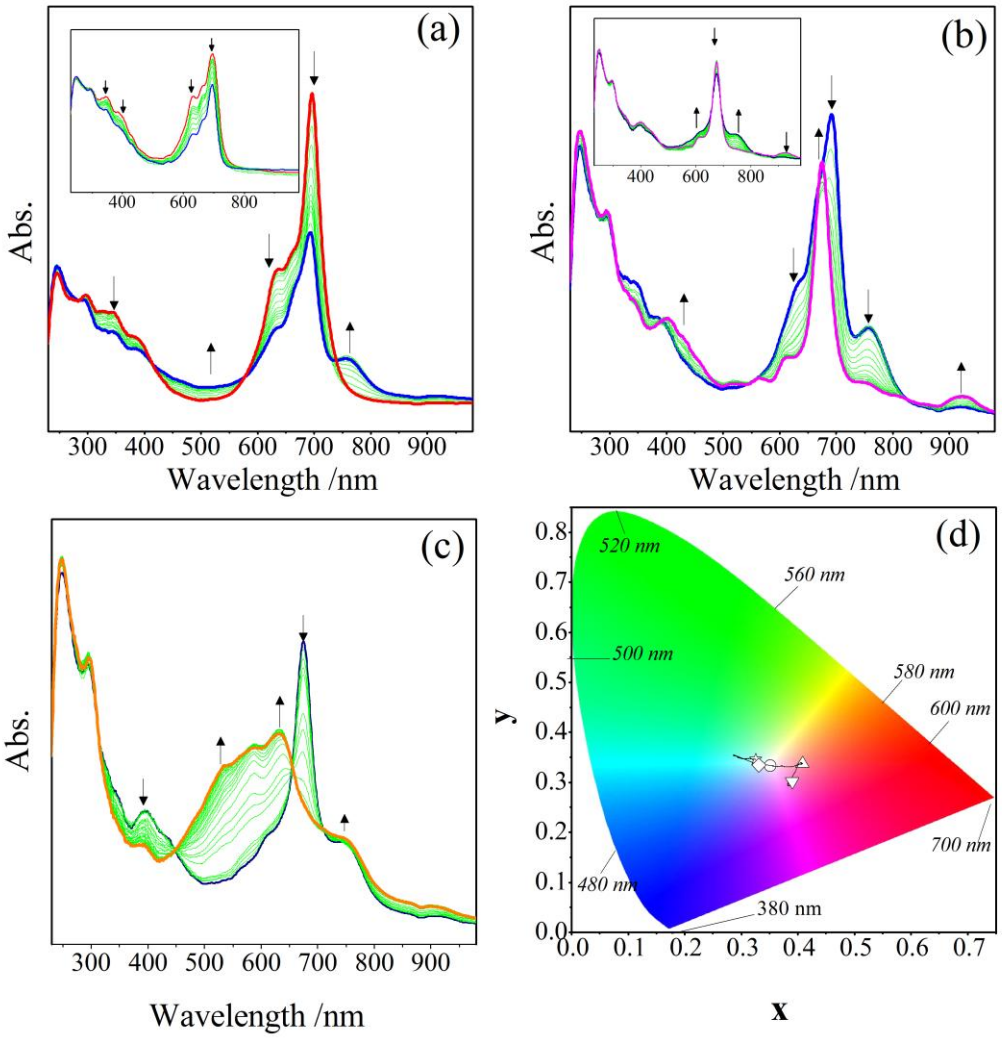


**Figure 3.23** In-situ UV-Vis spectral changes of TiOPc in DCM/TBAP. **a**) $E_{app}$= -0.60 V (inset: $E_{app}$= 1.00 V). **b**) $E_{app}$= -0.80 V (inset: $E_{app}$= -0.95 V). **c**) $E_{app}$= -1.20 V. **d**) Chromaticity diagram (each symbol represents the color of electro-generated species; □: $[Ti^{IV}OPc^{-2}]$, ◇:$[Ti^{IV}OPc^{-3}]^{-1}$; ○: $[Ti^{III}OPc^{-3}]^{-2}$; △: $[Ti^{III}OPc^{-4}]^{-3}$; ▽: $[Ti^{II}OPc^{-4}]^{-4}$; ☆: $[Ti^{IV}OPc^{-1}]^{+1}$.

### 3.2.3. Electrochemical Oxygen Sensing Measurements

During the voltammetric and in situ spectroelectrochemical measurements, it is noticed that penetration of molecular oxygen in the electrolytes alters the redox responses of MPcs due to the interaction between $O_2$ and MPcs. Due to this interaction, MPcs were used as electrocatalyst for the oxygen reduction reaction in different media. It was reported that MPcs having redox active metal centers, such as CoPc, MnPc and TiOPc, electrochemically catalyzed oxygen reduction reaction (ORR) [122,124,129-131]. It was also introduced that tailoring the MPcs with different substituents alters the catalytic activities of MPcs. Here we represent the electrocatalytic activity of MPcs having tetrakis 3-(4-methylphenyl)-5-phenyl-4H-1,2,4-triazol-4-yl]imino}methyl)phenoxy] substituent and substituent effects on the interaction between MPcs and molecular oxygen. During the electrocatalytic ORR measurements, we noticed that CoPc behaves as an electrosensor for molecular oxygen. CoPc represents similar SWV responses with those reported in some papers. This SWV responses could briefly represented like that; one electron reduced form of CoPc interact with $O_2$ and this interaction decreases the ORR potential and alters the second reduction reaction of CoPc. These voltammetric responses are well seen in **Fig. 3.24**. During the gradual increasing of $O_2$ in DCM/TBAP electrolyte, while the $R_1$ peak slightly decreases in current intensity, $O_2$ gives ORR at -1.25 V. Moreover $R_2$ peak of CoPc at -1.50 V shifts to the negative potentials gradually. This voltammetric data supports the electrocatalytic activity of CoPc for the ORR. In addition to the electrocatalytic activity, SWV responses of CoPc recorded at the anodic potentials of DCM/TBAP electrolyte during the gradual $O_2$ addition indicate the electrosensing activity of the complex. Without $O_2$, CoPc gives two oxidation couples $Oxd_1$ at 1.0 V assigned to the Pc based oxidation and $Oxd_2$ at 1.20 V assigned to the metal based oxidation process of CoPc. When $O_2$ concentration increases gradually, both of the anodic and cathodic peaks of $Oxd_2$ couple decrease and a new couple is recorded at just positive side of the $Oxd_2$ couple. Finally, $Oxd_2$ couple shifts form 1.20 V to 1.40 V due to the interaction with $O_2$. This voltammetric data indicates that CoPc interacts with $O_2$ and this interaction shifts the metal based oxidation couple of the CoPc to the positive potentials as a result of the increasing $O_2$ concentration.

These voltammetric results represent usability of CoPc as an oxygen sensor. Observation of a new couple at 1.40 V shows selectivity of the complex for $O_2$ and the peak current increases of this new couple and peak current decreases of $O_2$ couple could be used to determine the amount of $O_2$ in the solution.

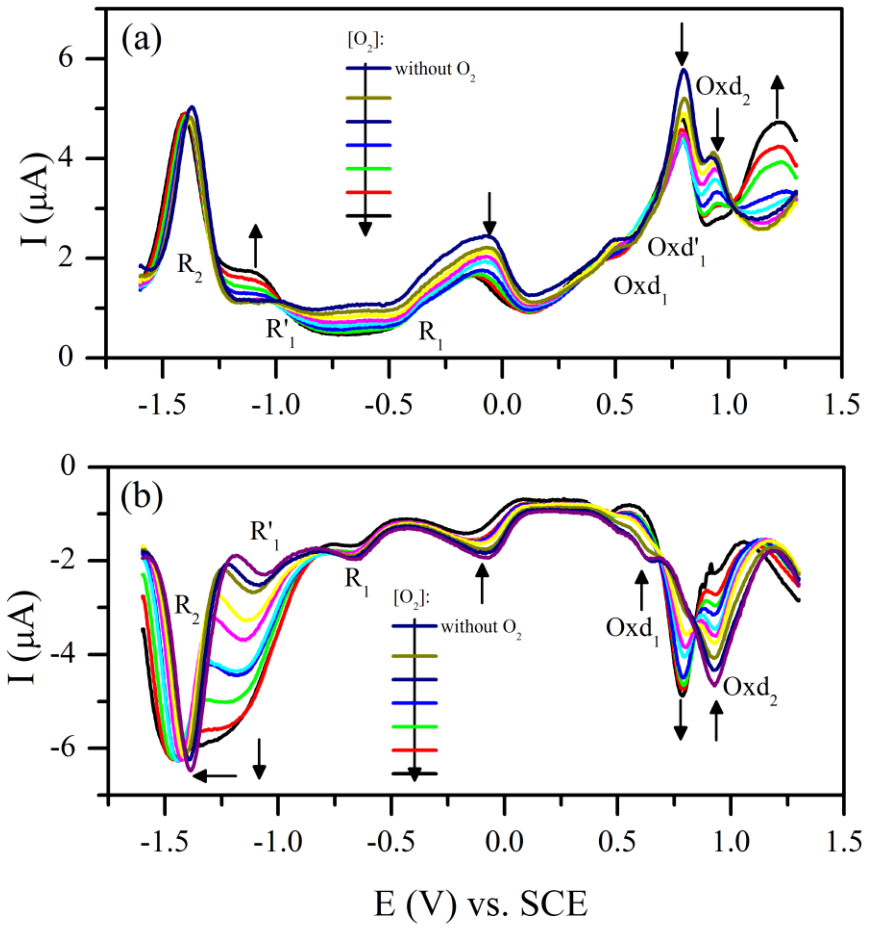


**Figure 3.24** SWV responses of CoPc recorded gas at 0.100 $Vs^{-1}$ scan rate on a Pt working electrode in DCM/TBAP which is gradually bubbled with $O_2$.

$O_2$ interaction of ZnPc, NiPc, and TiOPc were also tested. While ZnPc and NiPc did not interact with oxygen, the reduction processes of TiOPc alter due to the interaction with $O_2$ as shown in **Fig. 3.25**. With gradual increase in $O_2$ concentration, the metal-based reduction peaks ($R_2$ and $R_4$) of TiOPc disappear immediately, while the peaks of the first Pc based reduction couple $R_1$ decrease slightly in current intensity.

Moreover, the second Pc based reduction peaks $R_3$ shift to the negative potentials gradually. At the same time, ORR peaks are observed at -1.15 V.

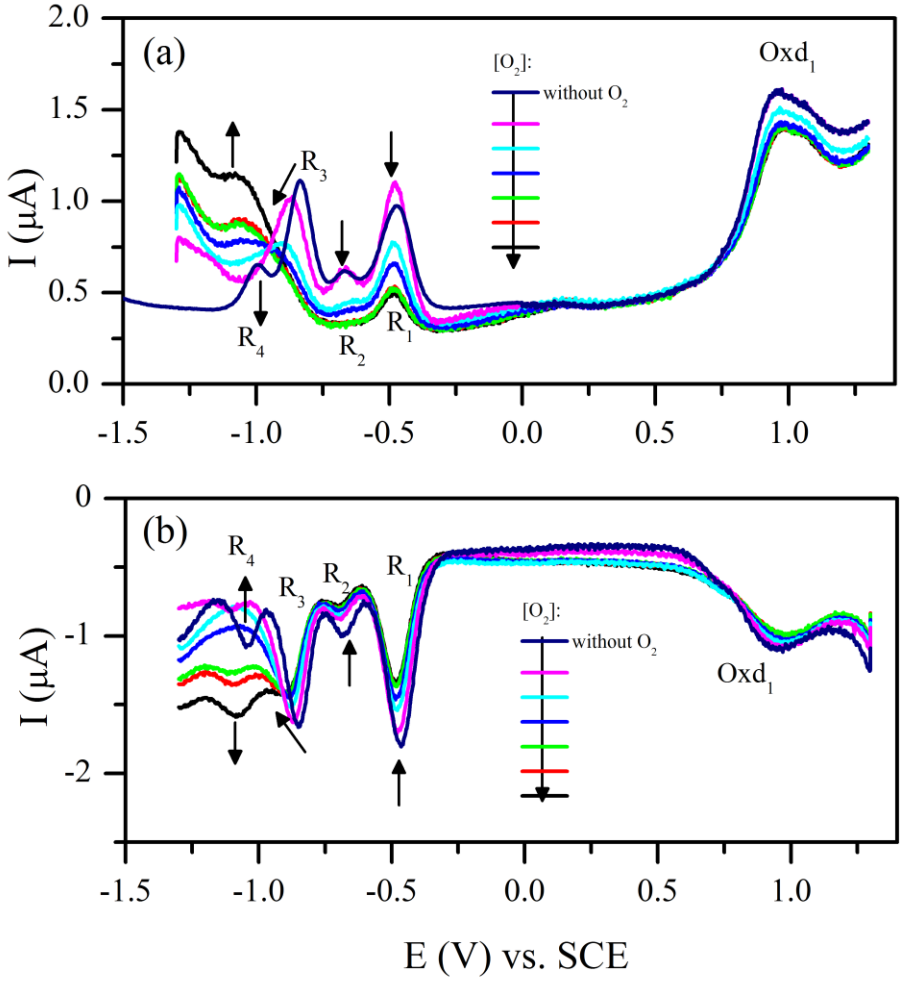


**Figure 3.25** SWV responses of TiOPc recorded gas at 0.100 $Vs^{-1}$ scan rate on a Pt working electrode in DCM/TBAP which is gradually bubbled with $O_2$.

These voltammetric data indicate that $Ti^{IV}O$ center of the TiOPc interacts with $O_2$ and this interaction catalyzes the ORR. While oxidation processes of CoPc are altered with increasing $O_2$ concentration, oxidation peaks of TiOPc do not change. Consequently, while CoPc and TiOPc behave as ORR electrocatalysts, only CoPc among the complexes studied here could be used as an oxygen sensor.

### 3.3. Octakis diethylamino-phenoxy Substituted Phthalocyanines ($H_2$Pc-odea, $Co^{2+}$ (CoPc-odea) and $Cu^{2+}$ (CuPc-odea)

The electropolymerization mechanisms and electrochemical responses of the insolubility of the electropolymerized films of MPcs bearing octakis diethylamino-phenoxy (odea) groups; $2H^+$ ($H_2$Pc-odea); $Co^{2+}$ (CoPc-odea) and $Cu^{2+}$ (CuPc-odea) were investigated **(Fig. 3.26)**.

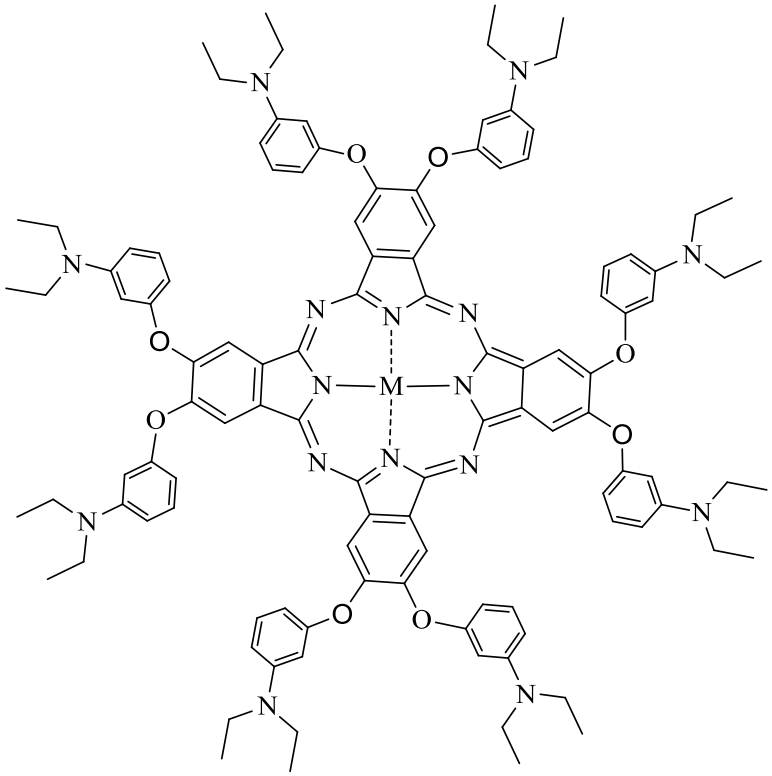

M: $2H^+$ ($H_2$Pc-odea), $Cu^{2+}$(CuPc-odea), $Co^{2+}$ (CoPc-odea)

**Figure 3.26** The Structure of metallophthalocyanines bearing octakis-[3-(diethylamino)phenoxy]-substituents (MPc-odea).

First, ITO/MPc-odea electrodes were constructed. Then electrochromic properties of the ITO/MPc-odea electrodes were studied in detail with various electrochemical, in-situ spectroelectrochemical and in-situ electrocolorimetric analysis methods.

### 3.3.1 Electrochemistry and Electropolymerization of the Complexes in Solution

Previous studies about the synthesis, electrochemical characterization and application of MPcs bearing redox active and/or electropolymerizable diethylamino-phenoxy substituents for usage in different electrochemical technologies was originated [44][138-140]. These complexes were especially synthesized, since diethylamino moieties on the substituents of a complex have electropolymerization potential [138,140]. As reported and illustrated in literature, similar complexes bearing different amino moieties and different number of amino groups, the type and number of alkyl on the amino moieties, the type and length of the chain between Pc ring and the amino groups, and finally type of the metal center of the Pc ring alter basic electrochemical responses of the MPc complexes [44][138-140]. In this study, the electrochemical properties of MPcs bearing octakis diethylamino-phenoxy susbtituents were studied [44]. It is aimed to facilitate electropolymerization ability of the complexes by using more electropolymerizable amino groups. Here modified ITO electrodes based on the electropolymerized MPc complexes were constructed and characterized in solution and in solid states and finally the electrochromic responses of the electropolymerized films of these complexes were examined.

Three different complexes, metal free octakis-[3-(diethylamino)phenoxy]-phthalocyanine ($H_2$Pc-odea ), copper (II) octakis-[3-(diethylamino)phenoxy]-phthalocyanine (CuPc-odea ) and cobalt (II) octakis-[3-(diethylamino)phenoxy]-phthalocyanine (CoPc-odea) were studied to illustrate the effects of the Pc core to the electrochemical and electrochromic responses of the complexes.

**Fig.3.27** shows CVs $H_2$Pc-odea in DCM/TBAP electrolyte system on GCE working electrode at 0.10 $Vs^{-1}$ scan rate. $H_2$Pc-odea gives two reversible reduction reactions $Red_1$ at-0.58 and $Red_2$ at -0.88 V at the cathodic side of the voltammogram. CPC analyses of the redox processes showed one-electron transfer nature of these processes. Analyses of these peaks with respect to changes of $E_{1/2}$, $\Delta E_{p,}$ $I_{pa}/I_{pc}$, and $I_{pa}$ vs. $\nu^{1/2}$ values as a function of scan rate indicate electrochemical and chemical reversibility of the reduction processes. These voltammetric responses are in harmony with the reported data of the similar

complexes in the literature. However $H_2$Pc-odea gives uncommon oxidation responses during the oxidation reactions. $H_2$Pc-odea gives a Pc based oxidation peak $Oxd_1$ at 1.00 V. When vertex potential of CV is slid to more the positive potentials, an uncommon huge wave $Oxd_2$ is also observed at 1.25 V. Without observation of $Oxd_2$ wave, all redox processes are stable at all scan rates and no any peak is affected from other processes. However when the potential is slid to the positive side of $Oxd_2$ wave, behavior of all waves changes during consecutive CV cycles. Observed voltammetric responses resemble to electropolymerization reactions. In order to investigate electropolymerization mechanisms, two different potential excitation protocols were applied.

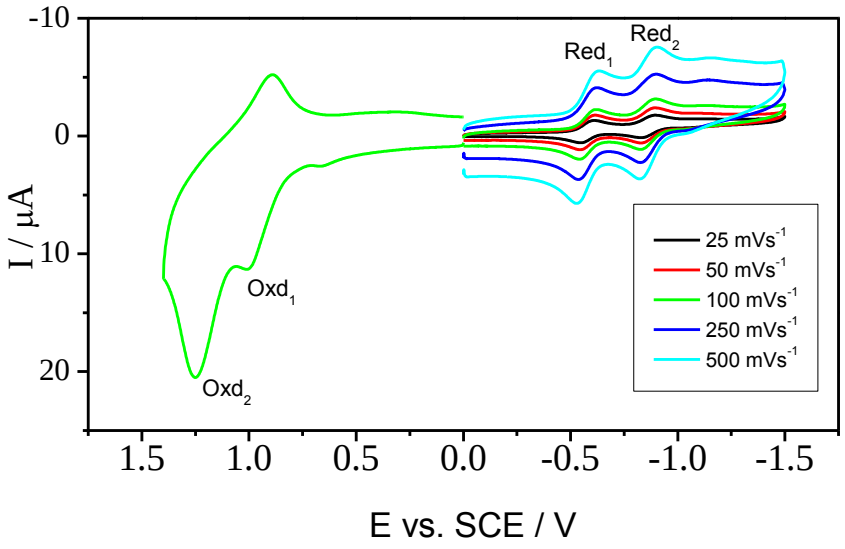


**Figure 3.27** CVs of $H_2$Pc-odea ($5.0\ 10^{-5}$ mol $dm^{-3}$) on a GCE at various scan rates in DCM/TBAP electrolyte system.

It is known that applied and/or scanned potential ranges alter polymerization reactions. Protocol 1 (*pro1*): Whole potential window of DCM/TBAP electrolyte system ($E_i$ =-1.50 V and $E_f$ = 1.50 V) was scanned at 0.10 $Vs^{-1}$ scan rate. Protocol 2 (*pro2*): anodic potential window of DCM/TBAP electrolyte system ($E_i$ = 0.0 V and $E_f$ = 1.50 V) was scanned at 0.10 $Vs^{-1}$ scan rate. **Fig.3.28a** represents the repetitive CV responses of $H_2$Pc-odea were recorded with "*pro1*" on GCE working electrode. These voltammetric responses are observed during the repetitive CV cycles: (*i*) Observation of new wave ($EP_1$) at around

0.62 V; (*ii*) increasing the peak current of $EP_1$ wave shifting towards positive potentials (up to 1.05 V); (*iii*) disappearance of the wave $Oxd_2$ at 1.25 V; (*iv*) increasing the peak current of both anodic and cathodic wave of $Oxd_1$ process; (*v*) disappearance of $Red_1$ and $Red_2$ processes; (v*i*) and finally observation of a new reduction wave ($EP_2$) at around -1.16 V with a shift towards negative potentials, as giving a huge anodic redox couple at around 0.70 V during the first CV cycle. All of these voltammetric responses indicate coating of $H_2$Pc-odea on the working electrode with an electropolymerization reaction. It is well known that observation of new waves with increasing peak currents as a function of the repetitive CV cycles show electropolymerization of the electroactive species on working electrode. As shown in **Fig.3.28a**, peak current increase continues until the 6$^{th}$ CV cycle.

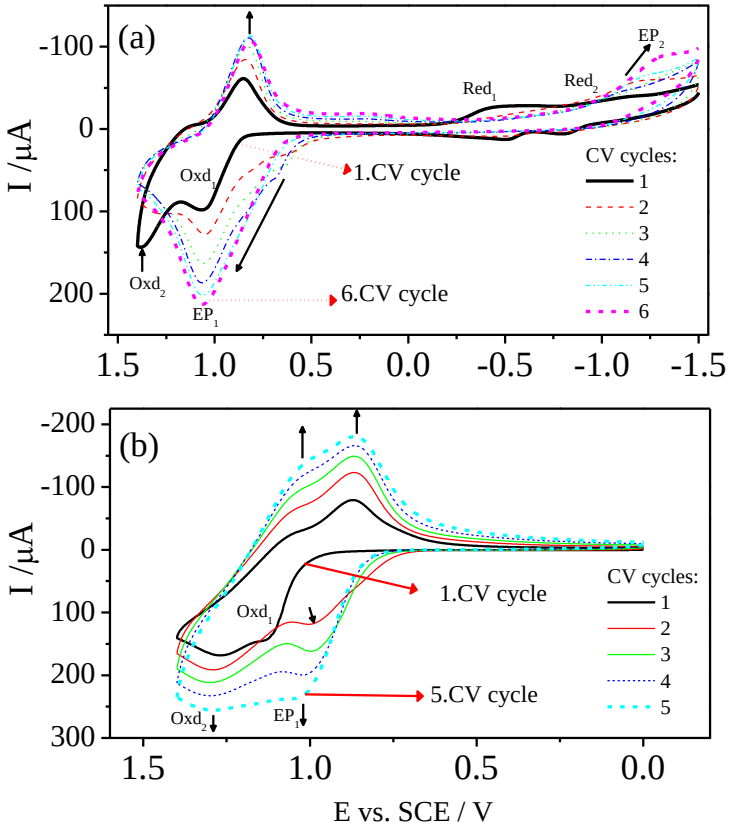


**Figure 3.28** Repetitive CVs of $H_2$Pc-odea (5.0 $10^{-5}$ mol $dm^{-3}$) on a GCE at 0.100 $Vs^{-1}$ scan rate (**a**) recorded in the whole potential windows and (**b**) recorded in anodic potential windows of DCM/TBAP electrolyte system.

After this point, peak current of the waves starts to decreases. This data indicates that electropolymerization process stopped after a particular film thickness. In order to investigate the effect of the applied potential range to the electropolymerization mechanism, repetitive CV responses of $H_2$Pc-odea were also measured with "*pro2"* **(Fig.3.28b)**. When **Fig.3.28a** ("*pro1"*) and **Fig.3.28b** ("*pro2"*) are compared with each other, it can be clearly distinguished that electropolymerization mechanisms alter, when different potential ranges are used for the electropolymerization reactions. While the electropolymerized film gives only one oxidation couple with "*pro1"*, it gives two oxidation couple in "*pro2"*. When $Oxd_1$ wave increases in current intensity in **Fig.3.28a**, it disappears and EP peak increases instead of $Oxd_1$ in **Fig.3.28b**. Moreover EP1 wave shifts in less extent and it is more reversible, when "*pro2"* is followed during the electropolymerization reaction. Thus, ITO/ $H_2$Pc-odea films were coated by using "*pro2"* and they were used for further characterization and application of modified ITO/ $H_2$Pc-odea electrode.

As shown in **Fig.3.29**, CuPc-odea shows very similar CV responses with those of $H_2$Pc-odea in DCM/TBAP electrolyte system on GCE working electrode at 0.10 $Vs^{-1}$ scan rate. CuPc-odea gives two reversible, diffusion controlled, and one-electron reductions at -0.69 V ($Red_1$) and at -0.97 V ($Red_2$) at the cathodic side of the voltammogram. It gives two oxidation reactions $Oxd_1$ at 0.95 V and $Oxd_2$ at 1.34 V.

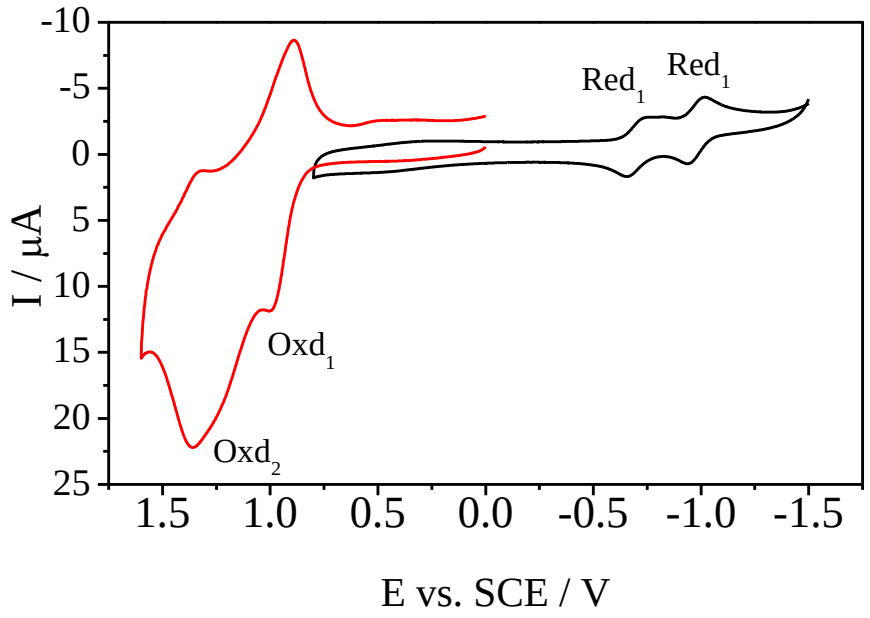


**Figure 3.29** CVs of CuPc-odea (5.0 $10^{-5}$ mol $dm^{-3}$) on a GCE at 0.100 $Vs^{-1}$ scan rate in DCM/TBAP electrolyte system.

Similarly CuPc-odea **(Fig.3.30)** is also electropolymerized during the oxidation reaction as $H_2$Pc-odea does. However, as shown in **Fig.3.30**, repetitive CV responses of CuPc-odea recorded with different potential ranges are rather different than those of $H_2$Pc-odea. While electropolymerized $H_2$Pc-odea film formed with "*pro1"* gives only EP1 wave after polymerization reaction, CuPc-odea film formed with "*pro1"* gives EP1 and *Oxd*$_2$ waves.

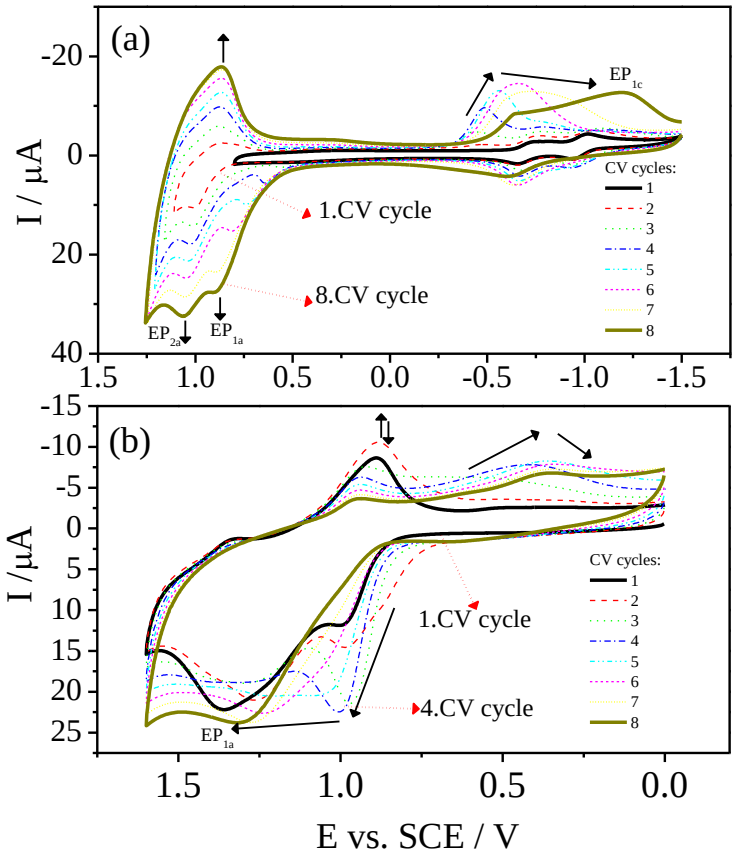


**Figure 3.30** Repetitive CVs of CuPc-odea (5.0 $10^{-5}$ mol $dm^{-3}$) on a GCE at 0.100 $Vs^{-1}$ scan rate (a) recorded in the whole potential windows and (b) recorded in anodic potential windows of DCM/TBAP electrolyte system.

Redox responses of $H_2$Pc-odea and CuPc-odea films prepared with "*pro2"* are also different from each other. These voltammetric responses indicate that changing $2H^+$ center of Pc ring with $Cu^{2+}$ cation influenced the electropolymerization reactions of the complexes in addition to the effects of the applied potential excitation types.

In order to investigate central metal effects, voltammetric and electropolymerization behaviors of CoPc-odea were also studied and compared with those of CuPc-odea . **Fig.3.31** illustrates CVs CoPc-odea in DCM/TBAP electrolyte system on GCE working electrode at 0.10 $Vs^{-1}$ scan rate. CoPc-odea gives a reversible metal based reduction reaction $Red_1$ at-0.02 V and a Pc ring based reduction reaction $Red_2$ at -1.30 V at the

cathodic side of the voltammogram. *Red$_1$* process of CoPc-odea is different from those of $H_2$Pc-odea and CuPc-odea due to the $[Co^{II}Pc^{2-}]$ / $[Co^{I}Pc^{2-}]^{-1}$ reduction process of the complex. It is known that $H_2$Pc-odea and CuPc-odea complexes can give only Pc ring based reduction reactions. Oxidation behaviors of CoPc-odea are similar with those of $H_2$Pc-odea and CuPc-odea. Like $H_2$Pc-odea and CuPc-odea, CoPc-odea also gives two oxidation couples (*Oxd$_1$* at 1.00 V and *Oxd$_2$* at 1.25 V) during positive potential scans. However, these waves have higher peak current than those of the reduction reactions, and CV responses of these wave changes continuously during consecutive CV scans. These behaviors illustrates electropolymerization of the complex, therefore electropolymerization mechanism of the complex was examined with repetitive CV measurements with "*pro1"* and "*pro2"*.

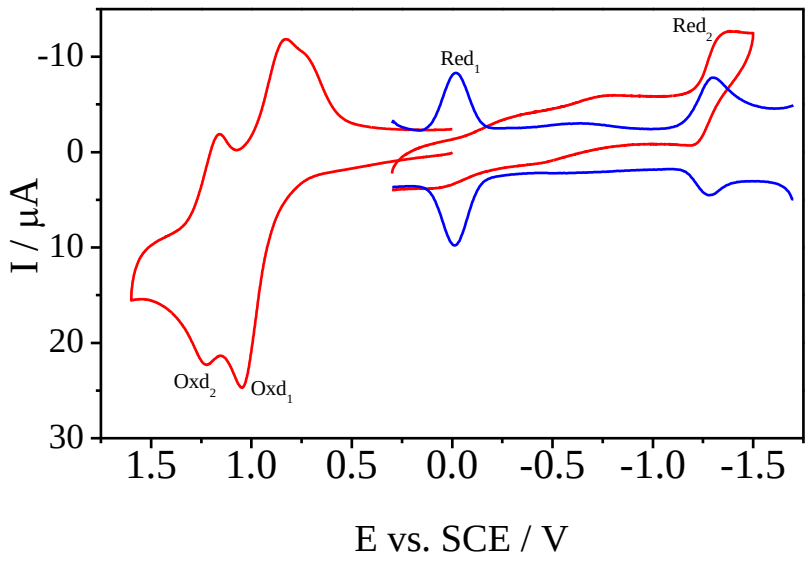


**Figure 3.31** CVs of CoPc-odea (5.0 $10^{-5}$ mol $dm^{-3}$) on a GCE at 0.100 $Vs^{-1}$ scan rate in DCM/TBAP electrolyte system.

As shown in **Fig.3.32**, while CV responses of CoPc-odea recorded with "*pro1"* **(Fig.3.32a)** are similar with those of $H_2$Pc-odea and CuPc-odea . Completely different responses are observed with "*pro2"* **(Fig.3.32b)**. Although peak current of polymerization processes ($EP_1$) of complexes stop just after a few CV cycles (5 cycles for $H_2$Pc-odea and 8 cycles for CuPc-odea), polymerization of CoPc-odea continues until 20$^{th}$ CV cycles.

During electropolymerization reactions, as $H_2$Pc-odea and CuPc-odea gives only $EP_{1a}$ polymer peaks, two polymer peaks $EP_{1a}$ and $EP_{2a}$ are observed during electropolymerization of CoPc-odea. This data illustrate that each complexes gives different polymerization reactions. It is known that same groups (amino moieties) on the complexes induce the electropolymerization reactions of the complexes. Although amino triggered polymers are formed for all complexes, due to the differences of the Pc core of the complexes, electropolymerization reactions give different voltammetric responses from each other.

General similarity of the electropolymerized films of the complexes is the insolubility. Although, all complexes are highly soluble in many organic solvents, DMSO, DCM, and AN, their electropolymerized films are insoluble in these solvents and water. Insolubility of the films makes application of these films possible in various electrolytic systems for different purposes. In order to decide the potential applications of the films formed with electropolymerization reactions, all complexes were coated on ITO electrodes with "*pro1*", and ITO/MPcs modified electrodes were constructed. Then ITO/MPcs electrodes were electrochemically characterized with CV measurements in MPc-free DCM/TBAP electrolyte. **Fig.3.33** illustrates CVs responses of ITO/MPcs electrodes recorded in MPcs-free DCM/TBAP electrolyte system at 0.10 $Vs^{-1}$ scan rate. As shown in **Fig.3.33**, each complex gives two oxidation reactions, $EP_{oxd1}$ and $EP_{oxd2}$. While oxidation reactions of ITO/$H_2$Pc-odea are completely irreversible, they are quasi reversible for ITO/CuPc-odea and ITO/CoPc-odea electrodes. As no color change was observable on the film of ITO/$H_2$Pc-odea electrode, cyan color of the films on ITO/CuPc-odea and ITO/CoPc-odea electrodes changed to reddish during oxidation reactions, which indicates possible electrochromic applications of the complexes.

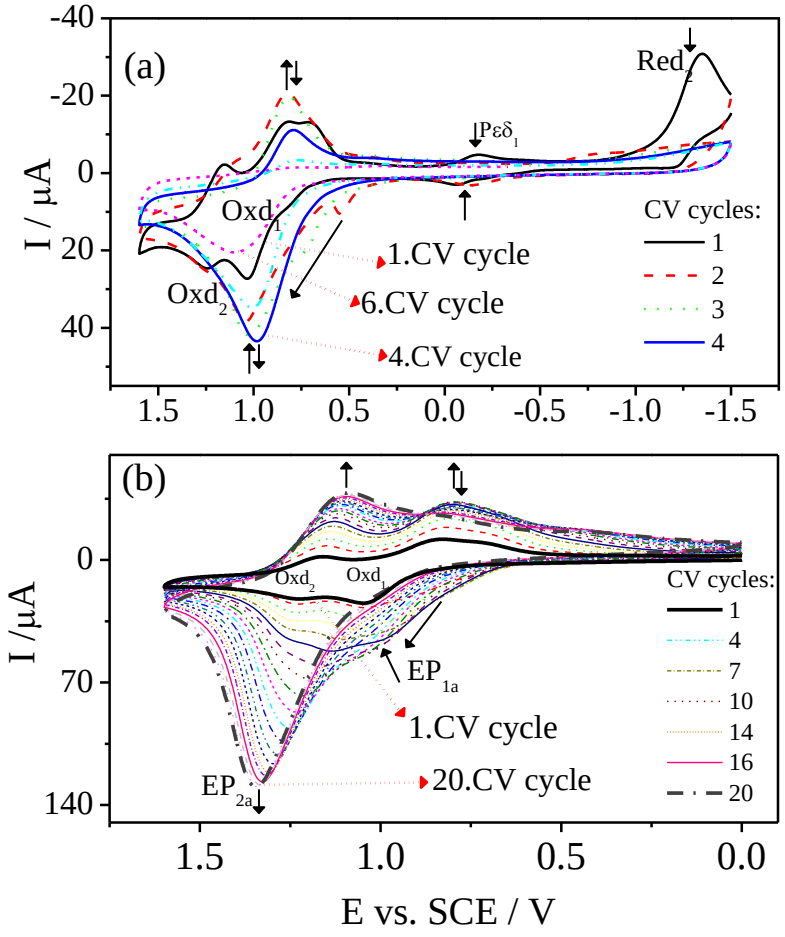


**Figure 3.32** Repetitive CVs of CoPc-odea (5.0 $10^{-5}$ mol $dm^{-3}$) on a GCE at 0.100 $Vs^{-1}$ scan rate (**a**) recorded in the whole potential windows and (**b**) recorded in anodic potential windows of DCM/TBAP electrolyte system.

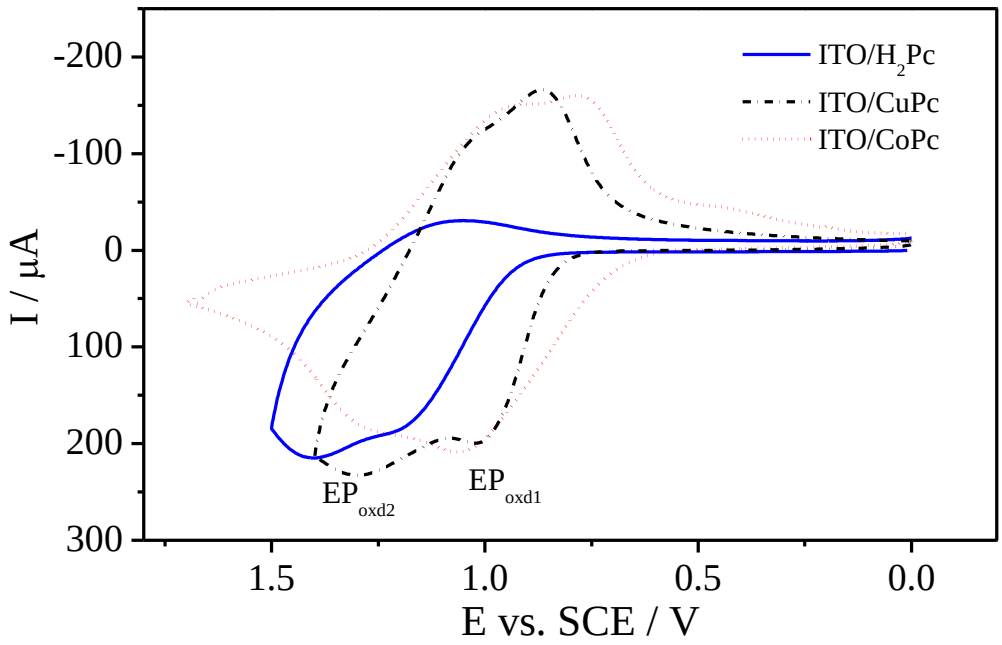


**Figure 3.33** CVs of ITO/MPcs-odea electrodes at 0.100 $Vs^{-1}$ scan rate in DCM/TBAP electrolyte system.

Electropolymerization of various MPcs bearing amino groups such as tetrakis diethyllamino-phenoxy-ethoxy substituents (MPcs-tdea) were investigated electrochemically and spectroelectrochemically in previous studies before. The electropolymerization properties and character of the electropolymerized films of octakis diethylamino-phenoxy substituted MPcs (MPcs-odea), were worked on here to investigate the effect of the number of the substituents to the electrochemical behaviors.

As shown in **Table 3.3**, there are distinct differences between the electrochemical and electropolymerization responses of MPcs-tdea and MPcs-odea. The main difference between these two MPc series is the reversibility of the electropolymerized films. ITO/MPcs-odea films give more reversible redox responses in DCM/TBAP electrolyte system than those of ITO/MPcs-tdea films. Improvement of the reversibility of the redox processes of functional species is one of the most desired properties for the practical applications.

**Table 3.3** Voltammetric data of octakis diethylamino-phenoxy and tetrakis diethyllamino-phenoxy-ethoxy substituted MPc complexes vs. SCE.

| Complexes | | ITO/MPcs oxidation waves $EP_{oxd2}$ | $EP_{oxd1}$ | Polymer waves $EP_{1a}$ | Redox reaction of monomeric complexes in solution $Oxd_1$ | $Oxd_2$ | $Red_1$ | $Red_2$ | Ref. |
|---|---|---|---|---|---|---|---|---|---|
| | [a]$E_{1/2}$ | 1.40 | 1.13 | (0.62-1.05)[f] | 1.25 | 1.00[d] (0.85)[e] | -0.58 | -0.88 | |
| **$H_2$Pc-odea** | [b]$\Delta E_p$ (mV) | - | 100 | | - | - | 65 | 64 | tw |
| | [c]$I_{p,a}/I_{p,c}$ | - | 0.25 | | - | - | 0.94 | 0.91 | |
| | [a]$E_{1/2}$ | 1.15 | 0.94 | (0.64-0.99)[f] | 1.34 | 0.95[d] (0.89)[e] | -0.69 | -0.97 | |
| **CuPc-odea** | [b]$\Delta E_p$ (mV) | 250 | 130 | | - | - | 61 | 65 | tw |
| | [c]$I_{p,a}/I_{p,c}$ | 0.86 | 0.85 | | - | - | 0.97 | 0.96 | |
| | [a]$E_{1/2}$ | 1.07 | 0.85 | (0.85-1.00)[f] | 1.03(0.83)[d] | 1.03[d] (0.83)[e] | -0.02 | -1.30 | |
| **CoPc-odea** | [b]$\Delta E_p$ (mV) | 200 | 125 | 1.3[g] | - | - | 150 | 80 | tw |
| | [c]$I_{p,a}/I_{p,c}$ | 0.90 | 0.88 | | - | - | 0.87 | 0.90 | |
| **$H_2$Pc-tdea** | [a]$E_{1/2}$ | | | | - | 0.76[d] (0.65)[e] | -0.76 | -1.08 | [139,143 |
| **NiPc-tdea** | [a]$E_{1/2}$ | | | | - | 0.86[d] (0.62)[e] | -0.97 | -1.26 | [139,143 |
| **CuPc-tdea** | [a]$E_{1/2}$ | | | | - | 0.85[d] (0.61)[e] | -0.96 | -1.22 | [139,143 |

**[a]:** $E_{1/2}$ values (($E_{pa}$+$E_{pc}$)/2) were given versus SCE and $Fc/Fc^+$ (in parenthesis) at 0.100 $Vs^{-1}$ scan rate. **[b]:** $\Delta E_p = E_{pa}-E_{pc}$. **[c]**: $I_{p,a}/I_{p,c}$ for reduction, $I_{p,c}/I_{p,a}$ for oxidation processes. **[d]**: $E_{pa}$ of wave recorded during the first CV cycle. **[e]**: $E_{pc}$ of wave recorded during the first CV cycle. **[f]**: $E_{pa}$ of the polymer film which shifted from the first value to the second one. **[g]**: $E_{pa}$ of the second oxidation of the polymer film.

### 3.3.2. Electrochromism of the Complexes

To investigate the possible usage of complexes as electrochromic materials, spectrochronocoulometric (SCC) analysis of the complexes were performed. For this purpose, firstly, in-situ spectroelectrochemical and in situ electrocolorimetric analysis of ITO/MPcs were carried out, if a ITO/MPcs film gives positive responses. Then the film was optimized with respect to basic parameters (potential ranges used for electropolymerization, film thickness, supporting electrolyte and solvent type, Pc core type of MPcs) to obtain desired electrochromic parameters.

First, ITO/$H_2$Pc-odea electrode was constructed with "*pro1"* and in-situ spectroelectrochemical and in situ electrocolorimetric analyses were carried out in DCM/TBAP electrolyte. Upon 1.50 V applied potential, spectrum and color of the film did not change. Changing film thickness and film preparation protocol did not give any spectral or color change under applied potential. This data indicates ITO/$H_2$Pc-odea electrode could not be used as electrochromic material. However, when ITO/CoPc-odea electrode was used instead of ITO/$H_2$Pc-odea electrode, significant spectral and color changes were observed as shown in **Fig. 3.34**. Without any potential application, ITO/CoPc-odea electrode gives two bands at 678 and 375 nm which are assigned to the Q and B bands of neutral CoPc-odea complex **(Fig. 3.34a)**. This spectrum of the complex gives blue color (point □ in **Fig. 3.34b**; x= 0.2821 and y = 0.3434) as shown in the chromaticity diagram. When 1.20 V is applied to ITO/CoPc-odea working electrode, spectrum of CoPc-odea immediately changes. As the Q band at 678 nm decreases in absorption intensity, two new bands are observed at 524 and 724 nm **(Fig. 3.34a)** and finally the blue spectrum is observed for the oxidized form of CoPc-odea. These spectral changes cause a color change from blue to red (point △ in **Fig. 3.34b**; x= 0.368 and y = 0.3054). When potential application is performed repetitively between 0.0 and 1.20 V with chronocoulometry (CC) technique, spectrum and color of the film is also changed reversibly between the spectrum and color of the neutral and oxidized CoPc-odea -odea .

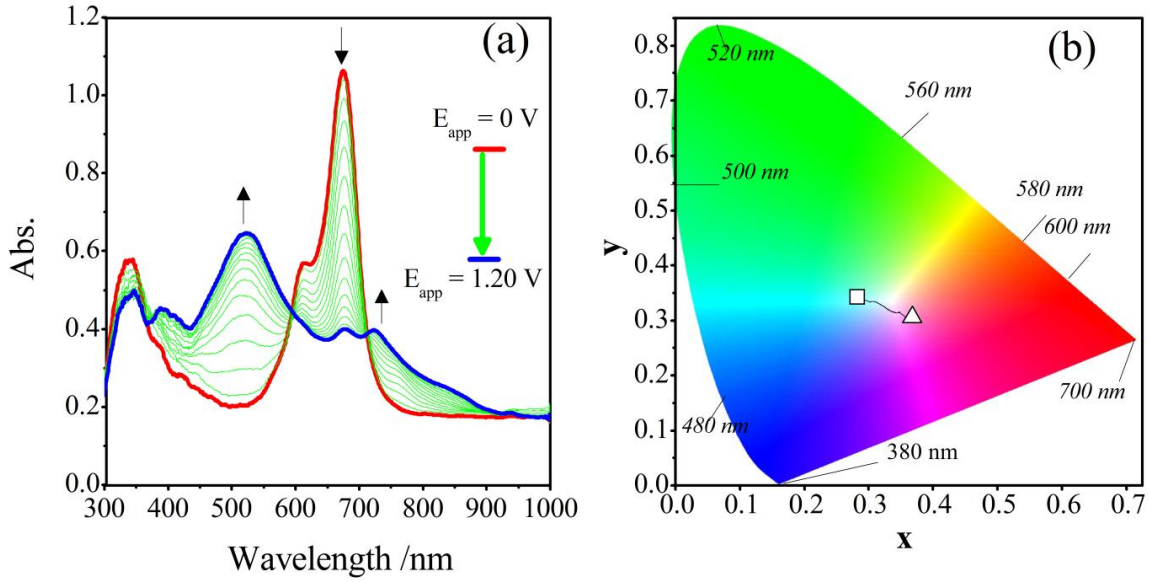


**Figure 3.34 a**) in situ spectroelectrochemical (%T vs. wavelength changes) and **b**) in situ electrocolorimetric analyses of ITO/CoPc-odea film in DCM/TBAP electrolyte recorded under 1.20 V applied potential.

It is known that electrochromic responses of an electrochromophore depends on the film morphology, film thickness, film preparation parameters, solvents and supporting electrolyte types, and type of the electrochromophore. All of these parameters were optimized to obtain the desired electrochromic parameters. In order to analyze the effects of film thickness, ITO/CoPc-odea electrodes were constructed with different number of CV cycles (2, 5, 10 and 15) and speed and stability of the spectral tests were performed with in situ SCC analyses of these electrodes in DCM/TBAP electrolyte system. In situ SCC analyses were performed by following T% vs time responses of the electrodes during repetitive CC excitations to the electrodes. CC excitations were done between 0.0 and 1.20 V with 100 s time intervals. As shown in **Fig.3.35**, different T% vs time responses are observed for different electrodes constructed with different number of repetitive CV cycles. The highest optical contrast and optical stability and the shortest response times are observed with ITO/CoPc-odea electrode modified with 5 CV cycles. When film gets thicker (CV cycles are more than 5), optical contracts start to decrease. The shortest

response times are found as 0.5 and 2.4 s for anodic and cathodic coloring processes respectively with ITO/CoPc-odea electrode modified with 5 CV cycles. Consequently, the film thickness controlled with 5 CV cycles within "*pro1"* is found as optimal film preparation condition. Thus, all electrodes were constructed with 5 CV cycles within "*pro1"* for further analyses.

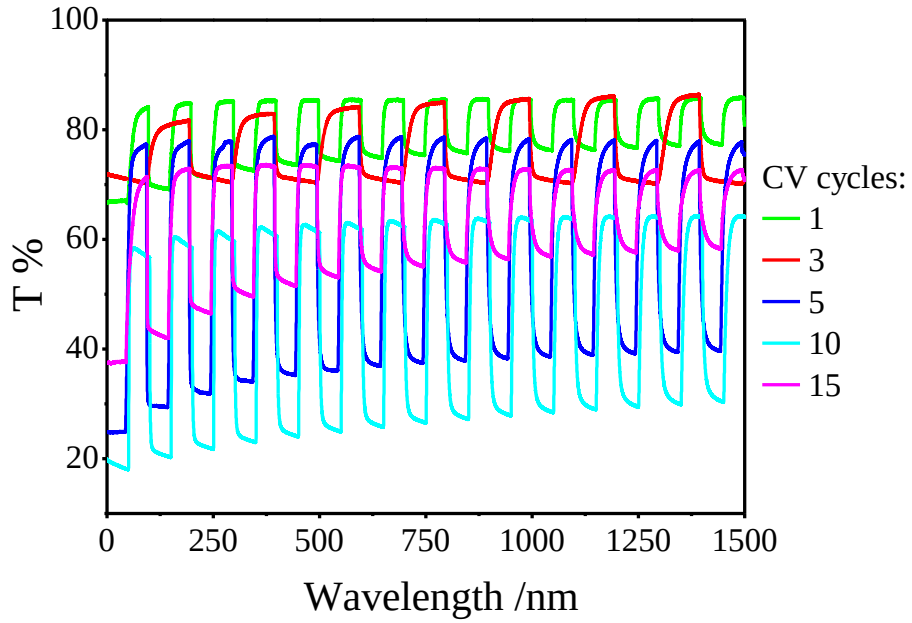


**Figure 3.35** %T (at 678 nm) versus time responses of ITO/CoPc-odea films prepared with different number of CV cycles in DCM/TBAP electrolyte system.

In order to find out the ideal solvent for the electrolyte system, SCC measurements of ITO/CoPc-odea electrode were performed in different solvents, DCM/TBAP, AN/TBAP, and $H_2O/LiClO_4$. ITO/CoPc-odea electrode did not give any spectral and color change in $H_2O/LiClO_4$, which indicates unsuitability of water as a solvent for the electrolyte system. When SCC analyses of ITO/CoPc-odea electrode were performed with respect to T% vs wavelength and T% vs time responses in DCM/TBAP and AN/TBAP, it is clearly shown that better electrochromic parameters are observed in DCM/TBAP **(Fig. 3.36a)** than those in AN/TBAP **(Fig. 3.36b)** electrolyte.

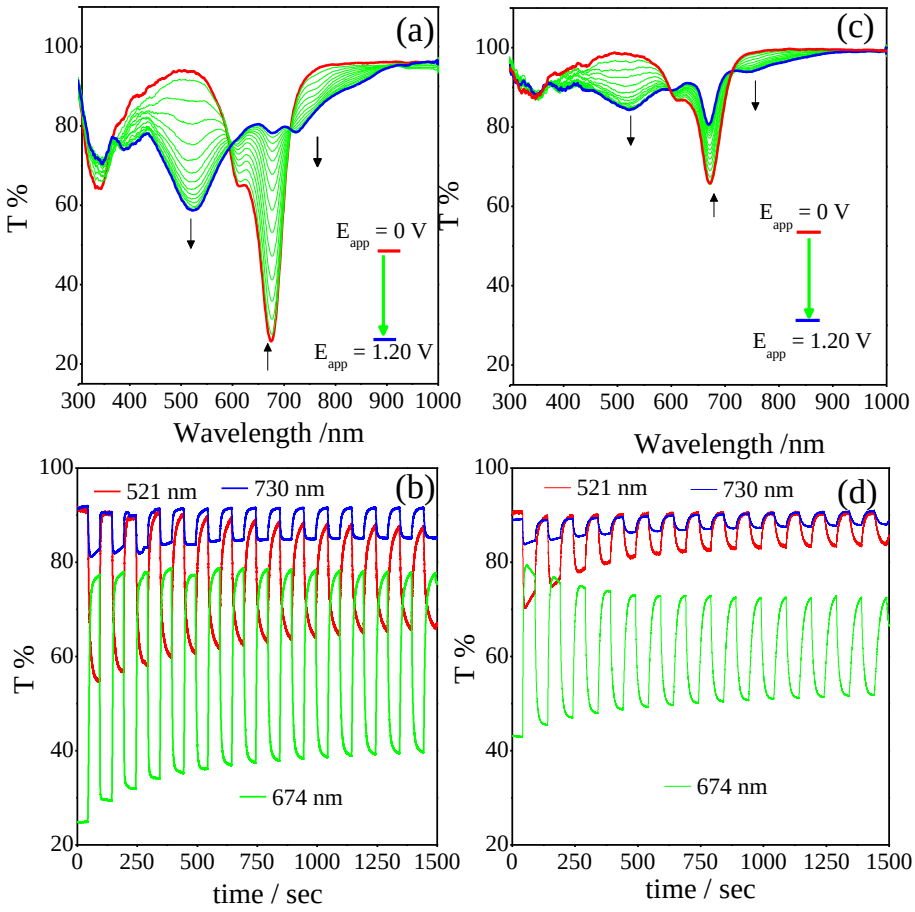


**Figure 3.36** SCC analyses of ITO/CoPc-odea film in different solvents. In situ spectroelectrochemical (%T vs. wavelength) changes (**a**: in DCM/TBAP and **c**: in AN/TBAP) and %T changes versus time (**b**: in DCM/TBAP and **d**: in AN/TBAP).

While %T of ITO/CoPc-odea electrode changes as 50 % at 678 nm and 35 % at 524 nm in DCM/TBAP **(Fig. 3.36a)**, these values are only 16% and 14% in AN/TBAP **(Fig. 3.36c)**. T% vs time responses of ITO/CoPc-odea electrode are followed at three different wavelengths and ITO/CoPc-odea electrode gives higher optical contrasts and optical stabilities and shorter response times at all wavelengths **(Fig. 3.36b and 36d )**. The best electrochromic parameters were derived from the T% vs time analyses carried out at 678 nm in DCM/TBAP as shown in **Fig. 3.36b**. While 0.5 s anodic coloring response time with 50 % optical contrast is observed at 678 nm in DCM/TBAP, these values decrease down to 3.4 s and 16% respectively in AN/TBAP **(Fig. 3.36d)**.

Consequently, further SCC measurements of ITO/CoPc-odea electrode were carried out in DCM/TBAP and electrochromic parameters were derived from the T% vs time analyses carried out at 678 nm (the Q band of the complex). To determine ideal supporting electrolytes, in situ SCC analyses were repeated by using different supporting electrolytes having different ionic sized anions. Since it's known that color changes arise from penetration and removing of anions to the oxidized cationic film. The suitability of the anion size to the porosity of the film determines the electrochromic character of the films. **Fig. 3.37** shows in situ spectroelectrochemical analyses of ITO/CoPc-odea in DCM with different supporting electrolyte. In order to explore the effects of anions to the electrochromic responses of ITO/CoPc-odea film, % T versus time responses of change of ITO/CoPc-odea film are followed under 1.20 V potential application.

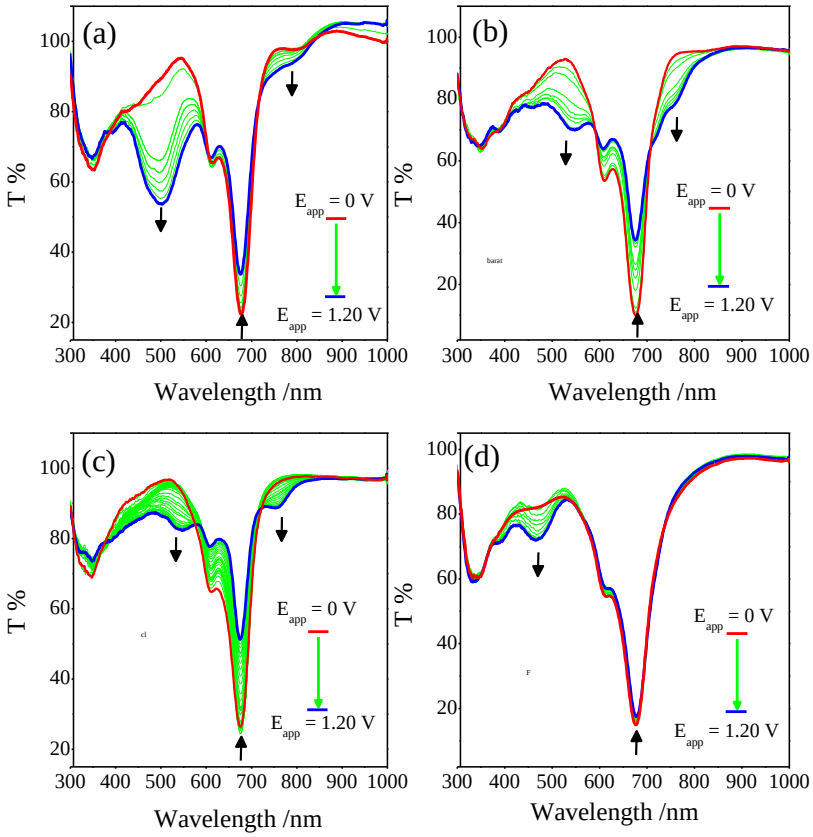


**Figure 3.37** In situ spectroelectrochemical (%T vs. wavelength) changes of ITO/CoPc-odea film in DCM solvent consisting different supporting electrolytes. **a)** TBAPF**, b)** TBAB, **c)** TBACl, **d)** TBAF.

Neutral CoPc-odea film gives the same transmittance bands in DCM with TBAP, TBAPF, TBAB, TBACl, and TBAF supporting electrolytes as shown in **Fig. .3.36a** and **Fig. 3.37**. When 1.20 V potential is applied to ITO/CoPc-odea electrode, CoPc-odea film gives different spectral changes with different electrolytes. While transmittance intensity of the Q band of CoPc-odea film at 678 nm decreases and disappears completely, two new bands are observed at 524 and 790 nm in DCM/TBAP **(Fig. 3.36a)**. When TBAPF is used however, intensity changes of the bands at 524 and 678 nm are smaller than those recorded in DCM/TBAP **(Fig. 3.37a)**. Moreover, the band at 790 nm shifts to 724 nm in DCM/TBAPF. This data indicates that neutral CoPc-odea film could not turn to fully oxidized CoPc-odea film due to unsuitability of hexafluorophosphate anion. It is known that for the oxidization of the film, anions of the supporting electrolyte should penetrate into the film with at least similar rate of the electron transfer reaction occurring on the electrode. When TBAB is used as the supporting electrolyte, the new increasing band assigned to the oxidized CoPc-odea film is observed at 550 nm instead of 524 nm recorded in DCM/TBAPF and DCM/TBAP. Moreover intensity change of this band is less than those observed in DCM/BAPF and DCM/TBAP **(Fig. 3.37b)**. ITO/CoPc-odea electrode also gives different spectroelectrochemical responses in DCM/TBACl **(Fig. 3.37c)** and DCM/TBAF **(Fig. 3.37d)** than those in DCM/TBAPF and DCM/TBAP **(Fig. 3.37b)**. While the new bands assigned to the oxidized CoPc-odea film are observed at 540 and 765 nm in DCM/TBACl **(Fig. 3.37c)**, the intensity of these bands are observed in less extent with respect to the changes observed in previous electrolytes. No any spectral changes are observed in DCM/TBAF **(Fig. 3.37d)** under 1.20 V potential application. When the spectral changes are compared with each other with respect to the intensity of the band at around 550 nm assigned to the oxidized CoPc-odea -odea, The order could be proposed for the proper electrocheromic response: TBAP > TBAP > TBAPF> TBACl >TBAF. This order is related with the ionic size of the anions of the supporting electrolytes. The most proper one is TBAP. The ions larger than TBAP (TBAPF) and smaller than TBAP are not proper for the porosity of CoPc-odea film for the neutralization of the oxidized film by penetrating into the film. This means that the size of the anion should be fitted into the porosity of the film.

Moreover, rate of the penetration into and out of the film should be fast enough as well as the electron transfer reaction rate on ITO/CoPc-odea electrode.

With respect to electrochromic analyses performed with different film thicknesses, solvents and supporting electrolytes, ITO/CuPc-odea and CoPc-odea films prepared with 5 CV cycles in "*pro1*" gives the best results in TBAP/DCM electrolyte system. Thus, SCC analyses of the complexes are performed with these optimized parameters to drive the basic electrochromic properties of the complexes. **Fig. 3.38** shows in situ SCC responses of ITO/ CoPc-odea electrode in TBAP/DCM electrolyte system. As shown in **Fig. 3.38a**, the highest transmittance intensity changes are observed at 524, 678, and 724 nm. Thus, %T vs. time changes are followed at these wavelengths during the repetitive chronocoulometric (CC) excitation between 0.0V and 1.20 V. As shown in the CC graph **(Fig. 3.38a)**, ITO/CoPc-odea film gives almost similar anodic and cathodic current responses and the film retains 85 % of its coulombic stability within 15 CC cycles then it almost keeps its coulombic stability. Observation of the same anodic and cathodic currents illustrates reversibility of the electron transfer and penetration of perchlorate ions in and out of the film. During repetitive CC excitations, %T responses of the electrode are observed at three different wavelengths with respect to elapsed time **(Fig. 3.38a)**. The highest optical contrast with the shortest response times are derived from the %T vs. time changes recorded at 524 nm.

While the transmittance changes at 724 nm retains 100 % of its optical stability, %T changes recorded at 524 and 678 nm lose 25% of its optical stability for neutralization reaction until $10^{th}$ CC cycle. Altough %T decreases during cathodic potential applications, it keeps its stability during anodic potential applications. After the $10^{th}$ CC cycle, completely stable %T changes are observed during both the anodic and cathodic potential applications. All electrochromic parameters, response times, optical contrast, optical stability, and coulombic stability, are derived from SCC analyses of ITO/CoPc-odea film and tabulated on **Table 3.3** High optical contrast (50%), short response times (0.85 s for cathodic and 1.5 s for anodic CC excitations), reasonable optical and coulombic stabilities of ITO/CoPc-odea film can provide most of the expectations of various display technologies.

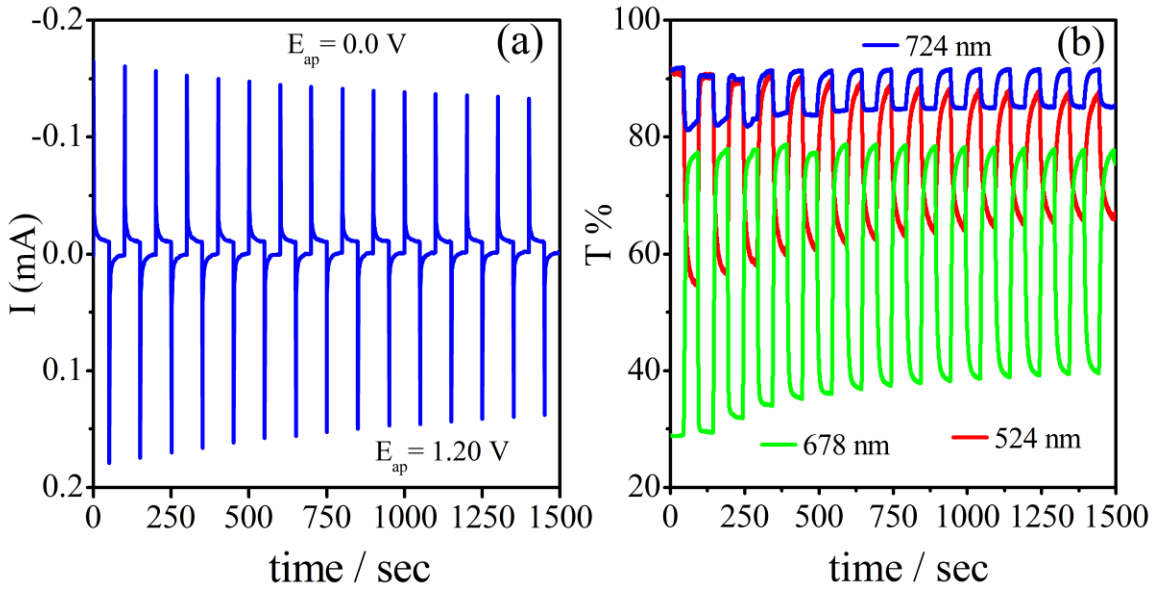


**Figure 3.38** SCC analyses of ITO/CoPc-odea film in DCM/TBAP electrolyte system. **a)** %T versus time changes at 490 nm (red) and 630 nm (green). **b)** Repetitive CC responses between $E_{app.}$=0.0 V and $E_{app.}$= 1.20 V within 50 s time intervals.

In order to investigate the effect of the metal center of MPcs to the electrochromic responses of the complexes, $H_2$Pc-odea and CuPc-odea complexes were also tested as possible electrochromic materials. As mentioned above, although $H_2$Pc-odea has similar redox activity with CoPc-odea and CuPc-odea complexes in solution and in solid state as ITO/ $H_2$Pc-odea film, No any spectral and color changes were observed in all tested electrolyte systems.

CuPc-odea film illustrates similar electrochromic responses with those of ITO/CuPc-odea film. As shown in **Fig. 3.39a**, during in situ spectroelectrochemical analysis of the ITO/CuPc-odea film, the Q band of the neutral CuPc-odea film increases in transmittance intensity at 682 nm, and a new band is recorded at 514 nm. Moreover, two new bands at 805 and 840 nm are also observed during the oxidation of the film. Originally neutral ITO/CuPc-odea film is light bluish green (point □ in **Fig. 3.39b**; x= 0.3099 and y = 0.3448) as shown in the chromaticity diagram, but its color turns to red (point △ in **Fig. 3.39b**; x= 0.3741 and y = 0.312) after oxidation reaction. Distinct spectral changes in the visible region of the spectrum, and clear color change indicates electrochromic usability of

the complex. To find out the electrochromic properties of the complex, ITO/CuPc-odea film was continuously reduced and oxidized with repetitive CC excitation between 0.0 and 1.20 V and, reversibility, speed, and stability of spectral and coulombic changes are followed.

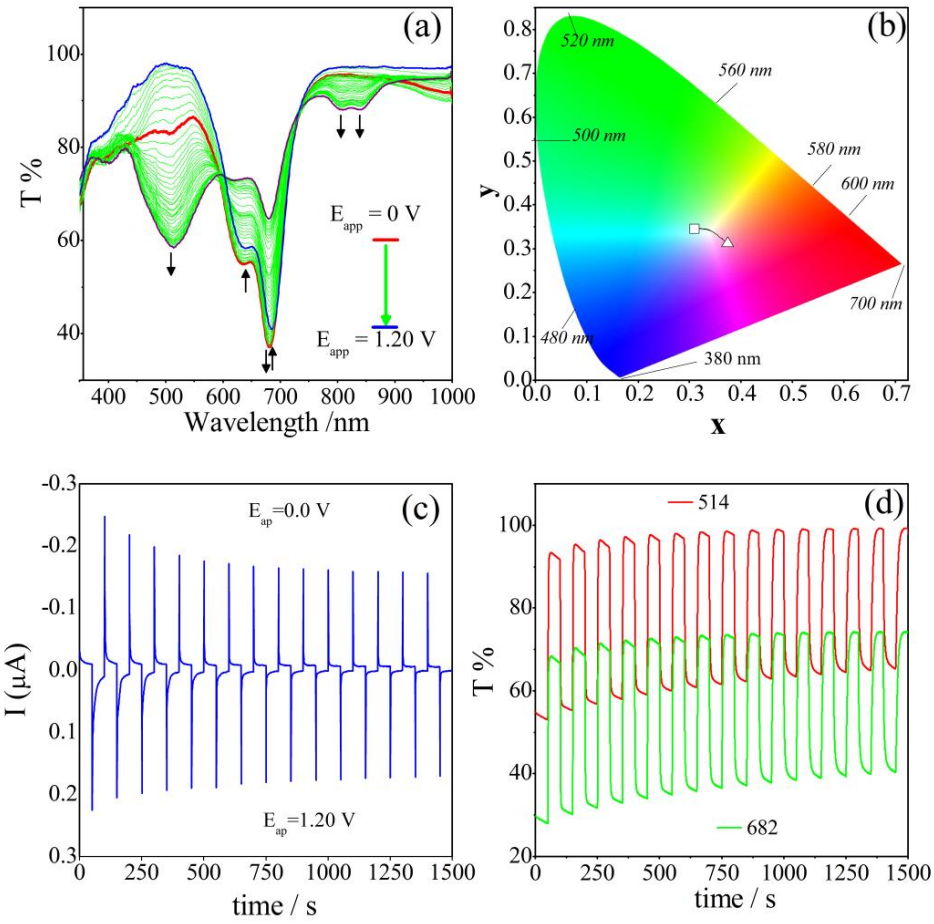


**Figure 3.39** SCC analyses of ITO/CuPc-odea film in DCM/TBAP electrolyte system. a) %T changes recorded during in situ spectroelectrochemical measurement under 1.20 V potential application. b) Chromaticity diagram of ITO/CuPc-odea film. c) Repetitive CC responses between $E_{app.}$=0.0 V and $E_{app.}$= 1.20 V within 50 s time interval. **d)** %T versus time changes at 682 nm (green) and 514 nm (red).

As shown in **Fig. 3.39c**, both the anodic and cathodic current responses of the electrode decreases until the 5$^{th}$ CC cycle, but after this point, completely reversible and stable current responses are observed during anodic and cathodic potential excitations. Under the

CC excitation signals, distinct transmittance changes are also observed. As shown in **Fig. 3.39d**, %T at 682 nm changes from 17% to 57%, when film is oxidized with the first CC cycle.

During consecutive CC cycles, %T values for the fully oxidized and neutralized film change and reach to a steady state after the $5^{th}$ CC cycle. Similar transmittance change (from 53% to 92%) is also observed at 514 nm. Response times for anodic and cathodic coloring processes are derived from %T at 682 nm as 0.9 and 0.6 s respectively. These values are found as 1.1 and 0.8 s, when %T changes at 524 nm are followed. When compared with ITO/CoPc-odea film, ITO/CuPc-odea film gives higher optical and coulombic stabilities and shorter response times. However, optical contrast of ITO/CoPc-odea film is higher than that of ITO/CuPc-odea film. When overall electrochromic parameters are taken into account, both of CoPc-odea and CuPc-odea complexes illustrate excellent electrochromic responses with respect to response times and optical contrasts in DCM/TBAP electrolyte system.

Electrochromic parameters of various electropolymerized film of MPcs bearing tetrakis diethyllamino-phenoxy-ethoxy substituents (MPcs-tdea) obtained in previous papers are tabulated in **Table3.4** for comparison with electrochromic properties of octakis diethylamino-phenoxy substituted MPcs (MPcs-odea) in this study. As shown in **Table 4**, when the electrochromic responses of MPcs-odea are compared with those of MPcs-tdea, it can be easily concluded that higher optical contrasts and shorter response times are observed with MPcs-odea film. Colors and color coordinates of these two different MPc series are also different from each other's. While ITO/MPcs-tdea films gave the best electrochromic response in AN/TBAP electrolyte, DCM/TBAP electrolyte is found as the best media for ITO/ MPcs-adea films. ITO/$H_2$Pc-tdea film gave reasonable electrochromic response with 40% optical contrast and 5.0 s response time between cyan and light yellow color, yet light green color of ITO/$H_2$Pc-tdea film did not change during oxidation. Consequently, it can be concluded that substitution of MPcs with octakis amino groups instead of tetrakis amino groups improve electropolymerization abilities, reversibility of the electropolymerized films, and electrochromic responses of these films.

**Table 3.4** Electrochromic parameters of octakis diethylamino-phenoxy and tetrakis diethyllamino-phenoxy-ethoxy substituted ITO/MPcs electrode.

| **Complexes** | **Electrolyte system** | $E_{app.}$ | %T[a] | Response time (s) [b] | Color | Color coordinates | Current stability loss [d] | %T stability loss [e] | Optical contrast [f] | Ref. |
|---|---|---|---|---|---|---|---|---|---|---|
| ITO/CoPc-odea | DCM/TBAP | *0.0 V* | 29 (91) | 1.50 | blue | x= 0.2821<br>y = 0.3434 | 4.0 (25) | 0.0 (1.2) | 50 | tw |
| | | *1.20 V* | 79 (54) | 0.85 | purple | x= 0.3680<br>y = 0.3054 | 7.0 (30) | 0.0 (8.0) | | |
| ITO/CuPc-odea | DCM/TBAP | *0.0 V* | 17 (92) | 0.6 | bluish green | x= 0.3741<br>y = 0.3120 | - | 1.0 (7.0) | 40 | tw |
| | | *1.20 V* | 57 (53) | 0..9 | red | x= 0.4181<br>y = 0.3368 | - | 1.5 (5.0) | | |
| ITO/NiPc-tdea | AN/TBAP | *0.0 V* | 59 | 1.8 | cyan | x= 0.3169<br>y = 0.3365 | - | - | 20 | [143] |
| | | *1.20 V* | 79 | 1.0 | red | x= 0.4181<br>y = 0.3368 | - | - | | |
| ITO/CuPc-tdea | AN/TBAP | *0.0 V* | 74 | 4.1 | greenish blue | x= 0.3176<br>y = 0.3326 | - | - | 17 | [143] |
| | | *1.20 V* | 91 | 3.2 | red | x= 0.3822<br>y = 0.332 | - | - | | |
| ITO/$H_2$Pc-tdea | AN/TBAP | *0.0 V* | 59 | 8.0 | cyan | x= 0.2988<br>y = 0.3315 | - | - | 40 | [143] |
| | | *1.20 V* | 99 | 5.0 | light yellow | x= 0.3577<br>y = 0.3507 | - | - | | |

**[a]:** maximum %T value reached at each anodic and cathodic CC excitations. **[b]:** Time needed to change the half of the total %T change. [c]: color coordinates (x: red and y: green) of the fully neutralized and oxidized films [d]: % current differences between the first and last CC excitations. [e]: % T differences between the first and last CC excitations. [f]: %T differences observed between the anodic and cathodic first cycle CC excitations.

## 4. CONCLUSIONS

Voltammetric and in situ spectroelectrochemical characterization of the $In^{III}$ClPc, $Mn^{III}$ClPc, and $Ti^{IV}$OPc bearing metal centers with higher oxidation states $In^{III}$, $Mn^{III}$, and $Ti^{IV}$ were performed in solution and in solid state as LB films. Metal based reduction reactions of $Mn^{III}$ClPc and $Ti^{IV}$OPc alter the electrochemical and in situ spectroelectrochemical behaviors of the complexes. Different colors of the redox forms of $Mn^{III}$ClPc and $Ti^{IV}$OPc recorded with in situ electrocolorimetric measurements show possible usage of the complexes in the display technologies, e.g. electrochromic and data storage application. Increasing redox activity of MPcs with incorporating redox active $Mn^{III}$ and $Ti^{IV}$ metal centers also increases the possibilities of the complexes for the application of functional materials in different electrochemical technologies. For this purpose, these complexes were investigated as electrocatalyst and electrosensor. Interaction of these complexes with molecular oxygen indicates the electrocatalytic and electrosensing activities of the complexes in solution as well as in aqueous solution as LB multilayer films.

Electrochemical and spectroelectrochemical results of the complexes convey the proposed structure of the complexes. Presences of $Co^{II}$ and $Ti^{IV}$O metal centers in the core of the Pc ring enhance the redox richness of the complexes due to the metal based redox processes of CoPc and TiOPc complexes. Distinct differences between the colors of the electrogenerated species recorded with in situ electrocolorimetric measurements indicate their possible application in the display technologies, e.g. electrochromic and data storage application. While the NiPc and ZnPc complexes did not interact with the molecular oxygen, CoPc and TiOPc complexes catalyzed ORR. Moreover, CoPc behaves as an oxygen sensor.

Electrochemical and spectroelectrochemical measurements indicates that $H_2$Pc-odea, CuPc-odea, and CoPc-odea complexes give common metal center and phthalocyanine based reduction processes during cathodic potential scans, and all are electropolymerized during the oxidation reactions. Although diethyllamino groups trigger electropolymerization of the complexes, altering the metal center of the Pc core of the complexes changes electropolymerization reactions. All complexes coated on ITO

electrode with the electropolymerization reaction and modified ITO/MPcs-odea electrodes were investigated as electrochromic materials. ITO/$H_2$Pc-odea film did not give any spectral and color changes as a result of oxidation reaction, but ITO/CuPc-odea, and ITO/CoPc-odea complexes represented excellent electrochromic responses with short response times and high optical contrasts. SCC analyses of films indicated that film thicknesses, solvent and supporting electrolyte types affect the electrochromic responses of the complexes. The best responses were observed in DCM/TBAP electrolyte system with the films coated with five CV cycles within the anodic potential window of DCM/TBAP electrolyte system.

## REFERENCES


[1] A.B.P.Lever et al., Pure & App. Chem., Vol. 58, No. 1 1, pp. 1467—1476, 1986.

[2] P. Gregory, (1999). Steamrollers, sports cars and security: phthalocyanine progress through the ages. Journal of Porphyrins and Phthalocyanines, 3(06), 468-476.

[3] R. P. Linstead, (1936), An unusual isomeric change in the three-carbon system, Journal of Chemical. Society, 57, 1016-1024.

[4] A.J Bard, Faulkner, L.R. (2001), Electrochemical Methods: fundamentals and applications, 2nd Edition, John Wiley & Sons, Inc., 1-430 New York, USA.

[5] N.B. McKeown, Phthalocyanine Materials: Synthesis, Structure and Function, Cambridge University Press, Cambridge, 1998.

[6] Jakub D. Baran & J. Andreas, Inversion of the shuttlecock shaped metal phthalocyanines MPc (M = Ge, Sn, Pb) a density functional study, Physical Chemistry Chemical Physics vol. 12, issue 23, p. 6179, *2010.*

[7] M. J. Schöning, & Poghossian, A. (2002). Recent advances in biologically sensitive field-effect transistors (BioFETs*).* Analyst, *127*(9), 1137-1151.

[8] A.B.P. Lever, C.C. Leznoff, "Phthalocyanines Properties, and Applications", vols.1–4, VCH, New York, (1989–1996).

[9] A. Kalkan et al., Polyhedron; 23, 3155-62, (2004).

[10] C.H. Lee, D.K.P. Ng, Tetrahedron Lett; 43, 4211-13, (2002).

[11] P.Gregory, Industrial Applications of Phthalocyanines. J Porphyrins and Phthalocyanines; 4:434, (2000).

[12] H.G. Tanner, ( E.I. du Pont de Numours & Co) U.S. Patent 2, 163, 768, (June 27, 1939).

[13] A. Sander, Die Chemie; 55, 255, (1942).

[14] M. Calvin, et al., Trans. Faraday Soc; 32, 1443, (1936).

[15] M. Polyani, Trans. Faraday Soc;34, 1191, (1938).

[16] C. Bull. Paquot, Soc. Chim; 8, 695, (1941).

[17] C. Bull. Paquot, Soc. Chim; 12, 450, (1945).

[18] N. Uni, Nature; 177, 1177, (1956).

[19] W.M. Brouwer et al., Chem; 128, 133, (1984).

[20] L.M. Santos, M. Baldwin, Anal. Chem; 58, 848, (1986).
[21] F.H. Moser & A.L. Thomas, "The Phthalocyanines", VoL.l, CRC Press, Boca Ration, F.L. (1983).
[22] H. Behret et al., J. ElectroanaI. Chem; 29,117, (1981).
[23] J. Zagel et al., J. Electroanal. Chem; 83, 207, (1977).
[24] T. Kuwana et al., J. Electroanal. Chem; 88,299, (1978).
[25] J.P. Randin, Electrochim Acta; 19,83, (1974). 151
[26] J. Zagal et al., J. Electrochem. Soc; 127, 1506, (1980).
[27] N. Kobayashi, Y. Nishiyama, J. Phys. Chem; 89, 1167, (1985).
[28] T.T. Osaka et al., Chem. Soc; 59, 2717, (1986).
[29] A. Elzing et al., J. Electroanal. Chem; 233, 113, (1987).
[30] J. Blomquist et al., Electrochem. Acta; 27,1445, (1982).
[31] Toshiba Corp. Jpn. Kokai Tokkyo Koho Jp. Appl. 81/41, 673,24 March 1981, CA. 1985, 102, 754174.
[32] M. Green, The promise of electrochromic systems, Chem. Ind. (1996) 641–644.
[33] D.R. Rosseinsky & R.J. Mortimer, Electrochromic systems and the prospects for devices, Adv. Mater. 13 (2001) 783–793.
[34] R.A. Colley et al., Poly[oxymethylene-oligo(oxyethylene)] for use in subambient temperature electrochromic devices, Polym. Int. 49 (2000) 371–376.
[35] H. Byker et al., Electrochromic Materials II, PV 94-2, Electrochem. Soc. Proc. Ser., Pennington, NJ, 1994, pp. 3–13.
[36] S. Somani Parakash & S. Radhakrishan, Electrochromic Materials and Devices: present and future, Materials Chemistry and Physics 77 (2002) 117-133.
[37] P.M.S. Monk et al., Electrochromism: Fundamentals and Applications, VCH, Weinheim, 1995.
[38] G.E Gunbas et al., A unique processable green polymer with a transmissive oxidized state for realization of potential RGB-based electrochromic device applications. Advanced Functional Materials. 2008;18(14):2026-30.
[39] B. Yigitsoy et al., Electrochromic properties of a novel low band gap conductive copolymer. Electrochim Acta. 2007;52(23):6561-8.

[40] S. Ozdemir et al.,Green to highly transmissive switching multicolored electrochromes: Ferrocene pendant group effect on electrochromic properties. React Funct Polym. 2011;71(2):168-74.
[41] A. Koca et al., Electrochemistry and spectroelectrochemistry of tert-butylcalix [4]arene bridged bis double-decker lutetium(111) phthalocyanine, $Lu_2Pc_4$ and dimeric lutetium(III) phthalocyanine, $Lu_2Pc_2(OAc)(2)$. Chem Phys. 2007;340(1-3):283-92.
[42] A. Yavuz et al., Electropolymerization of a New 4-(2,5-Di-2-thiophen-2-yl-pyrrol-1-yl)-Tetra Substituted Nickel Phthalocyanine Derivative. Journal of Applied Polymer Science. 2011;122(2):1293-9.
[43] H.K. Yildiz et al., 3,4-Ethylenedioxythiophene substituted phthalocyanines. Synthetic Met. 2011;161(17-18):1946-52.
[44] Faruk Demir et al., Electrochromism of Electropolymerized Metallophthalocyanines. Journal of The Electrochemical Society 2014;161(3):G1-G6.
[45] J.l. Miasik et al., J. Chem. Soc. Faraday Trans; 82, 1117, (1986).
[46] Sawa Seikosha Co., Ltd. Jpn. Kokai Tokkyo Koho JP 57, 108,652, 1982. CA 1983, 46165j.
[47] K. Shinbo et al., Colloids Surf. A 905, 198–200, (2002).
[48] M.I. Newton et al., Sensors Actuators B: Chem; 67, 307, (2000).
[49] M. Harbeck et al., Phthalocyanines as sensitive coatings for QCM sensors operating in liquids for the detection of organic compounds, Sensors and Actuators B: Chemical, 2010.
[50] D.D. Erbahar et al., Explosives Detection in Sea Water with Phthalocyanine Quartz Crystal Microbalance, Sensors and Actuators B: Chemical, 2012.
[51] D.D. Erbahar et al., Pesticide sensing in water with phthalocyanine based QCM sensors, Sensors and Actuators B: Chemical, 2012.
[52] Shahino Mah Abdullah, Temperature-sensitive chemical cell based on Nickel (II) phthalocyanine-tetrasulfonic acid tetrasodium salt Sensors and Actuators A: Physical 179 (2012): 146-150.

[53] M. Savy, (1974) Study of Reduction of Oxygen on Monomer and Polymer Phthalocyanines .2. Iron Polyphthalocyanines Impregnated on Carbon Blocks of Y Acetylene, Electrochimica Acta, 19(7), 403-411.
[54] S. Meshitsuka & K. Tamaru (1977) Photoelectrocatalysis by Metal Phthalocyanine Evaporated-Films in Oxidation of Oxalate Ion, Journal of the Chemical Society-Faraday Transactions, I 73, 236-242.
[55] C. Linkous et al., J. Electrochem. Soc;130, 1050, (1983).
[56] M.K. Halbert & R.P. Baldwin, Anal.Chem; 57,591, (1985).
[57] K.M. Korfhage et al., Anal. Chem; 57, 1514, (1984).
[58] H. Tachikawa & L.R. Faulkner, J. Am. Chem. Soc; 100,4379, (1978).
[59] F. Fu Ren & L.R. Faulkner, J. Am. Chem. Soc; 101,4779, (1979).
[60] H. Riel et al., Synthetic Met. 303, 111–12 (2000).
[61] K. Shinbo et al., IEICE Trans. Electron. E85-C 1233, (2002).
[62] Toshiba Corp. Jpn. Kokai Tokkyo, Koho lP. 57, 157.468(82, 157,468) 1982 CA. 1983, 75417.
[63] N. Doddapaneni, Eur. Pat. Appl. E.P 57, 986. 1982. CA 1983, 19510m.
[64] S. P. Keizer et al., (2003). Spectroscopy and electronic structure of electron deficient zinc phthalocyanines. Journal of the American Chemical Society, 125(23), 7067-7085.
[65] L. Guo et al., (1996). Ligand substitution effect on electronic structure and optical properties of nickel porphyrazines. Inorganic Chemistry, *35*(18), 5304-5312.
[66] W. Chidawanyika et al., (2007). Syntheses and photophysics of new phthalocyanine derivatives of zinc, cadmium and mercury.New Journal of Chemistry, *31*(3), 377-384.
[67] J. Obirai & T. Nyokong, (2005). Synthesis, spectral and electrochemical characterization of mercaptopyrimidine-substituted cobalt, manganese and Zn (II) phthalocyanine complexes. Electrochimica acta, 50(16), 3296-3304.
[68] M. J. Stillman & A. J. Thomson, (1974). Orbital reduction factors in the lowest excited state of the phthalocyanine ring and their measurement by magnetic circular dichroism spectroscopy. *J. Chem. Soc., Faraday Trans. 2, 70,* 805-814.

[69] A. B. P. Lever et al., (1981). Charge-transfer spectra of metallophthalocyanines: correlation with electrode potentials. Journal of the American Chemical Society,103(23), 6800-6806.

[70] A. Louati, et al., Inorg. Chem. 1985, 24, 1175.

[71] P.D. Hale, et al.,Chem. Soc. 1987, 109, 5943.

[72] A. B. P. Lever, Adv. Inorg. Radiochem. 1965, 7, 28.

[73] J. F. Myers et al., Inorg. Chem. 1975, 14, 461.

[74] M. J. Stillman & T. Nyokong, In Phthalocyanines. Properties and Applications Leznoff, C. C. and Lever, A. B. P. (eds.); VCH Publishers: New York, 1989, vol 1.

[75] T. S. Nyokong, Afr. J. Chem. 1995, 48, 23.

[76] K. Ban et al., J. Mater. Chem. 2000, 10, 1083.

[77] M.J. Stillman et al., In Phthalocyanines. Properties and Applications VCH Publishers: New York, 1993, vol 3.

[78] A.G. Gürek et al., J. Chem. Soc. Dalton Trans. 1994, 1419.

[79] K. Takahashi et al., Inorg. Chim. Acta. 1995, 232, 69.

[80] H. Matsuda et al., Proc. SPIE-Int. Soc. Opt. Eng. 1990, 1337, 105.

[81] Y. Suda et al., Proc. SPIE-Int. Soc. Opt. Eng., 1991, 1560, 75.

[82]http//www.biol.paisley.ac.uk/macro/Enzyme_Electrode/Chapter1/Cyclic_Voltammetry.html

[83] J. Wang, Analytical Electrochemistry 1994. VCH Publishers Inc: New York.

[84] D.B. Hibbert, Introduction to Electrochemistry 1993. Macmillan: London.

[85] M. A. C. Brett & A. M. O. Brett, Electrochemistry Principles, Methods and Applications 1993. Oxford University Press: New York.

[86] F. M. Hawkridge, Laboratory Techniques in Electroanalytical Chemistry, 2nd ed. Kissinger, P. T. and Heineman, W. R. (eds) 1996. Marcel Dekker Inc.: New York.

[87] T.P. Deangelis & W. R. Heineman (1976) Differential Pulse Anodic-Stripping Voltammetry in a Thin-Layer Electrochemical Cell, Analytical Chemistry, 48(14), 2262-2263).

[88] T.P. Deangelis & W.R. Heineman (1976) Electrochemical Experiment Using an Optically Transparent Thin-Layer Electrode, Journal of Chemical Education, 53(9), 594-597.
[89] W.R. Heineman et al., (1975) Mercury Film Nickel Mini-Grid Optically Transparent Thin-Layer Electrochemical Cell, Analytical Chemistry, 47(8), 1364-1369.
[90] A.E. Calik et al., J. Porphyr Phthalocya, 17 (2013) 1046-1054.
[91] V.P. Chauke et al., Polyhedron, 30 (2011) 2132-2139.
[92] N. Masilela et al., Journal of Photochemistry and Photobiology a-Chemistry, 201 (2009) 91-97.
[93] N. Nombona et al., Electrochim Acta, 53 (2008) 3139-3148.
[94] I.A. Akinbulu et al., J Solid State Electr, 15 (2011) 2239-2251.
[95] F. Demir et al., J Electroanal Chem, 703 (2013) 117-125.
[96] A. Erdogmus et al., Synthetic Met, 161 (2011) 1319-1329.
[97] G. Mbambisa et al., Polyhedron, 26 (2007) 5355-5364.
[98] M. Aric et al., Electrochim Acta, 87 (2013) 554-566.
[99] J.D. Blakemore et al., Brudvig, Dalton T, 41 (2012) 7681-7688.
[100] P. Tau & T. Nyokong, Polyhedron, 25 (2006) 1802-1810.
[101] A. Aktas et al., Dyes Pigments, 99 (2013) 613-619.
[102] E.R. Milaeva & G.S.a.A.B.P.L. The redox chemistry of metallophthalocyanines in solution, in: A.B.P.L. C.C. Leznoff (Ed.) The Phthalocyanines, Properties and Applications Wiley, 1992, pp. 162-227.
[103] I.A. Akinbulu et al., Electrochim Acta, 55 (2010) 7085-7093.
[104] F. Matemadombo et al., Electroanal, 20 (2008) 1863-1872.
[105] P.N. Mashazi et al., Electrochim Acta, 53 (2007) 1858-1869.
[106] C.L. Lin et al., J Electroanal Chem, 524 (2002) 81-89.
[107] A.K. Burat et al., Electroanal, 24 (2012) 338-348.
[108] B.J. Palys et al., J Electroanal Chem, 379 (1994) 89-101.
[109] A. Koca et al., Electrochim Acta, 56 (2011) 5513-5525.
[110] A. Koca et al., Electrochim Acta, 52 (2007) 2683-2690.
[111] B. Simicglavaski et al., J Electrochem Soc, 134 (1987) C130-C130.

[112] A. Koca et al., J Electroanal Chem, 616 (2008) 107-116.
[113] M. Canlica & T. Nyokong, Polyhedron, 30 (2011) 1975-1981.
[114] M. Kandaz & A. Koca, Polyhedron, 28 (2009) 2933-2942.
[115] Y. Liu & X.Q. Lin, Chinese J Anal Chem, 27 (1999) 1026-1028.
[116] A.I. Adebayo & T. Nyokong, Polyhedron, 28 (2009) 2831-2838.
[117] C.C. Leznoff et al., Inorg Chim Acta, 359 (2006) 2690-2699.
[118] A. Koca, J Electroanal Chem, 655 (2011) 128-139.
[119] A.L. Ugur et al., Polyhedron, 29 (2010) 3310-3317.
[120] A. Koca et al., Electroanal, 22 (2010) 310-319.
[121] A. Alemdar et al., Synthetic Met, 160 (2010) 1556-1565.
[122] I.A. Akinbulu & T. Nyokong, Polyhedron, 29 (2010) 1257-1270.
[123] B. Ortiz et al., J Electrochem Soc, 143 (1996) 1800-1805.
[124] W.A. Nevin et al., J Electroanal Chem, 213 (1986) 217-234.
[125] F. Demir et al., Phys Chem Chem Phys, 15 (2013) 15926-15934.
[126] I. Ozcesmeci et al., Electrochim Acta, 56 (2011) 5102-5114.
[127] A. Koca et al., Electroanal, 22 (2010) 1623-1633.
[128] P. Sen et al., Synthetic Met, 161 (2011) 1245-1254.
[129] G. Gumrukcu et al., Synthetic Met, 161 (2011) 112-123.
[130] Z. Odabas et al., Polyhedron, 26 (2007) 3505-3512.
[131] P. Matlaba & T. Nyokong, Polyhedron, 21 (2002) 2463-2472.
[132] B.O. Agboola et al., Electrochim Acta, 51 (2006) 6470-6478.
[133] E.F. Perez et al., Electroanal, 10 (1998) 111-115.
[134] A.B.P.L. C. C. Leznoff, Phthalocyanines, Properties and Applications, 4 ed., Wiley-VCH, 1996
[135] P. Tau & T. Nyokong, J Electroanal Chem, 611 (2007) 10-18.
[136] P. Tau & T. Nyokong, Electrochim Acta, 52 (2007) 3641-3650.
[137] H.R.P. Karaoglu et al., The synthesis and electrochemistry of novel, symmetrical, octasubstituted phthalocyanines. Synthetic Metals. 2013;182:1-8.

[138] S. Karadag et al., Synthesis and electrochemical properties of a double-decker lutetium (III) phthalocyanine bearing electropolymerizable substituents on non-peripheral positions. Dyes and Pigments. 2013.
[139] V. Cakır et al., Synthesis, characterization, electrochemical and spectroelectrochemical properties of metal-free and metallophthalocyanines bearing electropolymerizable dimethylamine groups. Dyes and Pigments. 2013.
[140] A. Aktas et al., Synthesis, characterization, electrochemical and spectroelectrochemical properties of peripherally tetra-substituted metal-free and metallophthalocyanines. Dyes and Pigments. 2013;99(3):613-9.
[141] H.J. Yen & G.S. Liou, Solution-processable triarylamine-based electroactive high performance polymers for anodically electrochromic applications. Polym Chem-Uk. 2012;3(2):255-64.
[142] P.M. Beaujuge & J.R. Reynolds, Color Control in pi-Conjugated Organic Polymers for Use in Electrochromic Devices. Chem Rev. 2010;110(1):268-320.
[143] F. Demir et al., Electrochromism of Electropolymerized Metallophthalocyanines. Journal of the Electrochemical Society. 2014;161(3):G1-G6.

# AUTOBIOGRAPHY

**Name - Surname** **:** Mehmet AYDEMİR

**Date of Birth** **:** İstanbul /1972

**Language** **:** English

**E-mail** **:** cascade34@hotmail.com

**Education**

| Degree | Section / Program | University / High School | Graduation Year |
|---|---|---|---|
| **High School** | Maths | Hayrullah Kefoğlu | 1989 |
| **University** | Chemistry | M.E.T.U | 1995 |

**Publication**

Altuğ Mert Sevim, H. Yasemin Yenilmez, ***Mehmet Aydemir***, Atıf Koca, Zehra Altuntaş Bayır, Synthesis, electrochemical and spectroelectrochemical properties of novel phthalocyanine complexes of manganese, titanium and indium, *Electrochimica Acta*, 2014, DOI: 10.1016/j.electacta.2014.05.149.